

Y3. A17

AEC

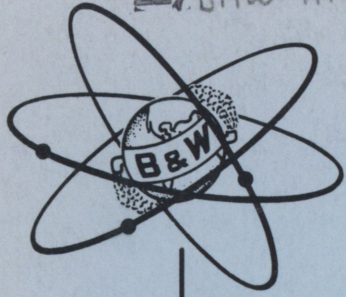
22/BAW-1116

RESEARCH REPORTS

BAW-1116

UC-81

AEC R&D Report



UNIVERSITY OF
ARIZONA LIBRARY
Documents Collection

JUN 1

LIQUID METAL FUEL REACTOR
EXPERIMENT

QUARTERLY TECHNICAL REPORT

APRIL 1958 - JUNE 1958

THE BABCOCK & WILCOX COMPANY

ATOMIC ENERGY DIVISION

metadc100984

— DISTRIBUTION NOTICE —

This report is distributed to TISE and OTS according to the Category "Reactors-Power" as given in the "Standard Distribution Lists for Unclassified and Scientific Technical Reports," TID-4500 (15th Ed.), August 1, 1959. Individual contractors have been supplied previously under Category C-81 of M-3679 (23rd Ed.).

— LEGAL NOTICE —

This report was prepared as an account of Government sponsored work. Neither the United States, nor the Commission, nor any person acting on behalf of the Commission:

A. Makes any warranty or representation, expressed or implied, with respect to the accuracy, completeness, or usefulness of the information contained in this report, or that the use of any information, apparatus, method, or process disclosed in this report may not infringe privately owned rights; or

B. Assumes any liabilities with respect to the use of, or for damages resulting from the use of any information, apparatus, method, or process disclosed in this report.

As used in the above, "person acting on behalf of the Commission" includes any employee or contractor of the Commission, or employee of such contractor, to the extent that such employee or contractor of the Commission, or employee of such contractor prepares, disseminates, or provides access to, any information pursuant to his employment or contract with the Commission, or his employment with such contractor.

Printed in U. S. A.

PRICE \$3.00

Available from the

OFFICE OF TECHNICAL SERVICES
U. S. DEPARTMENT OF COMMERCE
WASHINGTON 25, D. C.

BAW-1116
UC-81
AEC R&D Report

LIQUID METAL FUEL REACTOR
EXPERIMENT
QUARTERLY TECHNICAL REPORT
APRIL 1958 - JUNE 1958

AEC CONTRACT NO. AT(30-1)-1940
B&W CONTRACT NO. AEJ-46

SUBMITTED TO THE
UNITED STATES ATOMIC ENERGY COMMISSION
BY
THE BABCOCK & WILCOX COMPANY

TABLE OF CONTENTS

	Page
List of Figures	v
List of Tables	vi
References	vii
Summary	ix

PART ONE DESIGN STUDIES AND RELATED WORK

I. PHYSICS AND MATHEMATICS	3
A. LMFRE-I Design	3
B. Critical Experiment	6
II. REACTOR ENGINEERING	20
A. LMFRE-I Conceptual Design	20
B. Thermal Analysis	20
C. Instrumentation and Control	23
D. Nuclear Analysis	24
III. SYSTEMS ENGINEERING	25
A. Systems Design	25
B. Component Development	29
IV. MECHANISMS ENGINEERING	30
A. LMFRE-I Maintenance Scheme	30
B. Machine Designs for Critical Experiment	30
C. Prototype Conceptual Designs	31
D. Manpower Scheduling Charts	31
E. Canyon Bridge Crane	31
V. CHEMISTRY	32
A. Fuel Processing	32
B. Analytical Chemistry	42
VI. MATERIALS AND INSPECTION	44
A. 4-in. Utility Loop	44
B. ETR Test Loop	44
C. Vapor Deposited Coating on Graphite	44
D. Bismuth	44
E. Specifications	44

TABLE OF CONTENTS (CONT'D)

APPENDIX

	Page
REACTOR KINETICS	49
A. Formulation of the Problem	49
B. Results of Calculations.	61

PART TWO RESEARCH AND DEVELOPMENT PROGRAM

I. CHEMISTRY	83
A. Chemical Methods of Analysis.	83
B. Chemical Cleaning and Decontamination	86
C. Fuel Solution Stability	87
D. Uranium Solubility	87
E. Fuel Preparation	88
F. Sodium Bismuth Leak Test.	97
G. Slurry Development.	99
H. Uranium Carbide Formation	103
I. Electrolysis	104
J. Fuel Oxidation	104
K. ETR Loop Off-Gas Handling	104
II. INSTRUMENTS AND CONTROL	105
A. Non-Nuclear Instrumentation	105
B. Nuclear Instrumentation	110
III. MATERIALS TESTING	111
A. Dynamic Test Loops	111
B. Static and Capsule Tests	118
C. Miscellaneous Metallurgical Investigations	129
D. Graphite-to-Metal Seal	135
E. Alternate Impregnants for Graphite	136
F. Coated Graphite	147
G. Beryllium Thimble Development	147
H. Application of Molybdenum Coating	147
IV. PROTOTYPE TESTING	148
A. Reactor Port Thimble Joints	148
B. 2 1/2-in. Loop.	148
C. Valve Testing	148
D. Degassing Sparger Plate	149
E. 60-Cycle Induction Heating	149
F. Bellows Testing	151
G. Cavitation Testing - Rotating Disc	151
H. Bismuth Filters	151
I. Flange Testing	154

TABLE OF CONTENTS (CONT'D)

	Page
V. REMOTE MAINTENANCE	155
Remote Welding	155
VI. IN-PILE WORK	161
A. In-Pile Test Loop at ETR.	161
B. In-Pile Test Loop at MTR	163
C. In-Pile Test Loop at BNL.	163

LIST OF FIGURES

Figure		Page
1. Thermal Neutron Flux Distribution from Plane Source		10
2. k_{eff} vs. Core Radius.		11
3. k_{eff} vs. Core Height		12
4. k_{eff} vs. Fuel Concentrations		13
5. k_{eff} vs. Poison Fraction		14
6. k_{eff} vs. Core Voids		15
7. k_{eff} vs. Graphite Density		16
8. k_{eff} vs. σ_a (Carbon)		17
9. Energy Release vs. Step Input		18
10. Energy Release vs. Slope of Ramp Input.		19
11. LMFRE Reactor Arrangement		21
12. LMFRE-I Heat Exchanger		26
13. LMFRE-I Pump		27
14. Cold Trap Operation, Trap Temperature = 300 C		34
15&16. Cold Trap Operation, Trap Temperature = 300 C		35
17. Uranium Cold Trap Operation, Initial Concentration = 1000 ppm		40
18. Heat Generation from One Year's Accumulation of Fission Products Plus Po-210		41
19. Power vs. Time for Ramp Inputs		63
20. Mean Fuel Temperature vs. Time for Ramp Inputs.		64
21. Pressure of Fuel in Core (P_C) and Pressure of Gas (P_p) vs. Time for 1.5 Percent/Sec Ramp		66
22. Excess Multiplication vs. Time for 1.5 Percent/Sec Ramp . . .		67
23. Graphite Temperatures vs. Time for 1.5 Percent/Sec Ramp. .		68
24. Power vs. Time for Step Inputs		69
25. Mean Fuel Temperature vs. Time for Step Inputs		70
26. Graphite Temperatures vs. Time, 8 Percent δk Step Input . .		71
27. Excess Multiplication vs. Time, 8 Percent δk Step Input. . . .		72
28. Power vs. Time with Control Rod Operation		73
29. Excess Multiplication vs. Time		74
30. Fraction of Weight Remaining as a Function of $k\tau$ for Various Values of w_o/w_q		93
31. $k\tau$ for Complete Dissolution vs. w_o/w_q		94
32. Sodium-Bismuth Leak Test		98
33. Thermocouple Response Time (Test Apparatus Schematic) . . .		106

LIST OF FIGURES (CONT'D)

Figure	Page
34. Test for Liquid Level Indicators (Schematic)	108
35. 2 1/2-in. Loop for 3/4-in. Flowmeter Testing (Schematic) . .	109
36. Corrosion Results	114
37. Corrosion Results	115
38. Corrosion Results	116
39. Corrosion Results	117
40. Capsule Cycled 3203 Hr	122
41. Gamma Graph of Capsule No. 351 after 3000 Hr.	124
42. Gamma Graph of Capsule No. 329 after 3714 Hr.	125
43. Comparison of Creep-Rupture Properties - 1.25 Cr - .50 Mo	131
44. Creep Curve for 1.25 Cr - .50 Mo	132
45. Comparison of Min. Creep Rates of 1.25 Cr - .50 Mo	133
46. Hydraulic Press	138
47. Punches and Dies used for Dry Pressing	139
48. Electric Furnace Air Atmosphere	140
49. Graphite-Aluminum Samples after Firing (1500 F)	141
50. Graphite-Aluminum Samples after Firing (1000 F)	142
51. Percent Weight Loss for Graphite Pellets	143
52. Percent Volume Increase for Graphite Pellets	144
53. Carbon Tube Furnace	146
54. Test to Determine 60-Cycle Induction Heating Requirement . .	150
55. Apparatus - Rotating Disc Cavitation Test	152
56. Apparatus - Bismuth Filter Development	153
57. Gas-Shielded Metallic Arc Weld in Croloy 2-1/4 Pipe	157
58. High-Frequency Induction Forge Welding	158
59. High-Frequency Induction Forge Welding	159
60. Induction Forge Welding Equipment	160
61. Test Area - ETR Loop	162
62. Main Panel Board - ETR Loop	162

LIST OF TABLES

Table	Page
1. Status of Test Loops June 25, 1958	112
2. Summary of Tilting Capsule Test	119
3. Summary of Tilting Capsule Test	120
4. Tilting Capsule Test	126
5. Tilting Capsule Test	127
6. Tilting Capsule Test	128
7. Impact Strength, Ft-Lb at 885 F	134

REFERENCES

1. BAW-1019, LMFRE Reference Design Report (Aug. 1957)
2. BAW-1052, LMFRE-I Reference Design Report (June 1958)
3. Bethe, H. A., Tonks, L., Hurwitz, H., Neutron Penetration and Slowing Down at Intermediate Distance Through Medium and Heavy Nuclei, Physical Review, Vol 80, p 11 (Oct. 1950)
4. Paynter, H. M., Takahashi, Y., Report Prepared for ASME Meeting (June 1955)
5. BAW-1104, LMFR Research and Development Program (June 1958)
6. BAW-1107, LMFRE Quarterly Technical Report (Jan. - March 1958)
7. A. D. Little, Inc., Report on Continuous Uranium Monitoring of an LMFR (Jan. 1958)
8. Gilhart, J. S., "Graphite-to-Metal Seal Screening Tests," Report No. 7043, BAW-1053,(Sept. 23, 1957)

SUMMARY

Preparation of spectrographic standards for chemical analyses included several new procedures for the purification of bismuth to decrease iron, chromium, etc. Analytical work for various LMFRE tests included 1,642 separate determinations on 307 samples. Mercury and mercury vapor procedures were used in the cleaning of specimens, components, and a bismuth test loop. Alliance's work on uranium solubility was completed and a report is being written.

The test apparatus for sodium-bismuth leak testing has been completed and the size of the controlled leak was calibrated using water.

Results of corrosion work in the dynamic test loops have shown the value of the zirconium additive in reducing corrosion. Improvements to the loops have reduced cold locations which could collect uranium and reduce loop concentrations. Corrosion of hot zones and metal transport of the loop material to cold areas have been noted, particularly on the loops with low zirconium concentration.

Capsule testing has shown metal transport and corrosion at the higher temperatures under which this screening test has been operating. In addition to Croloy 2-1/4 and 1-1/4 the capsules have now included beryllium, tantalum, and other alloys, preparatory to use in test loops.

The initial stress-rupture and creep information on Croloy 2-1/4 and 1-1/4 in liquid bismuth fuel solutions compares well with that in an air atmosphere. Impact data at operating temperature show an improvement after aging.

The outgassing of graphite has begun and other graphite projects have been discussed. Graphite seals and weepage tests await receipt of specimens. Preparation of graphite pellets with impregnant materials included, indicates that subsequent oxidation to form the metal oxides will be difficult. The formation of carbides appears promising and is now under investigation.

Design of apparatus and test procedures for checking instrumentations for temperature, pressure, liquid level, and flow is complete. Most of the apparatus is complete and tests will begin as prototype instruments are received.

Work on the prototypes of various components is very active. Beryllium is on hand and dry box equipment and other health safety requirements are being prepared for development of the "thimble". The 2 1/2-in. test loop for the testing of valves and other components is almost complete.

Initial induction heating tests have indicated excessive gradients, and revisions are now being tested. Test apparatus for cavitation and for new projects on the testing of valves, filters, and bellows are complete in most cases and await receipt of specimens for the initial proof tests. A sparging device tested with water and mercury is being placed in the first in-pile test loop.

Assembly of the in-pile loop for the ETR reactor is almost complete. The in-pile section for the critical facility test as Arco has been shipped. Design of loop No. 3 (MTR) is almost complete and construction of components is underway.

The investigation of welding procedures for remote operation has produced successful welds on 2 1/2-in. OD x .250-in. wall and 6 5/8-in. OD x .313-in. wall steels. Additional work is underway on other sizes and with tubing on which a bismuth film remains from operation. The consumable arc, gas-shielded welding process has been discontinued.

The Engineering Prototype Development Facility has been leased and renovated for the developmental testing of LMFRE-I maintenance equipment and operational mechanisms. The facility has approximately 5700 sq ft of floor space of which nearly 4500 sq ft will be used for AEC purposes. The remaining 1200 sq ft will be used by B&W as a light duty machine and weld shop.

The first draft of a maintenance reference design report has been prepared and released. This report elaborates upon functions of maintenance equipment, more fully explains techniques and procedures to be utilized in typical plant maintenance operations, and presents information on associated research and development programs.

Magnesium, selenium, and zirconium have been tried as dispersing agents of slurries. It was found that magnesium reduces thoria to thorium metal. The stability of the slurry and the effect of agglomerates are being studied. The bismuth in the slurry test loop has been dumped into the sump and is being kept molten with the intent of starting circulation upon determination of detailed slurry specifications.

Croloy 1-1/4 was selected as the reactor secondary containment material because it meets design temperature requirements (1050 F), and all welds made in the field can be stress relieved during original system heatup.

PART ONE
DESIGN STUDIES AND RELATED WORK

I. PHYSICS AND MATHEMATICS

Physics work has centered around the establishment of a new reference design for the LMFRE-I and the design and construction of the critical experiment facility.

A. LMFRE-I DESIGN

1. Core Size

The core size and reflector thickness have been computed on the basis of the revised reactor parameters previously reported.

V _{Bi} / V _c in core:	0.5
Average Temperature:	817.5 F
Core Geometry:	Cylinder H = D, 3 in. U-Bi plenum at top and bottom of core
Overall diameter of core + reflector	7 ft 10 in.
End reflector thickness	2 ft

The criticality calculations were made for several N₂₅/N_{Bi} ratios and for the case of bismuth penetration into all graphite at the rate of 0.3 g/cc. Four-group diffusion theory was used in all criticality calculations. A four-group, multiregion code utilizing coefficients prepared by a 38-group spectral calculation was employed throughout the study. The results are listed below.

N ₂₅ /N _{Bi} (ppm)	Core (cm)	Diameter (inches)	Reflector Thickness (cm)	Reflector Thickness (inches)	Bismuth Penetration (g/cc)
525	127	50	55.9	22	none
*712	105	41.4	69.4	27.3	none
990	91	35.8	74	29.1	none
623	105	41.4	69.4	27.3	0.3

*Reference Design

2. Isotope Buildup

The buildup of uranium isotopes during operation of the experiment is important because of the limitation of uranium solubility in bismuth. The sources of additional uranium requirements are given below.

a. Higher uranium isotopes

- (1) U-236 and U-237 buildup
- (2) U-238 - initial inventory
- (3) U-238 added with U-235 to compensate fuel burnup
- (4) U-238 added with U-235 to overcome poison buildup

b. Additional U-235

- (1) Override equilibrium Xe-135
- (2) Override equilibrium Sm-149
- (3) Override other fission product poisons

Since the LMFRE-I will be designed for a total heat output of 8 1/3 MW, the total uranium content of the U-Bi fuel was calculated after one year of full power operation at 8.33 MW. The results are summarized below for the present reference design (initial $N_{25}/N_{Bi} = 712$ ppm).

URANIUM CONTENT OF U-BI FUEL AFTER ONE YEAR AT 8.33 MW

Isotope	N_U/N_{Bi} (Atom Ratio)	M_U/M_{Bi} (wt. Ratio)
	ppm	ppm
U-235, initial concentration	712	800
U-235, Equilibrium Xe override	57*	64
U-235, Equilibrium Sm override	16	18
U-235, other fission products	20	23
U-236 and U-237	20	23
U-238, initial concentration assuming 93.5% enriched fuel	49	56
U-238 added with U-235 for burnup	8	9
U-238 added with U-235 to override poisons	6	7
Total	888	1000

* This is an upper limit based on the assumption that all xenon remains in the core.

3. Control Rods

Control requirements are as follows.	<u>$\Delta k / k$, percent</u>
Temperature coefficient	3.5
Xe-135 and Sm-149	2.0
Shutdown	3.0
Periodic fuel addition	0.5
Gain in delayed neutrons	0.3
Total	<u>9.3</u>

Calculations indicate that a ring of four rods located on a radius of 22 cm is sufficient for control.

4. Thermal Flux With an Artificial Source

Thermal flux profiles have been generated for startup conditions in the LMFRE-I core. A four-group code, which solves four-group diffusion equations with an artificial neutron source, was used to predict the thermal flux outside the reflector for both Po-Be and Sb-Be sources located at the core center. Results indicate that the spectrum of the source exerts little influence on the value of the thermal flux without fuel or other highly absorbing material in the core.

<u>Reactor (Design)</u>	<u>Source</u>	<u>Source Strength (neuts/sec)</u>	<u>Method of Calculation</u>	ϕ_{th} (outer reflector surface) <u>(neuts/cm²-sec)</u>	ϕ_{th} (detector)
Phase I ¹	Po-Be	10 ⁸	2-group (hand)	502	
Phase I	Po-Be	10 ⁸	4-group (code)	463	
Phase I	Sb-Be	10 ⁸	4-group (code)	434	
Phase I	Fission	10 ⁸	4-group (code)	463	
Reference ²	Sb-Be	10 ⁸	4-group (code)	1570	21.2

In an effort to compare diffusion theory with other methods for large distances away from the source, calculation of slowing down density as a function of distance from a plane source was made by the method of Bethe, Tonks, and Hurwitz³. The slowing down density was converted to neutron flux, comparative results being shown in Figure 1.

B. CRITICAL EXPERIMENT

1. Status

Effort has been exerted toward finalizing the mechanical design of the facility, the procurement of materials, and the preparation of a hazards analysis. The design work is complete, and all major components have been received and installed. All core and reflector materials have been received except the U-Al fuel strips which are being fabricated by the vendor.

Assembly of core and reflector materials has begun, for the purpose of checking out the mechanical equipment and the operational procedures. Licensing action has been initiated, and critical experiments are expected to begin in August.

2. Design

a. Backscattering Effects

Calculations indicate that backscattering of neutrons from the concrete walls of the bay and the steel superstructure could add as much as 1 percent in reactivity to an unprotected assembly.

The movable table on which the assemblies will be built is constructed of 2-in. steel. Backscatter from the table provides a potential increase in reactivity of 0.2 percent. These effects are insignificant, however, when a high cross section neutron absorber is placed between the graphite reflector and the scattering materials. The critical assemblies will be covered on all sides and both ends will be covered with a cadmium sheet.

b. Parametric Study of Criticality Effects

To develop the best procedures for operation of the critical experiment, the effects of various parameters on the criticality of the assembly were investigated. The parameters and their range of values are listed below.

Radius of core:	45.88 - 61.12 cm
Height of core:	76.52 - 137.48 cm
N_{25}/N_{Bi} :	650 - 900 ppm

Σ_a (poison) / Σ_a :	0-0.06
Void fraction in core:	0.01 - 0.03
Graphite density:	1.60 - 1.75 g/cm ³
$\bar{\sigma}_a$ (graphite):	0.0040 - 0.0050 barns

The results of this study are shown in Figures 2 through 8.

3. Power Excursions

a. Summary

The amount of energy released during power excursions in the LMFRE critical experiment have been calculated.

The excursions were assumed to be initiated by reactivity disturbances of the step and ramp types. Steps from 0 to 2 percent and ramps from 0 to 2 percent/sec were considered. The ramps were assumed to rise to 2 percent and remain at that value.

The total energy release as a function of step input is plotted in Figure 9. Figure 10 shows the energy release as a function of the slope of ramp inputs.

(1) Curves 1

The curves numbered 1 in Figures 9 and 10 represent the energy release when it is assumed that: all of the energy generated remains in the U-Al alloy, and that the transient is terminated by boiling of U-Al alloy.

(2) Curves 2

The curves numbered 2 in Figures 9 and 10 represent the energy release when it is assumed that: some of the energy generated is transferred to the graphite and bismuth, and that the transient is terminated by boiling of the U-Al alloy.

(3) Curves 3

The curves numbered 3 in Figures 9 and 10 represent the energy release when: some of the energy produced is transferred to the graphite and bismuth, and the transient is terminated by the temperature coefficient of reactivity when the graphite temperature becomes sufficiently large.

(4) Maximum Energy Release

The energy release for a given reactivity input is given by curves 2 and 4, whichever is lower.

The maximum energy release occurs for the input corresponding to the point of intersection of curves 2 and 4.

b. Energy Release Without Heat Transfer

(1) Calculation Methods

The calculations using the simple model in which all energy remains in the fuel have been done in two ways: a Datatron program, "LMFRE Critical Experiment Kinetics", and an IBM-704 program, "Thermonetics," borrowed from Pratt & Whitney.

The principal difference in the programs is that the latter handles the calculation in a more refined manner during the boiling phase. The results compare favorably.

(2) Results

Results indicate that most of the energy release, without heat transfer, is used to boil the fuel; hence, the total energy release is relatively independent of the magnitude of the reactivity input.

c. Effects of Heat Transfer

The temperature of any component (graphite, fuel, or bismuth) can be written

$$T = \int_0^t K(t - \tau) P(\tau) d\tau.$$

The functions $K(t - \tau)$ were calculated by the SHED Program.

A unit temperature was inserted in the fuel and the resulting mean fuel, graphite and bismuth temperatures were calculated as functions of time.

The power levels in the step cases were approximated by analytic expressions of the form ae^{bt} .

The power levels in the ramp cases could not be approximated easily by simple formulae, and the actual values from the Datatron

calculations (section a) were used. Therefore, data were available only up to the time of boiling (with no heat transfer) and figures for later times were obtained by extrapolation.

The integration was done numerically.

(2) The energy releases, assuming transient termination by boiling, and assuming termination by temperature coefficient, were calculated for both step and ramp cases. The results are shown in Figures 9 and 10.

(3) The heat transfer calculation assumed a model consisting of regions of graphite, air, graphite, fuel tape, bismuth, air and graphite. The outer boundaries were insulated. This model is an approximation of the "one tape per bismuth block" geometry (600 ppm).

FIG. 1: THERMAL NEUTRON FLUX DISTRIBUTION
FROM PLANE SOURCE OF STRENGTH
1 NEUTRON/CM²-SEC

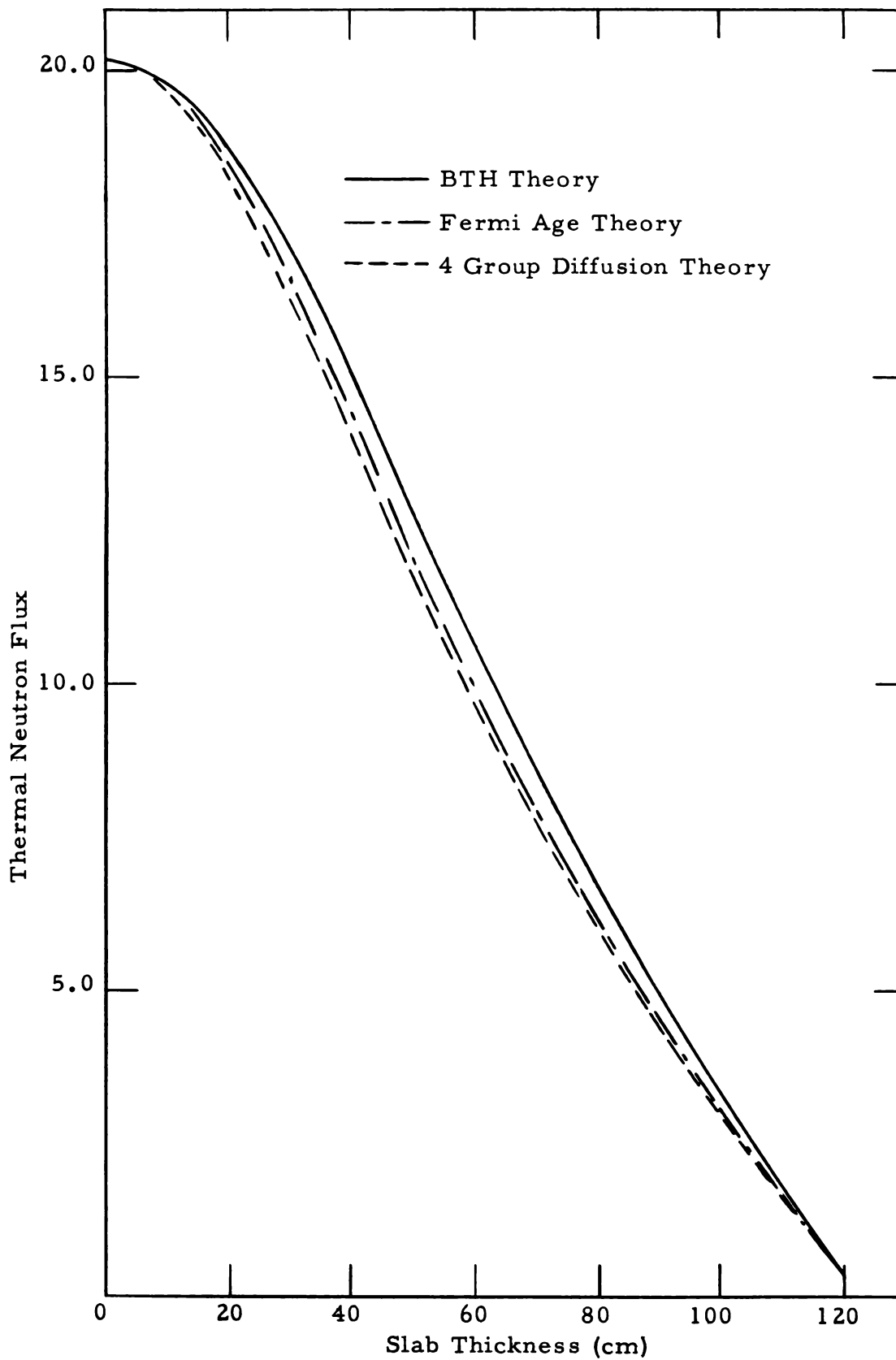


FIG. 2: k_{eff} VS. CORE RADIUS

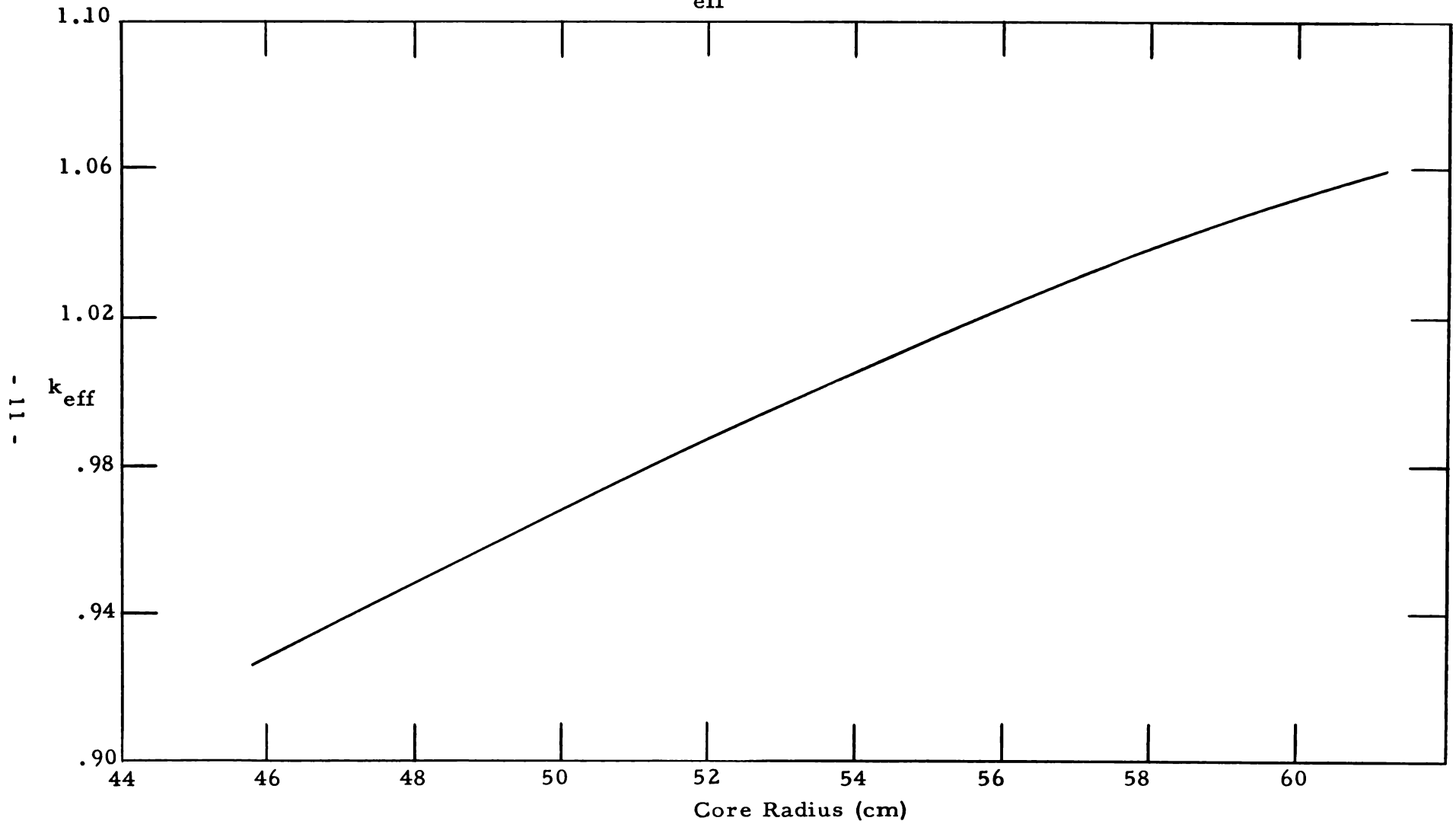


FIG. 3: k_{eff} VS. CORE HEIGHT

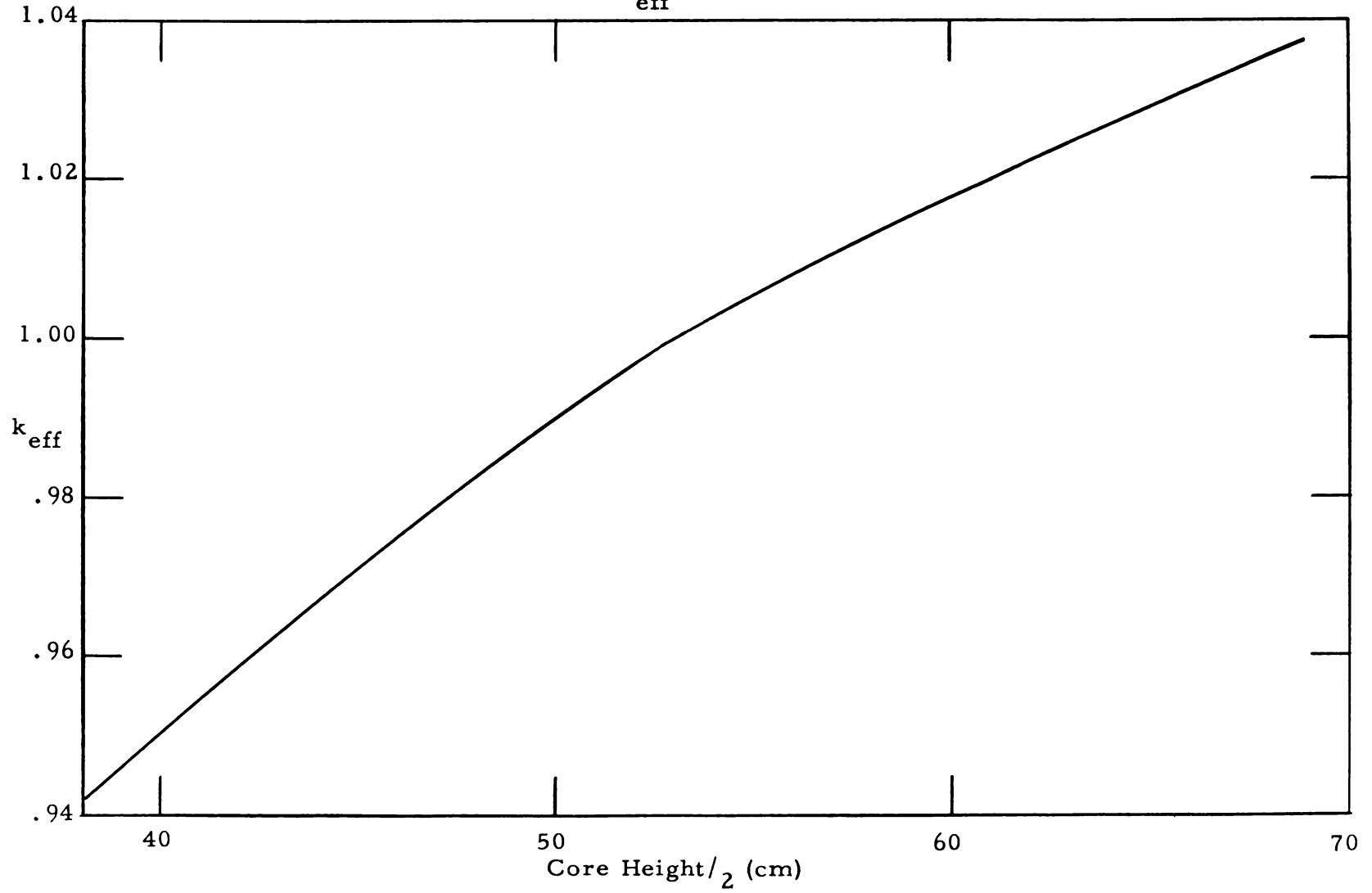


FIG. 4: k_{eff} VS. FUEL CONCENTRATIONS

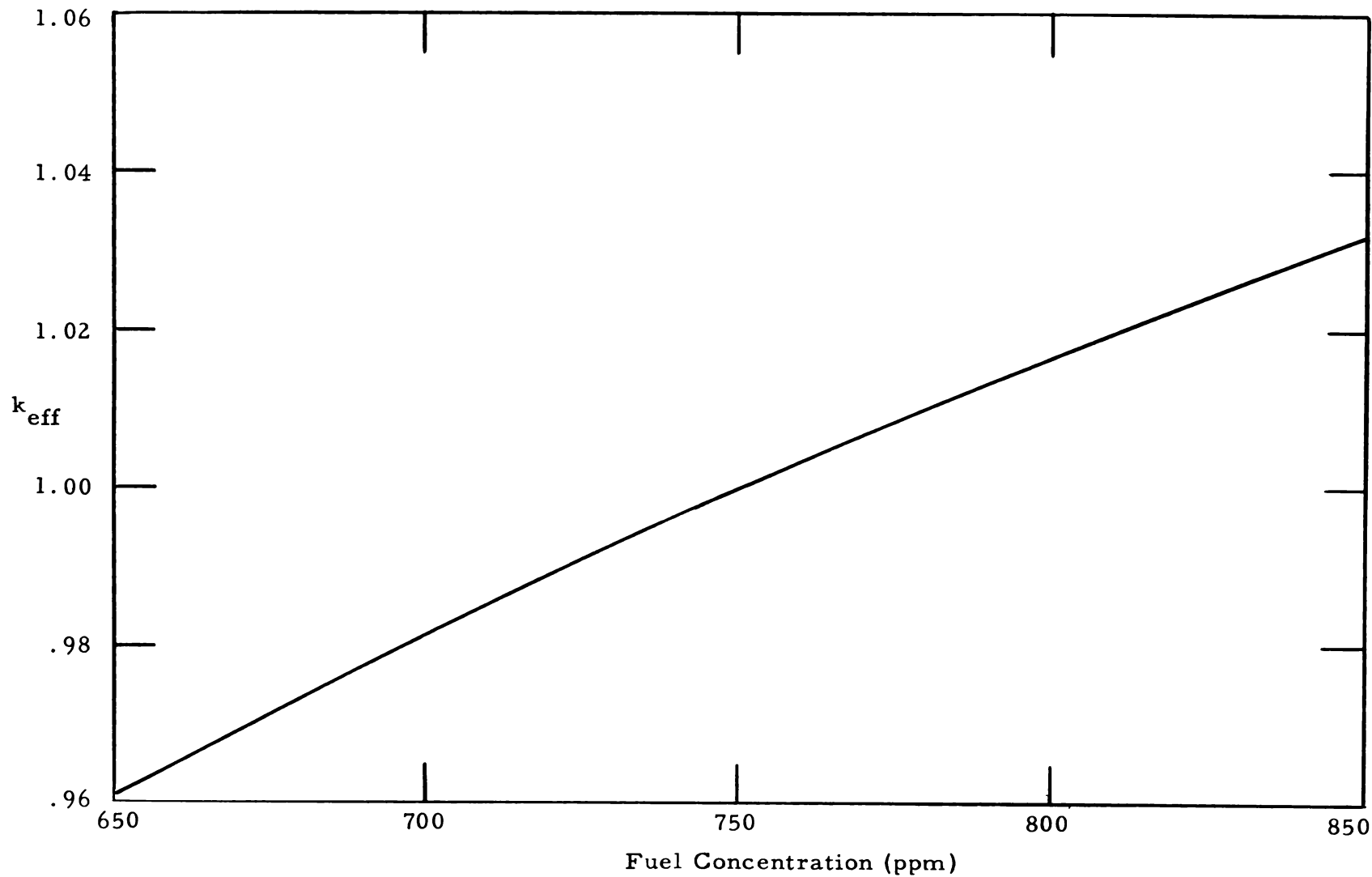


FIG. 5: k_{eff} VS. POISON FRACTION

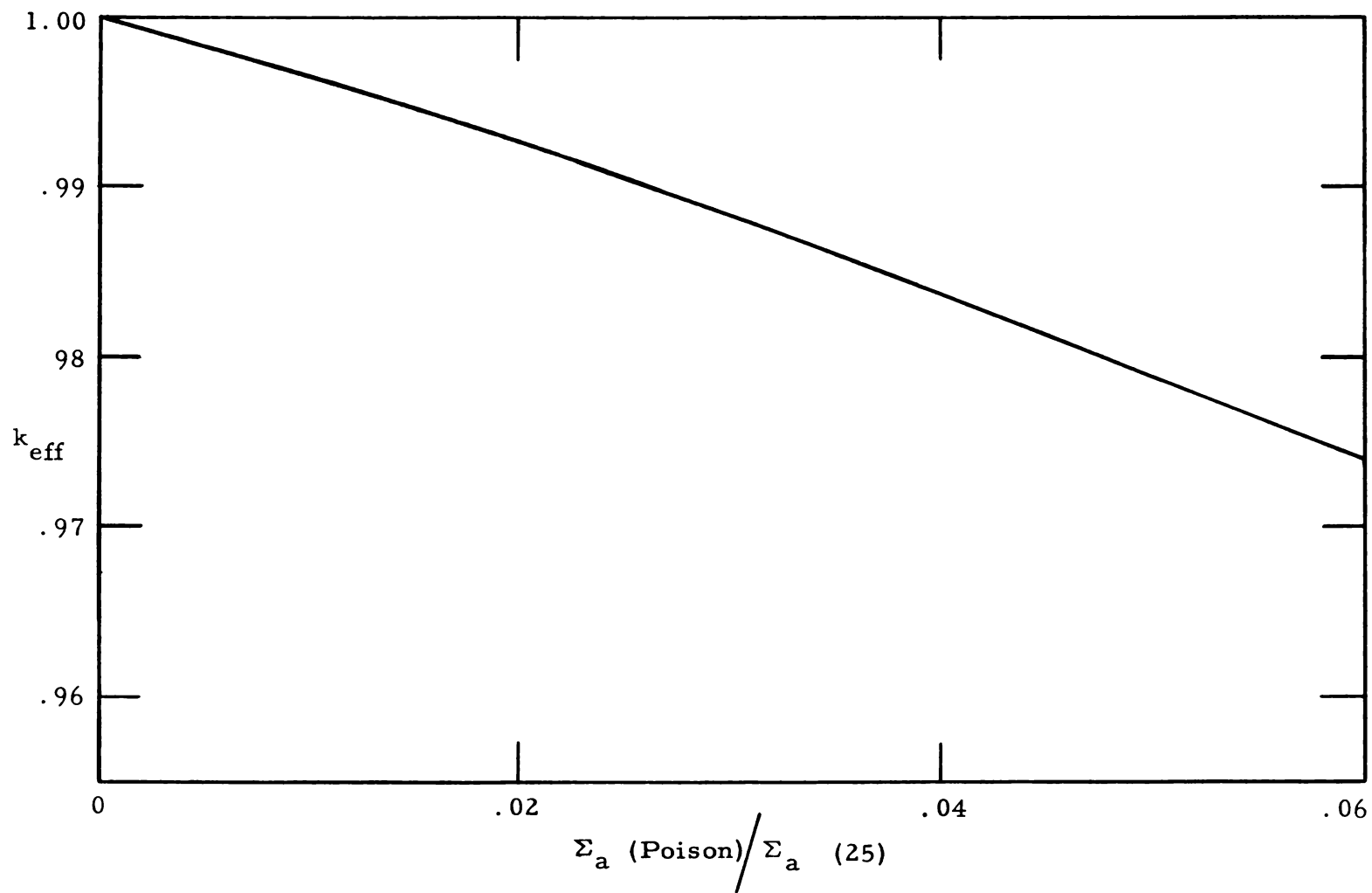


FIG. 6: k_{eff} VS. CORE VOIDS

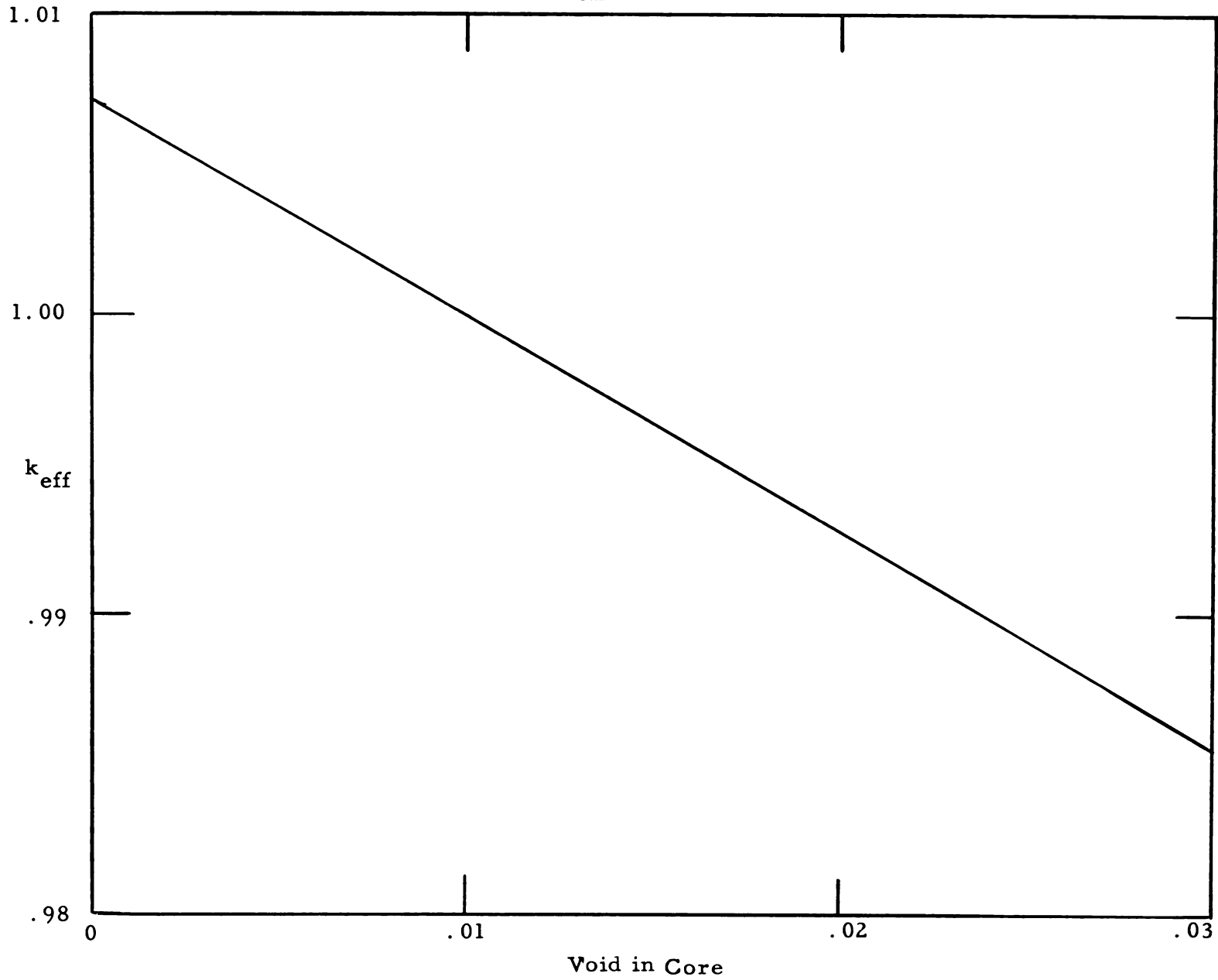


FIG. 7: k_{eff} VS. GRAPHITE DENSITY

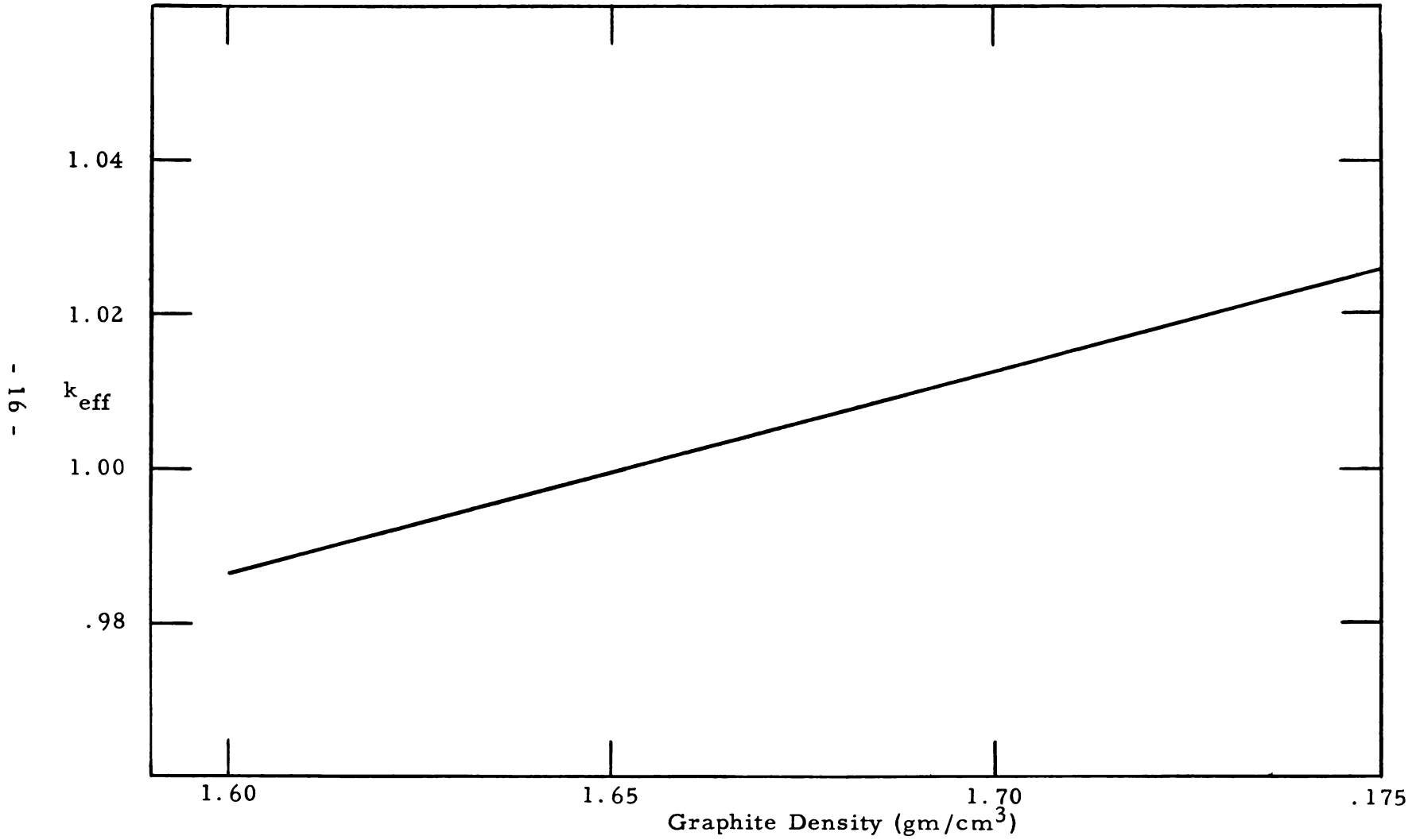


FIG. 8: k_{eff} VS. σ_a (CARBON)

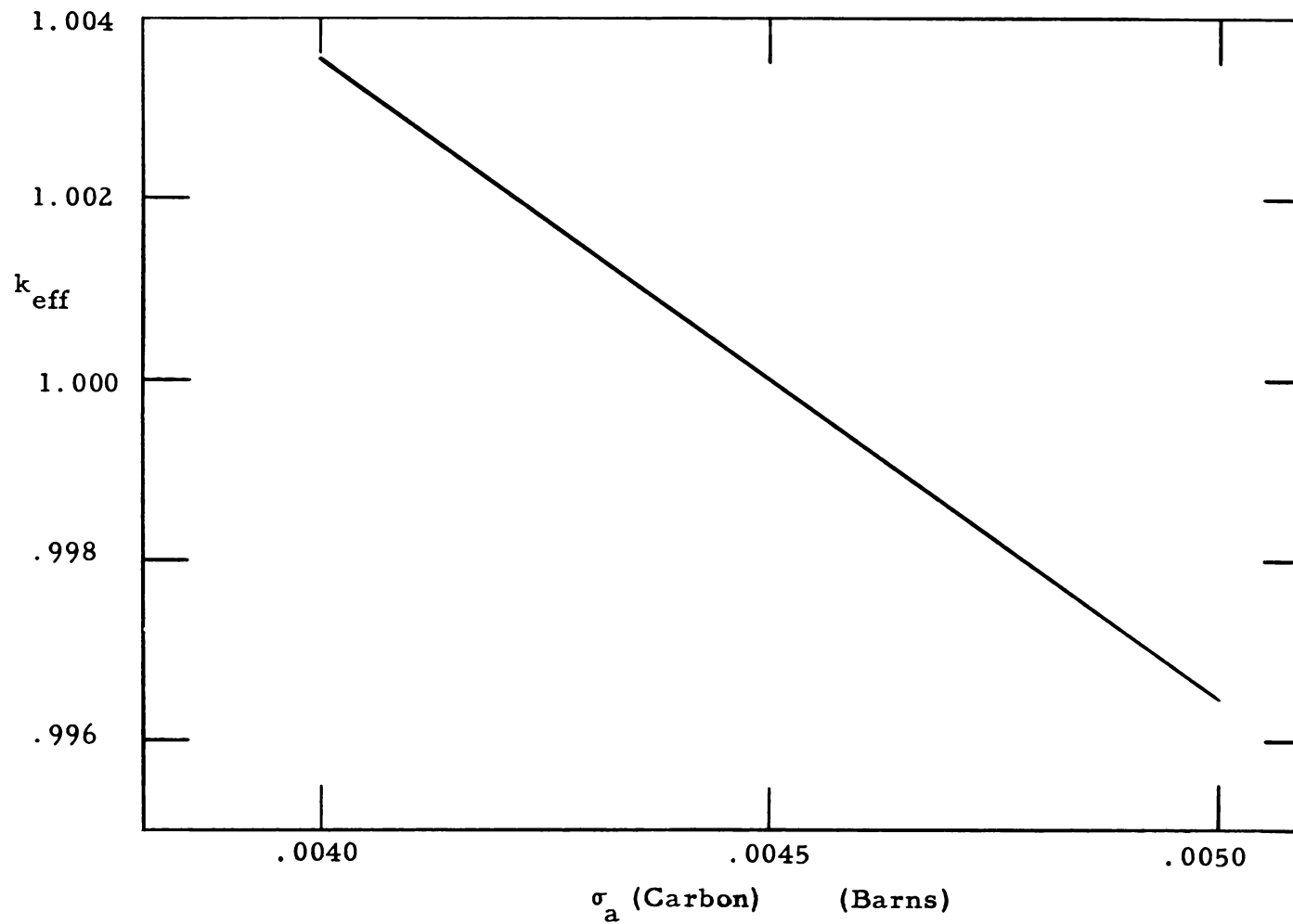


FIG. 9: ENERGY RELEASE VS. STEP INPUT

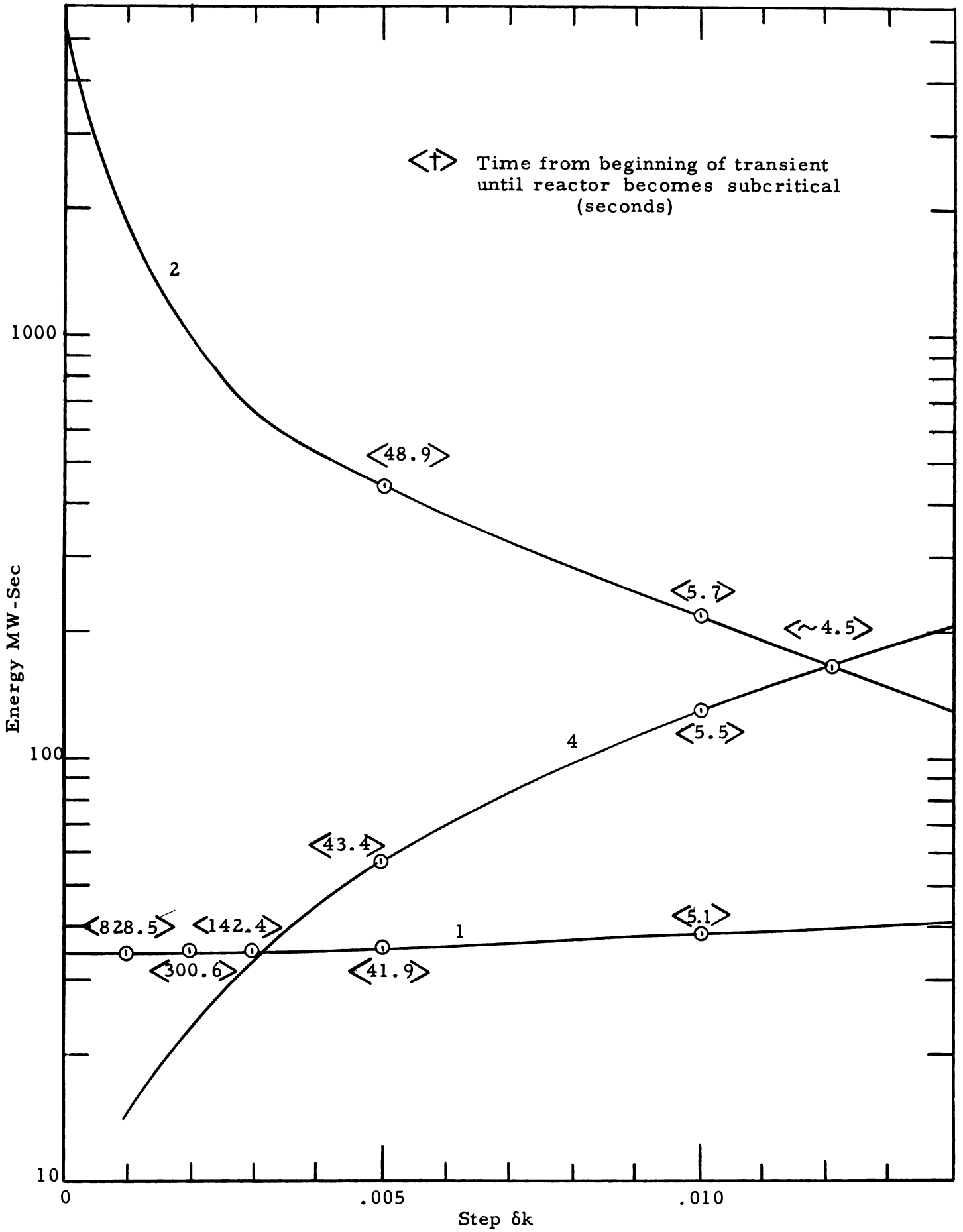
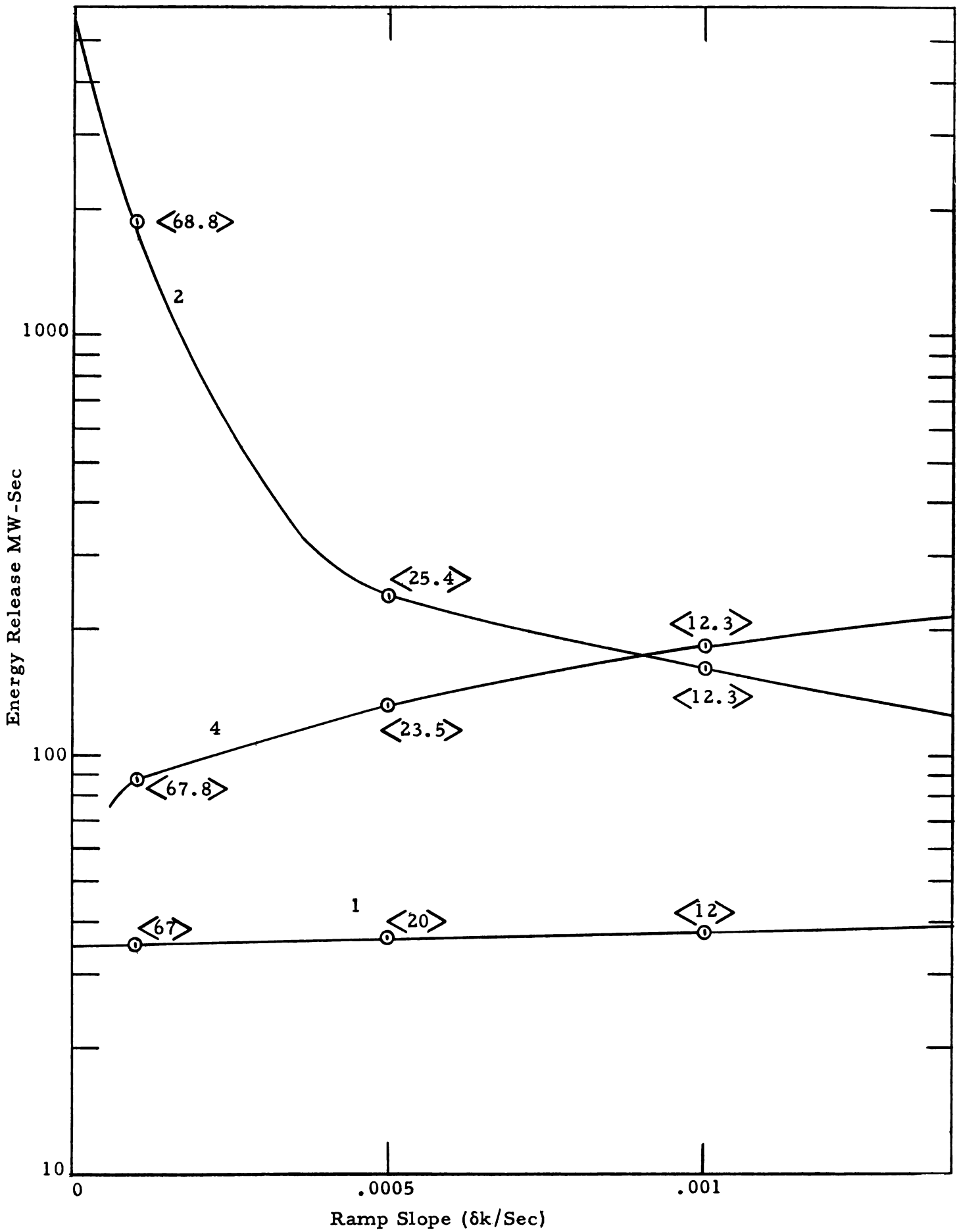


FIG.10: ENERGY RELEASE VS. SLOPE OF RAMP INPUT



II. REACTOR ENGINEERING

A. LMFRE-I CONCEPTUAL DESIGN

Basic arrangement drawings for the Reference Reactor Design were completed. These drawings, as described in BAW-1052,² are identical except for the control rods and control rod drive system. The reference design features liquid-metal-column control rods; the alternate design uses conventional mechanical control rods and drives.

The design requirements for reactor (non-nuclear) instrumentation, sampling mechanisms, and gas connections to the reactor (for outgassing and degassing operations) were reviewed, and tentative designs established. Figure 11 illustrates these conceptual designs.

A method of sealing the tantalum sheathed thermocouples to the reactor vessel (notation 17, Fig. 11) with tantalum compression fittings is being investigated. The outer annulus baffle (10) will accommodate thermal differential expansion between the reactor primary vessel and the graphite internals, and provide proper flow distribution (2 percent total flow) through approximately 121 quarter-in. diameter holes.

The effect of possible flow unbalances on temperature distribution in the reactor was investigated. The major areas of expected flow unbalances are in the outer annulus and at the core entrance. Measuring flow distribution on a scale model of the LMFRE at the Research Center should be initiated during the next quarter.

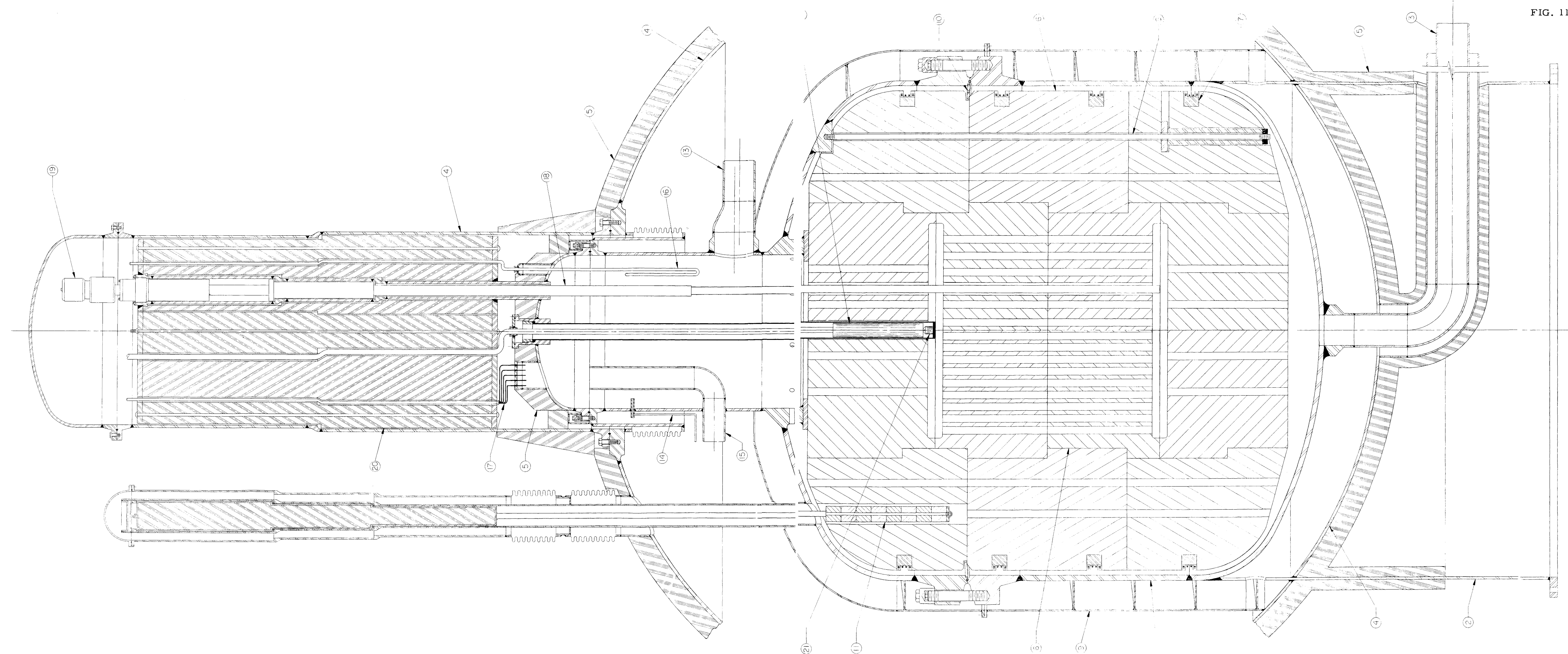
B. THERMAL ANALYSIS

1. Reflector Cooling

A study of cooling requirements for the LMFRE-I side reflector was completed. The maximum temperature and thermal stress in the graphite, based on parameters that would yield the highest values, were

FIG. 11: LMFRE REACTOR ARRANGEMENT

VERTICAL SECTION



LEGEND

- (1) - REACTOR VESSEL
- (2) - SUPPORT SKIRT
- (3) - FLUID INLET CONNECTION
- (4) - CONTAINMENT VESSEL
- (5) - THERMAL INSULATION
- (6) - GRAPHITE CORE & REFLECTOR ASSEMBLY
- (7) - CIRCUMFERENTIAL CLAMPS - 4 REQ'D.
- (8) - VERTICAL HANGER RODS - 8 REQ'D.
- (9) - HEATING GAS SHROUD
- (10) - ANNULUS BAFFLE
- (11) - GRAPHITE SAMPLES
- (12) - NEUTRON DETECTOR - 1 REQ'D.
- (13) - FLUID OUTLET CONNECTION
- (14) - DEGASSING CONNECTION
- (15) - EVACUATION CONNECTION
- (16) - LIQUID LEVEL INDICATOR - 1 REQ'D.
- (17) - THERMOCOUPLE LEADS
- (18) - LIQUID COLUMN CONTROL UNITS - 4 REQ'D.
- (19) - CONTROL UNIT DRIVES - 4 REQ'D.
- (20) - CONTROL DRIVE SHIELDING

calculated to be 1355 F and 880 psi. These values were based on a power level of 8 1/3 MW, graphite thermal conductivity of 8 Btu/hr-ft² -°F/ft fuel pickup of 0.3 g of Bi/cc³ - graphite, and two rows of 32 one-in. holes places 28 and 36 in. from the core center. The coolant flow rate necessary to provide approximately the same ΔT through the reflector cooling holes and outside annulus as through the core proper was calculated to be 5.12 x 10⁵ lb/hr and 6.96 x 10⁴ lb/hr, or 15 and 2 percent full flow respectively.

Orificing of the flow in the outer annulus is necessary to provide the proper flow distribution in the annulus and reflector cooling holes. Approximately 121 quarter-in. diameter holes were found to provide the necessary flow restriction in the annulus for proper coolant temperature rise and pressure drop.

2. Decay Heat in Reactor

The temperature rise of the primary system fuel stream after a reactor shutdown was calculated. The heat source calculation assumed that all fission product gamma and beta energy was absorbed in the fuel solution and that no cooling of the fluid was available. The total primary steam temperature approached the boiling point of bismuth (approximately 2700 F) after 24 hr, assuming the reactor had operated at full power (8 1/3 MW) for at least 800 hr.

3. Radiation Heat Generation in Primary Vessel Flange

The temperature rise caused by the absorption of radiation energy in the full-opening vessel flange was calculated. Gamma sources considered in the calculations were (1) core, (2) reflector, (3) outlet pipe, (4) reflector annulus, (5) reactor outlet surge volume and (6) gammas resulting from n,γ reactions in the metal. The maximum temperature calculated in the flange was found insignificant (13 F above the fuel temperature in the outer annulus). These values are based on continuous reactor operation at 8 1/3 MW, and a fuel absorption in the graphite of .3 g fuel/cc of graphite.

C. INSTRUMENTATION AND CONTROL

1. System Analysis

The system analysis (analog) program subcontract was prepared in final form and negotiated with the vendor. This contract will cover a 9-month period and involves the simulation and analysis of the primary system.

The theoretical transfer functions of the intermediate heat exchanger (IHX) have been developed in conjunction with systems and components engineering. These functions have a form similar to the expressions developed by Paynter and Takahashi⁴. Four such expressions were obtained for the IHX at constant flow conditions.

One of the four possible transfer functions for variable flow $\left(\frac{\text{change in outlet temperature of primary fluid}}{\text{change in primary system flow}} \right)$ has been obtained and will be used to complete the analysis of the IHX.

A comprehensive analysis was made of the speed-torque characteristics for an all-electrical speed control system for a liquid metal pump. This system consists of a prime mover (induction motor), a magnetic coupling, a.c. generator and drive motor. The final expressions derived relate the machine torques to the frequency of the a.c. generator, the control (driving) signal to the magnetic coupling, the pump torque demand, and the physical constants of the electrical machinery.

A digital study will be conducted to determine the response of the system to various driving inputs and will aid in the flow control analysis of the primary and intermediate systems.

2. ETR Test Loop Monitoring

A radiation monitoring system capable of detecting gross activity of $10^{-6} \mu\text{ c/cc}$ and particulate activity as low as $10^{-12} \mu\text{ c/cc}$ has been designed for the ETR test loop No. 2. This system will monitor for any leakage from the loop and monitor the air for activity when the loop is disassembled. The particulate activity monitor is composed of two channels, one to detect for α 's (to be used for Po-210 monitoring) the other for β - γ activity. The gross activity monitor will be used to detect gaseous fission products that may be present in the sampled air.

D. NUCLEAR ANALYSIS

1. Argon Activity in Stack Gas

The dose rate for various weather conditions was calculated for A-41 emitted from a stack 20 to 80 meters high. The A-41 is formed by activation of argon in the reactor cell air between the secondary containment and the biological shielding. The maximum ground dose level expected for the recommended stack height of 150 ft and a reactor cell-to-stack air flow of 600 cfm is approximately 8.4×10^{-3} rep/week, a factor of 36 lower than the acceptable gamma dose rate of .3 rep/week.

2. Liquid Metal Control Rod Rupture

The effect of a liquid column control rod rupture, with subsequent release of the liquid metal rod alloy to the fuel solution, was investigated.

A 40 percent cadmium - 60 percent bismuth eutectic and a control rod material volume of 250 cc transmitted to the primary system would render the reactor inoperable; i. e. , sufficient uranium with the design solubility limit could not be added to the system to maintain criticality. The control rod system must be designed so that the probability of a rod rupture is insignificant. Possible column designs will be investigated further to determine the best solution to the problem.

3. Cell (Air) Cooling Water Activity

The induced activity in the cell (air) cooling water was calculated, based on water containing relatively large amounts of dissolved salts and activated by both thermal and fast flux. The maximum activity, based on a power level of 8 1/3 MW at a distance of 4 in. from the cooling water exit, is less than tolerance levels (7.5 mr/hr).

4. Uranium Solubility

The effect of uranium solubility decrease in the presence of zirconium on the core and reflector size and on power density is being investigated. Reactor parameters must be reevaluated before the problem can be solved. Three possible solutions appear possible: higher reactor inlet temperature, reevaluation of the safety factors for temperature and critical experiment, and increase in core size.

III. SYSTEMS ENGINEERING

A. SYSTEMS DESIGN

1. General

Alternate system designs were investigated, and existing designs were refined.

System designs were prepared and included in the LMFRE-I Reference Design Report.²

2. Work Related to the Semi-Contact Scheme of Component Replacement

a. Heat Exchanger

The vertical, straight tube, floating head heat exchanger design was further developed by Barberton personnel.

Changes included improvement of (1) provisions to allow for differential expansion between downcomer and tubes, and (2) the seals at the top of the unit. These improvements are incorporated in the latest design, shown in Figure 12.

b. Pump

The pump design was similarly developed, using as a model the design prepared for the Brookhaven 4-in. utility test loop. The manufacturer has asserted that this design can be modified to suit LMFRE-I conditions. The resulting design is shown in Figure 13.

Specifications were sent to several manufacturers after being assured of the feasibility of a pump using the semi-contact maintenance approach. The pump finally used for the LMFRE-I may not be identical to the design of Figure 13, but will have many similar features:

- (1) Designed for disassembly from the top and contains internal shielding.

FIG. 12: LMFRE-I HEAT EXCHANGER

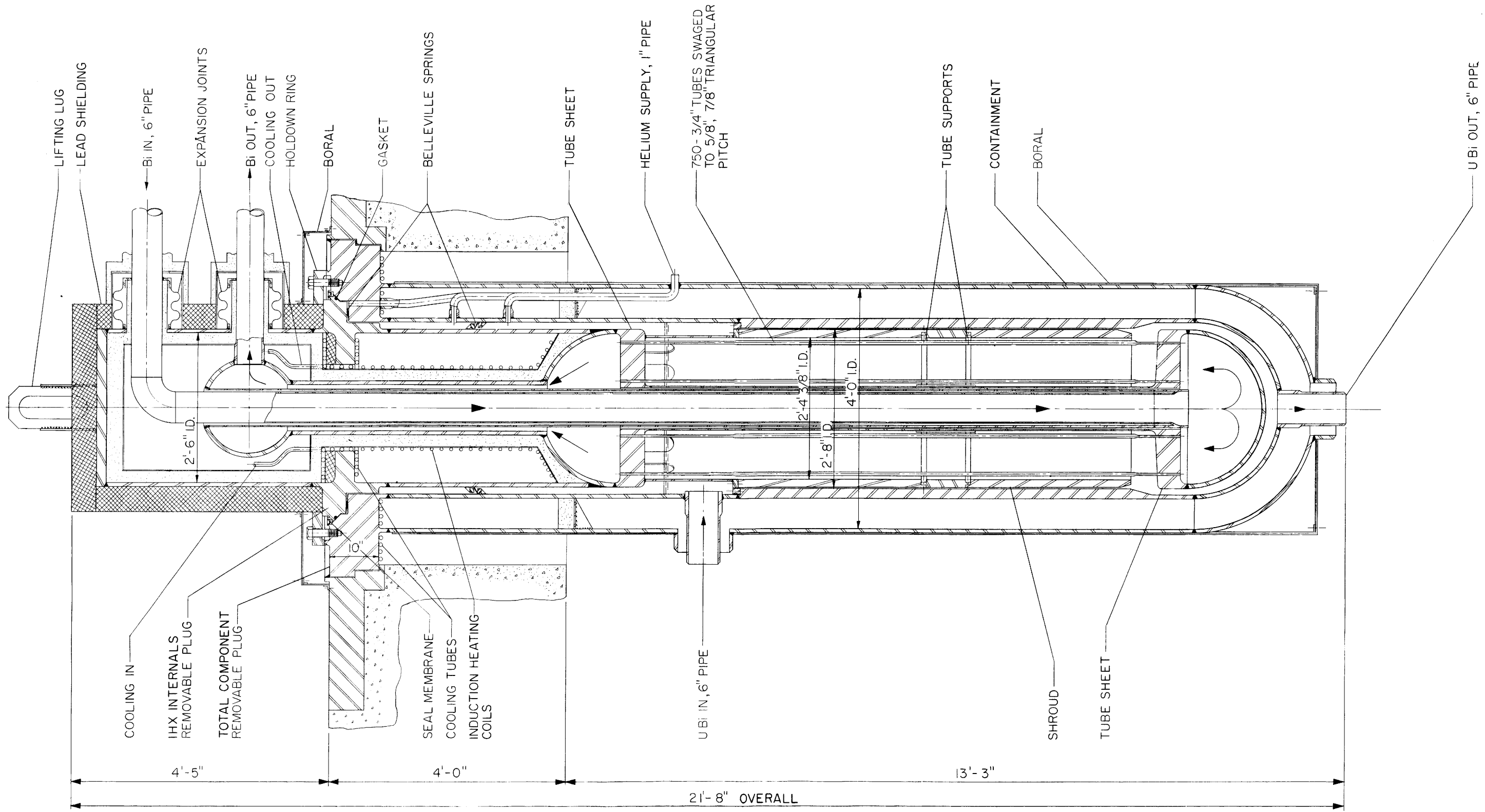
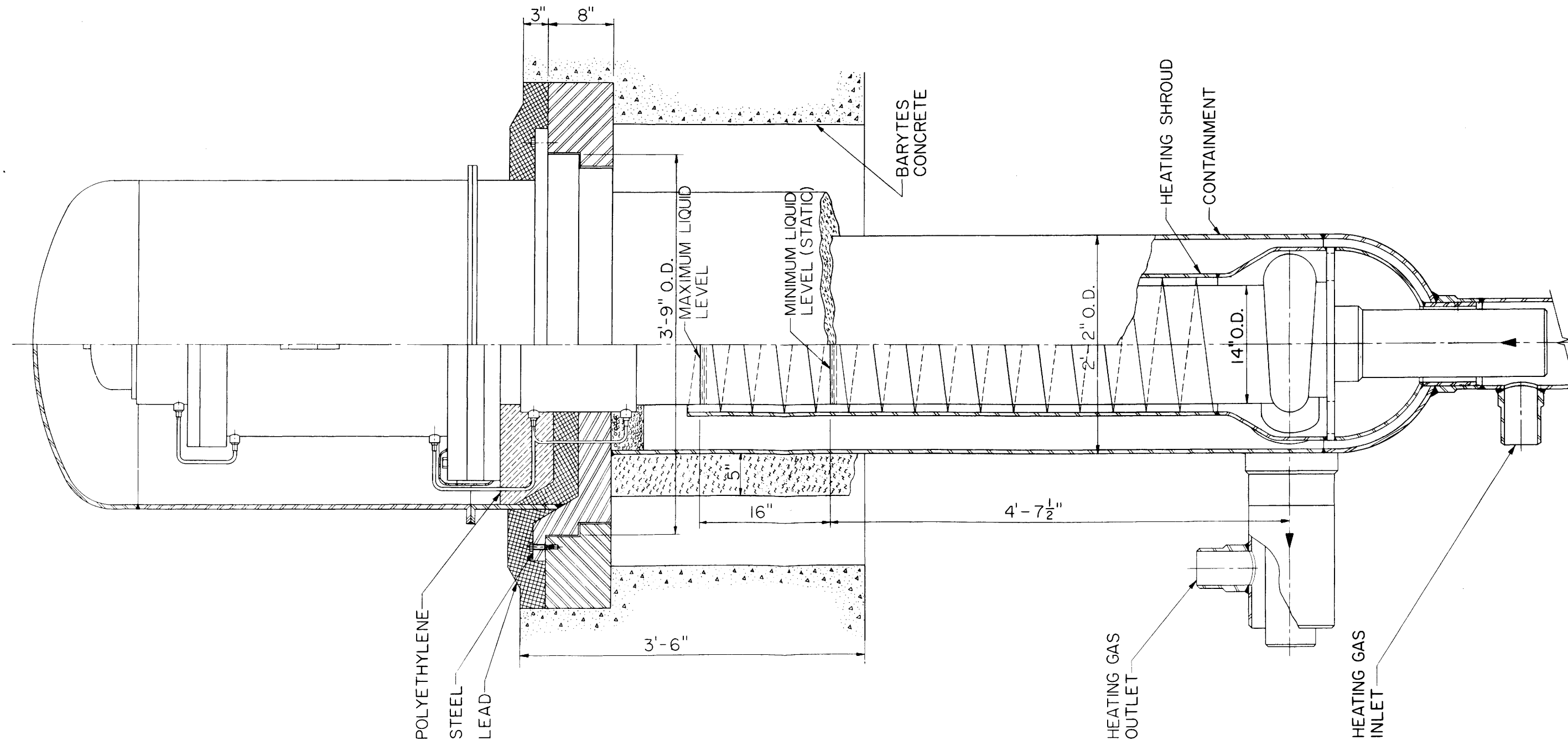


FIG. 13: LMFRE-I PUMP



- (2) Designed so that bismuth seeks its own level inside the pump.
- (3) The liquid level for the primary system will be established by a free surface in the reactor.
- (4) The liquid and gas spaces of the reactor and suction side of the pump will be interconnected, fixing liquid level in the pump.

The later approach, used instead of a liquid level control, will prevent flooding of the pump motor with radioactive fuel.

Beginning this year, reference pump design will be developed in the 4-in. utility test loop at Brookhaven, and experience may indicate necessary changes in the LMFRE-I unit. A prototype LMFRE-I pump will be tested at Alliance next year.

3. Containment

Design of containment for the primary system proved to be closely associated with design of the startup heating and decay heat removal system. It is also allied with an evaluation of the maximum credible accident. From the point of view of containment, the latter was tentatively concluded to be rupture of the primary system, releasing about 20 cu ft of bismuth, at its boiling point, into the reactor containment. This spill heats the gas in the containment, raising its pressure to about 50 psia.

Containments other than the reactor containment are designed to cope with bismuth spills at normal operating temperature.

It was found that containment of spills, and heating and cooling, was best provided by constructing close fitting jackets around each component as shown in Figure 12 and 13. Helium is circulated through the jackets for heating and cooling. At dead ends, the other areas where gas flow patterns may be poor, backup induction heaters will be used.

Induction heaters will be used throughout the intermediate system, where there are no containment requirements. Confidence in this method has been increased by Alliance's recent success in heating a pipe in this manner.

The size of the dump tanks was increased to allow room for an excess of bismuth.

B. COMPONENT DEVELOPMENT

Dump Valves

Dump valves for the LMFRE-I are designed for semi-contact maintenance and have horizontal stems. This design was selected because the valves were some 20 ft below the canyon floor. By projecting them through the side wall of the primary system area, a compact valve design could be obtained. Procurement of such a valve is planned.

Subsequent investigation revealed that a dump valve with a vertical stem presents some advantages although it is large. The number of maintenance mechanisms would be reduced and plant layout would be simplified since dump lines would not have to be lead to the edge of the primary system area. Therefore, proposals on vertical stem, semi-contact valves were requested from a number of valve manufacturers. A series of conferences will be held to acquaint valve manufacturers with the problems.

IV. MECHANISMS ENGINEERING

A. LMFRE-I MAINTENANCE SCHEME

The proposed LMFRE-I plant arrangement and maintenance scheme has been developed for release. The scheme was formulated from two basic concepts:

1. The use of component internals that are bayonet-mounted within through-shield mounted component shells. Component heads protrude above the shield, which is the canyon floor. The head is seal welded to the shell so that by contact cutting the seal weld and removing a bolted holddown ring, the head attached internals are free to be remotely extracted for transfer to the "hot" storage pool by the canyon bridge crane.

2. The use of mobile truck mounted manipulators and television viewing equipment. The truck and equipment will be battery powered and radio controlled. This equipment is provided predesigned access to areas beneath the canyon floor, where it will be used to cut and weld pipe; assist in component shell removal by the canyon crane (after the component internals are removed and the component pipes are cut); assist in the remote replacement of reactor, dump tanks, and other auxiliary components; and to cleanup spills, etc. Other trucks will be used as tow trucks and maintenance equipment carriages in remote maintenance and handling operations. These trucks may be used in any part of the plant to which they have been given predesigned access.

B. MACHINE DESIGNS FOR CRITICAL EXPERIMENT

Machine designs for the LMFRE Critical Experiment have been developed and checked out for the table drive, fuel element removal crane, and draw bridge hoist.

C. PROTOTYPE CONCEPTUAL DESIGNS

Prototype conceptual designs have been issued for mobile manipulator, liquid-metal-column control rod, fuel sampling mechanism, metallurgical sampling stations, fuel addition mechanism, seal welder and cutter, and component transfer container.

D. MANPOWER SCHEDULING CHARTS

Manpower scheduling charts and time estimates are being prepared for future mechanisms engineering efforts on the LMFRE-I project.

E. CANYON BRIDGE CRANE

Preliminary detailed specifications for the LMFRE-I canyon bridge crane have been prepared.

V. CHEMISTRY

A. FUEL PROCESSING

1. Uranium Removal from Primary Loop Solution

The problems involved in cold trapping as a means of uranium removal have been considered: some are formidable enough to preclude this method from use in LMFRE-I. A dilution system is much simpler and will be used, when required, to lower uranium concentration.

Cold Trap Design Problems

(1) General

A number of problems must be considered in the design of a suitable cold trap for the removal of uranium from the liquid in the primary loop. These problems can be divided into the categories of trap location, trap operation, heat removal, and trap design. The first three will be considered in detail. A basic consideration to all of these problems is whether the cold trapped material will be reused in the primary loop. Since zirconium and corrosion products and uranium probably will precipitate in the trap, there will be a reduction in the zirconium concentration in the primary loop. The cold trapped uranium (and zirconium) should be returned to the primary loop as needed after any cold trapping operation because

- (a) The amount of uranium consumed by the experiment will be held at a minimum
- (b) The problem of handling precipitated material will be avoided
- (c) Trap design should be simpler

- (d) The zirconium trapping can be tolerated by using an initial maximum permissible zirconium concentration consistent with mutual solubility effects
- (e) The cold trapped material is a volumetric heat source, making physical transfer out of the system difficult.

(2) Location

Two locations have been considered. It can be built directly as part of the primary loop or as an auxiliary system. Either could be used to adjust concentration without a complete dump of the primary system. The primary loop location poses some problems of flow and level control which could be met but which must be critically controlled during reactor operation. An auxiliary system is favored because it affords flexibility and safety although requiring extra fuel inventory for maximum usefulness.

The extra fuel inventory and tank capacity are required to permit batchwise cold trapping of some fuel during reactor operation. The dump tank capacity must be capable of holding the primary loop volume plus the extra fuel inventory in the auxiliary cold trap system.

(3) Operation

There are two distinct methods of operating a cold trap. One, described in Figure 14, continuously mixes the cold trap effluent with the main body of the inventory being processed. The cold trap feed composition changes with time. The other method (described in Fig. 15) withdraws a fluid of constant composition, processes it through the cold trap, and accumulates the effluent. Intermittently this material may be mixed with the main inventory to achieve a lowering of uranium concentration. In practice this may not be applicable directly to the operating reactor since it involves an unsteady level in the primary inventory. Figure 16, the recommended design, is a variation of the previous method. This achieves the same result in the same manner but maintains constant level in the primary inventory volume.

FIG. 14: COLDTRAP OPERATION TRAP, TEMPERATURE = 3000 C

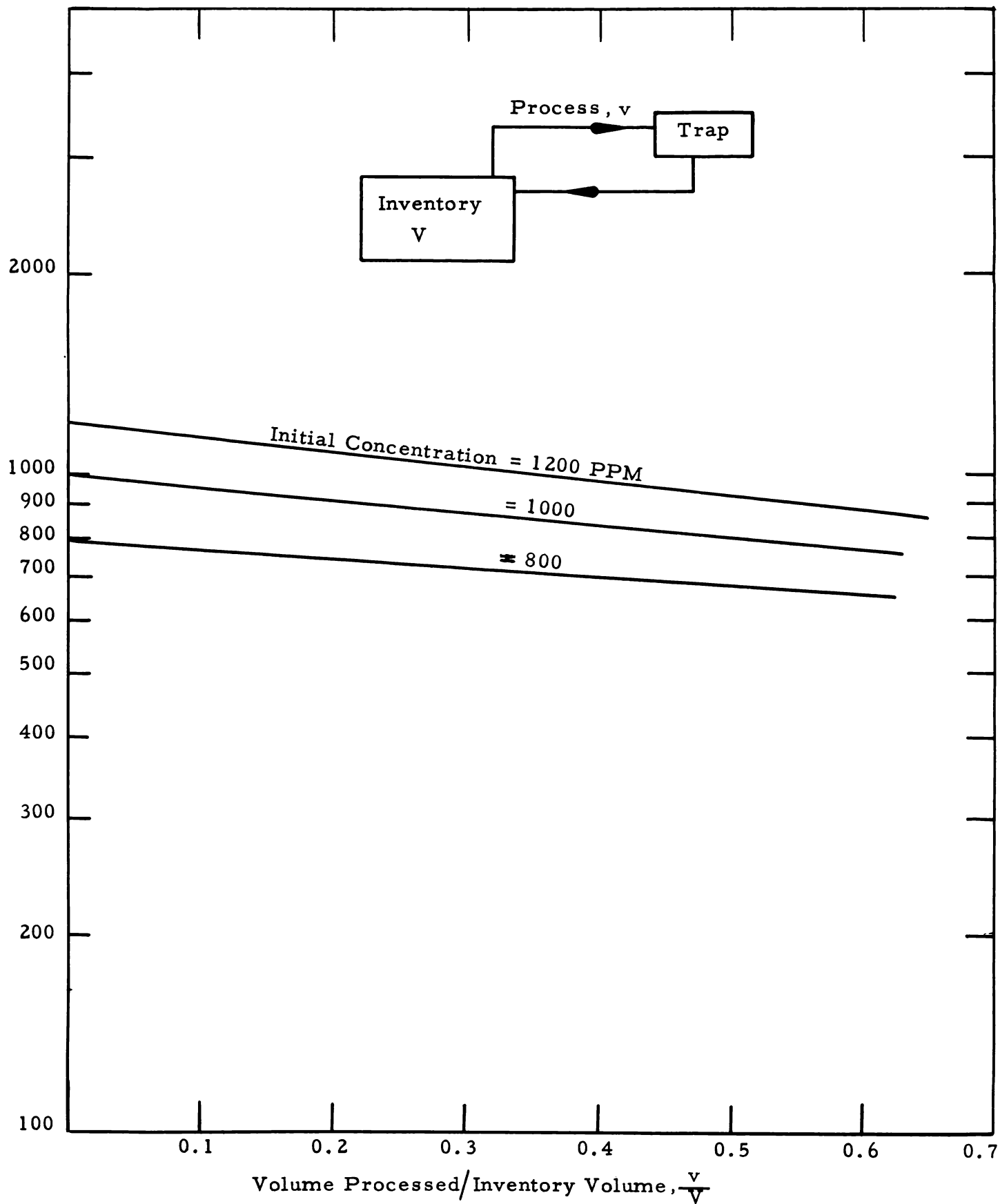
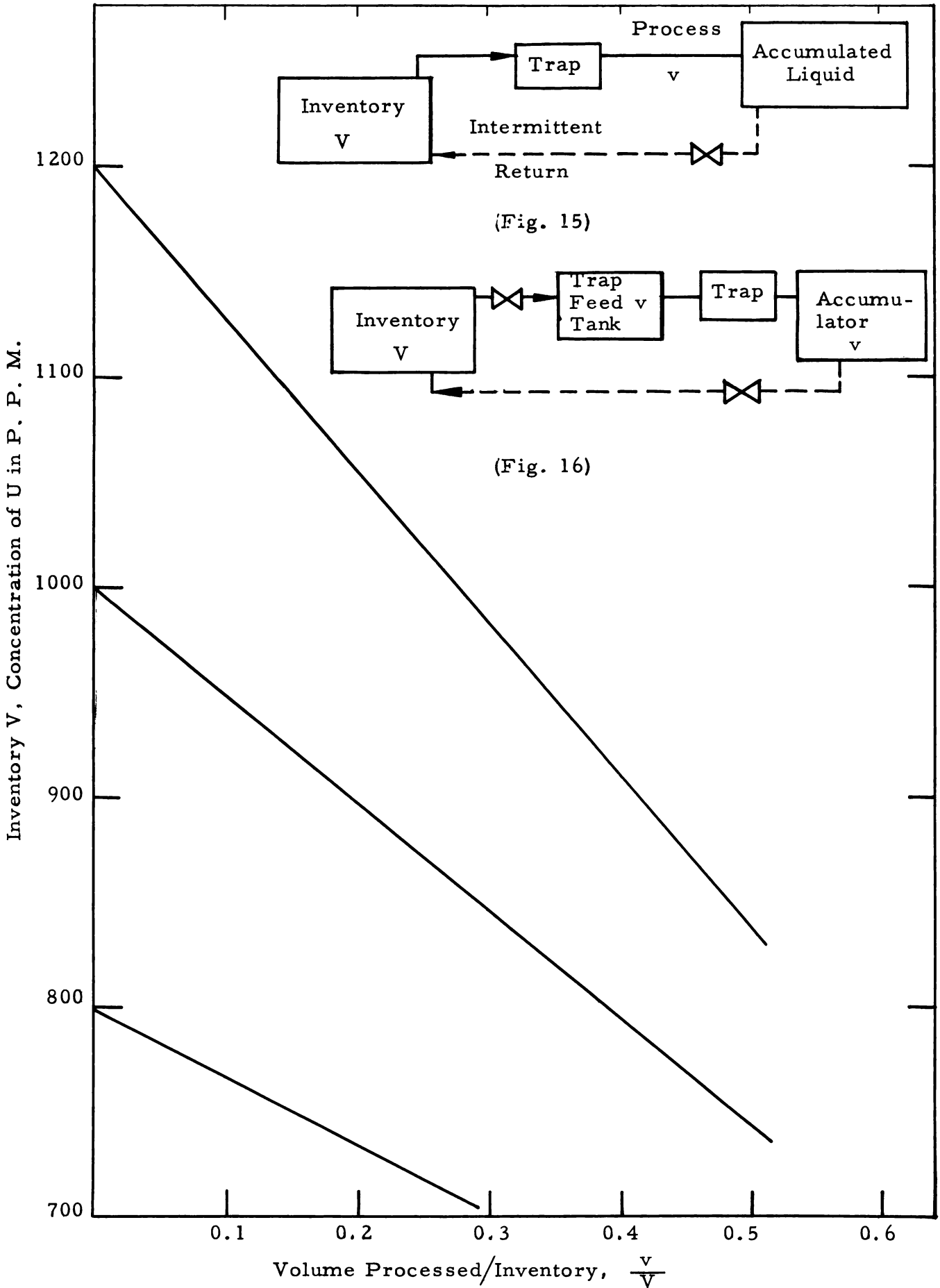
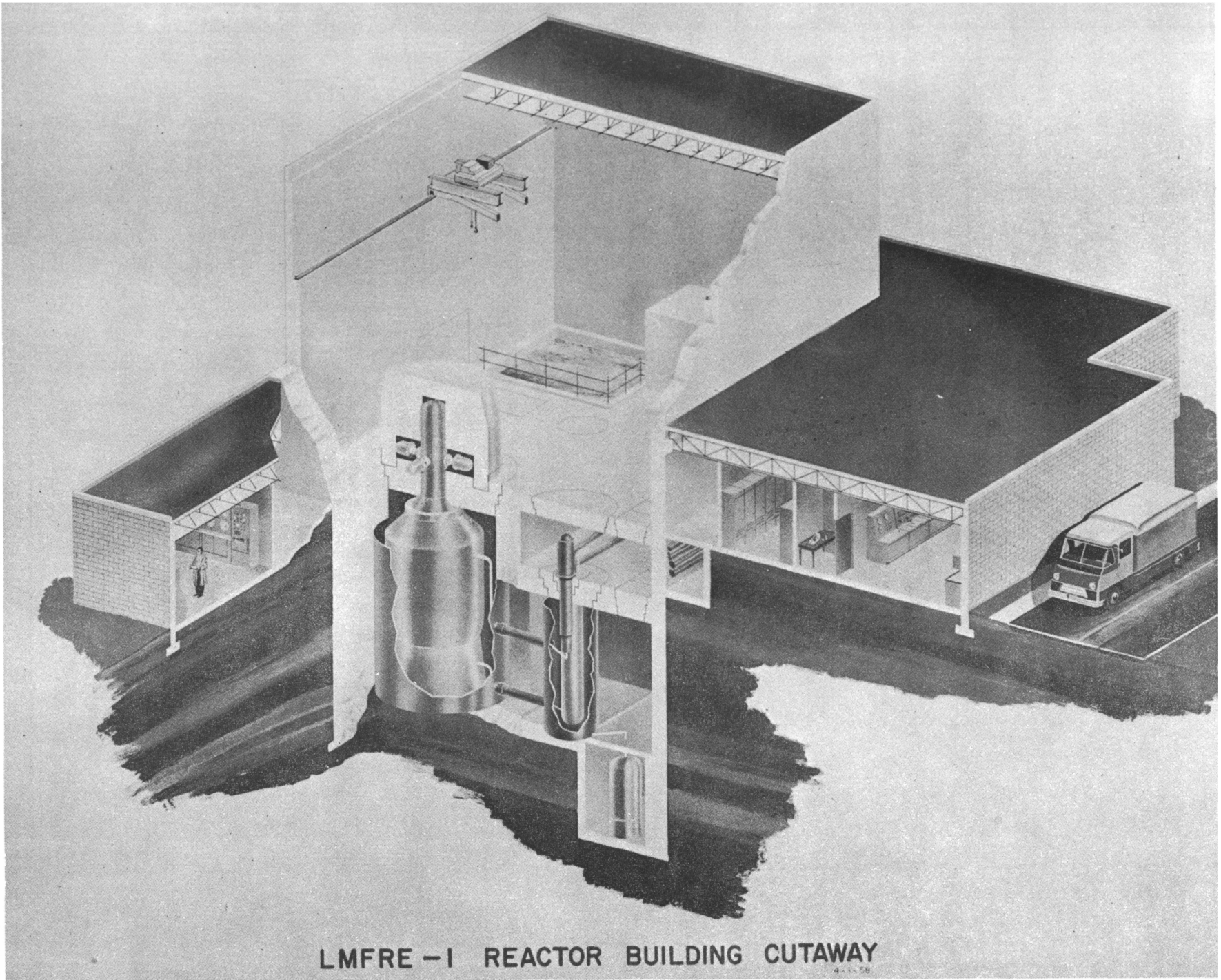


FIG. 15 & 16: COLD TRAP OPERATION,
TRAP TEMPERATURE = 300 C





LMFRE-1 REACTOR BUILDING CUTAWAY

4-1-78

Method I (See Fig. 14)

Let

system volume, main inventory	= V, ft ³
system concentration	= C, ppm uranium
cold trap return concentration	= b, ppm uranium
amount circulated to trap	= v, ft ³
total uranium inventory	= W lbs.

For uranium deconcentration,

$$-dW = Cdv \frac{610}{10^6} - bdv \frac{610}{10^6}$$

$$dW = Vdc \frac{610}{10^6}$$

$$-Vdc = (C-b)dv$$

$$\frac{v}{V} = \ln \left(\frac{C_1 - b}{C - b} \right) \text{ Where } C_1 \text{ is the initial concentration,}$$

and b is the constant dependent only on cold trap temperature.

Method II (See Fig. 15)

Let

total system volume	= V, ft ³
processed liquid volume	= v, ft ³
initial concentration, bulk inventory	= C ₁ ppm uranium
final concentration, bulk inventory	= C ₂ ppm uranium
cold trap return concentration	= b ppm uranium

Then

$$C_2 = C_1 - (C_1 - b) \frac{v}{V}$$

Method III (See Fig. 16)

Let

primary loop volume	= V, ft ³
processes liquid volume	= v, ft ³
initial loop concentration	= C ₁ ppm uranium
loop concentration after partial dump and remix with processed liquid	= C ₂ ppm uranium
cold trap effluent concentration	= b ppm uranium

Under ideal operating conditions a volume of fluid (V-v) at concentration C_1 will be mixed with a volume of fluid (v) at a concentration (b) to yield a volume of fluid (V) at concentration C_2 .

$$C_2 = \frac{C_1 (V - v) + bv}{V}$$

$$C_2 = C_1 - (C_1 - b) \frac{v}{V}$$

As stated previously the latter two methods operate identically. The last method however, has a system inventory (V+v) while in Method II, the total inventory is only V.

(4) Heat Removal

Figure 17 describes the sensible heat removal requirement. Assuming the fuel enters the cold trapping system at 395 C and leaves at 300 C, about 3900 Btu/ft³ processed must be removed as sensible heat. The recommended volume to be held up for processing is about 0.2 of the primary loop inventory, about 20 ft³ of fuel. A reasonable processing time might be 8 hr, which gives a heat rate of 9800 Btu/hr. Regenerative cooling may be provided to reduce part of this load.

Actually the cooling system for the cold trap cannot be designed solely on the above consideration. Experience in bismuth liquid metal systems indicates that trace elements tend to occlude and precipitate out with intermetallic compounds of thorium and bismuth (protactinium distribution coefficients, $C(\text{Pa})_p / C(\text{Pa})_l^{**}$ are 60 and greater). Therefore, it must be assumed that fission products and Po-210 will be occluded in the UBi_2 solids formed in the trap. The heat rate from this source builds up and is approximately proportional to the volume of fuel put through the trap. There is no way to use regenerative cooling to reduce this load. Figure 18 can be used to estimate the cooling requirements (at the trap) imposed by this heat source. If the fuel is held up in the trap feed tank for 3 days, its heat generation rate is about

** $C(\text{Pa})$ = concentration of protactinium
 Subscript l = liquid phase
 Subscript p = solid phase (in particles)

1000 Btu/hr ft³. If 20 ft³ of this material is put through the trap and all the fission products and Po-210 are assumed to be stripped out in the trap, this volumetric source will generate heat at a rate of 20,000 Btu/hr. The strength of this heat source remains fairly constant. This means that no more uranium can be removed once the trap has accumulated a source strength equivalent to the trap cooling capacity.

The above consideration of the heat removal problem influences several things.

(a) Physically removing cold trapped material does not seem feasible. The concentrated heat source would require cooling during any transfer operation.

(b) A simple continuous cold trap to be used directly on the primary loop does not seem feasible. The cold trapped fission products would have a high specific activity since there would be no cooling time.

(c) There is a practical minimum time limit between successive cold trapping runs set by the capacity of the cooling system because the trap cooling system is designed to remove only a specified amount of heat at a given temperature drop from fuel to coolant. The fuel temperature will decrease only after the decay heat source degenerates with decay time.

(d) A filter-type trap, rather than a cold surface trap, does not seem feasible because the filter surface probably will be difficult to cool.

Figure 18 has been plotted on a basis of one year's accumulation of fission products. If the trap is put in operation prior to one year after reactor startup, the heat generation will be somewhat less.

(5) Design

Figure 16 reveals that for a loop containing 1000 ppm of uranium, the uranium concentration can be reduced by 100 ppm in one step if 20 percent extra fuel inventory is provided. These numbers are purely arbitrary, but sufficient extra volume should be provided to give flexibility to the system design in case a large reduction in concentration is required.

FIG. 17: URANIUM COLD TRAP OPERATION,
INITIAL CONCENTRATION = 1000 ppm

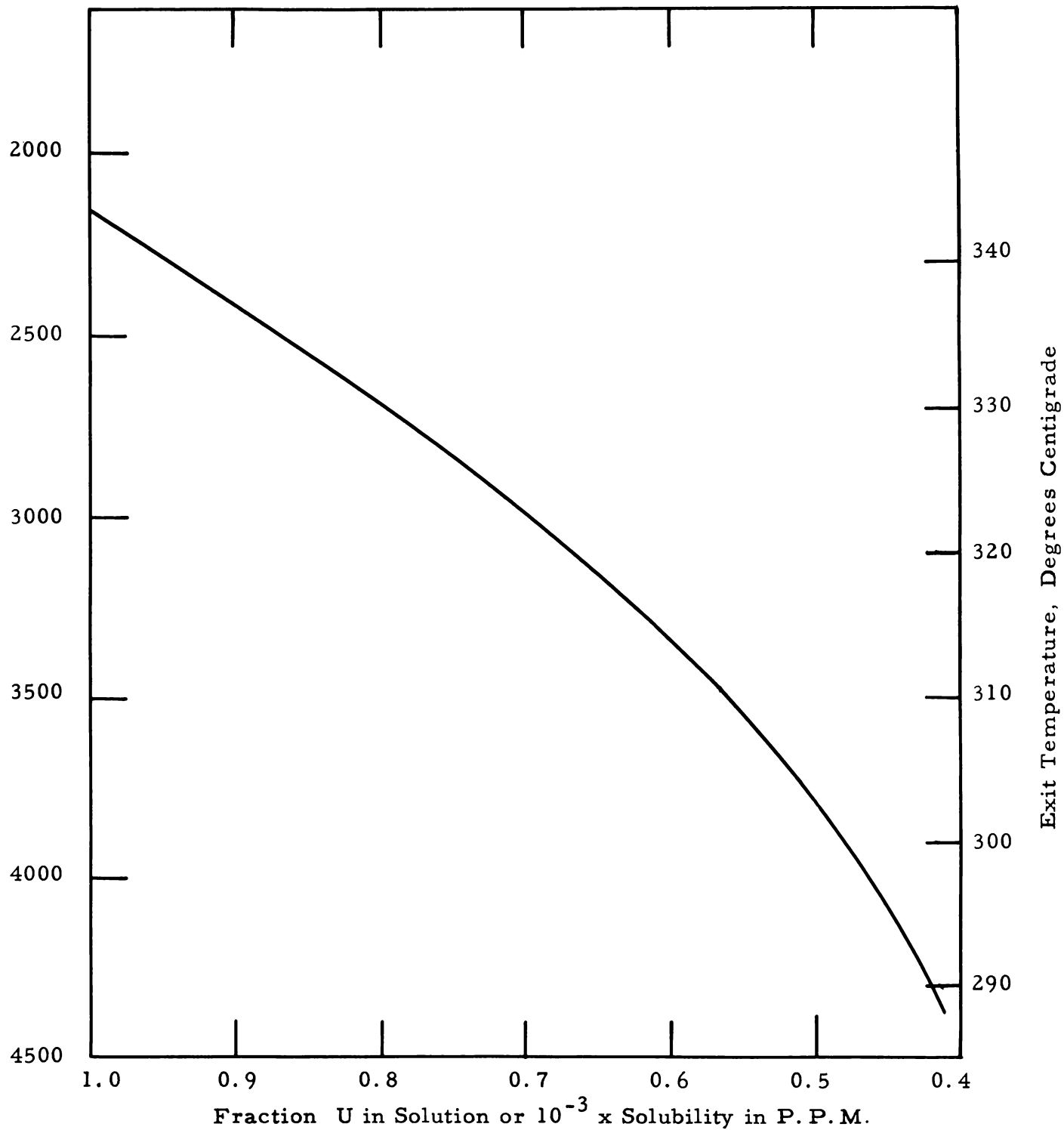
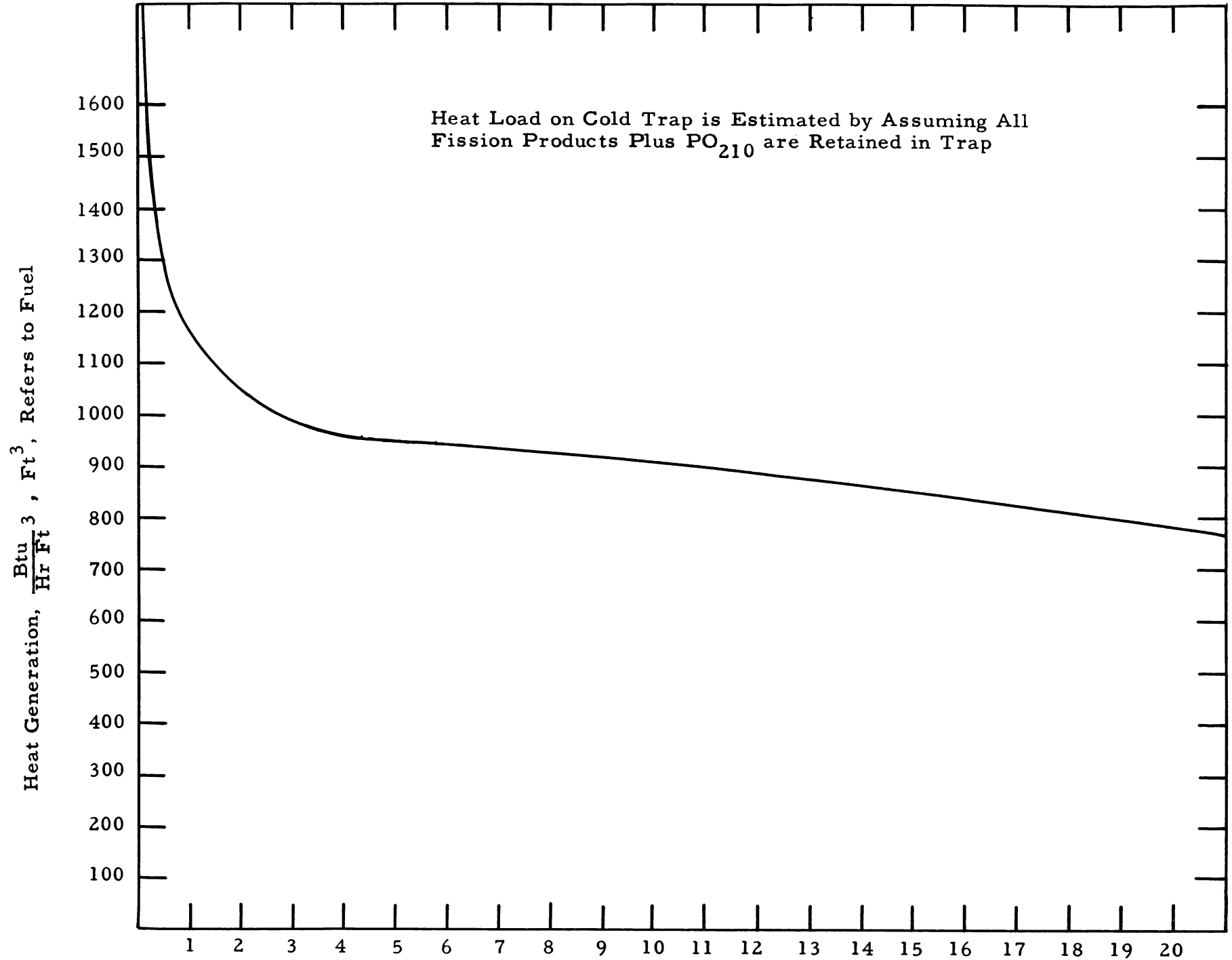


FIG. 18: HEAT GENERATION FROM ONE YEARS ACCUMULATION
OF FISSION PRODUCTS PLUS PO_{210}



There are two basic types of traps. One is a "flow through type", the other is a "cold finger dip type." Both have drawbacks. The flow through type presents the danger of melt down in the event of cooling system failure. This is not a serious problem in the cold finger dip type since it would be located in a large tank of fuel which would dissolve the UBi_2 as it heated up. However, the original configuration of the freezeout mass at the cold finger could not be controlled as in a flow through type trap. In the cold finger dip type the whole tank will approach temperature equilibrium with the cold finger. Under these circumstances it is improbable that all crystal growth will take place at the cold finger, and tank temperature control will be critical.

2. Slurry Processing

A preliminary treatment of an alternative to aqueous (solvent extraction) processing of uranium and thorium oxide fuel slurries was prepared. The method, a modification of the fluoride volatility process, consists of

- (a) Separation of the solid from the liquid phase
- (b) Processing of the solid phase using mercury washing, fluoride volatilization, reduction, and reconstitution of the oxide particles by calcination
- (c) Processing of the liquid phase to convert fission products, protactinium, and residual thorium and uranium oxides to fluorides, and transfer of these fluorides to the salt phase.

The potential usefulness of such a process in LMFR fuel processing must be determined by research and development. After the chemical feasibility of the process is demonstrated, the economics can be evaluated.

B. ANALYTICAL CHEMISTRY

The role of analytical chemistry in the operation of LMFRE-I has been preliminarily defined in BAW-1052.² Analytical equipment and personnel will be limited to that required for emergency and control analyses that must be obtained within a couple days after sampling. Arrangements will be made to obtain off-site analytical services for all other requirements.

The chief function of the LMFRE-I laboratory will be the analysis of the fuel solution for uranium, magnesium, zirconium, and corrosion products. The preparation of samples for shipment to other laboratories will be handled by this laboratory.

The reference design report contains a new, but still preliminary, laboratory layout, including the necessary hot cell and caves and the expected sample flow.

VI. MATERIALS AND INSPECTION

A. 4-IN. UTILITY LOOP

A graphite base material was recommended as a replacement bearing for one of the loop pumps. This material was selected because of its compatibility in bismuth and its good bearing characteristics when operated under low loading. Molybdenum - 0.5 percent titanium and tantalum were recommended as materials for replacement impellers on the pumps.

B. ETR TEST LOOP

A 410 stainless steel filter for filtering the charge to the loop was recommended for use on the melt tank. This method of cleaning the bismuth is used satisfactorily at BNL and is not so hazardous as hydrogen firing.

C. VAPOR DEPOSITED COATING ON GRAPHITE

Application of such a coating was discussed with a vendor. The coating would prevent the absorption of U-Bi by the graphite, eliminating any radiation damage that would occur in the graphite internals.

D. BISMUTH

Refining of high purity bismuth and the possible reclamation of bismuth taken from various dynamic test loops were discussed with a major bismuth manufacturer.

E. SPECIFICATIONS

1. Issued In Final Form

a. Test Program on the Effects of Irradiation on the Tensile and Impact Properties of Molybdenum - 0.5 Percent Titanium

- b. Dynamic Corrosion Testing of Croloy 1-1/4 in Liquid Bismuth
- c. Capsule Testing of Materials for Liquid Bismuth Service
- d. Dynamic Corrosion Testing of Croloy 2-1/4 in Liquid Bismuth
- e. Zirconium Nitride and Zirconium Carbide Film Theory Test

Program

- f. Cemented Graphite Joint Test Program

2. Issued In Preliminary Form

- a. Liquid Metal Control Rod Corrosion Program
- b. Welding of Croloy 2-1/4 and Croloy 1-1/4 for Liquid Bismuth Service
- c. Procedure for Cleaning of Croloy 2-1/4 and Croloy 1-1/4 Exposed to Liquid Uranium-Bismuth

APPENDIX

REACTOR KINETICS

A. FORMULATION OF THE PROBLEM

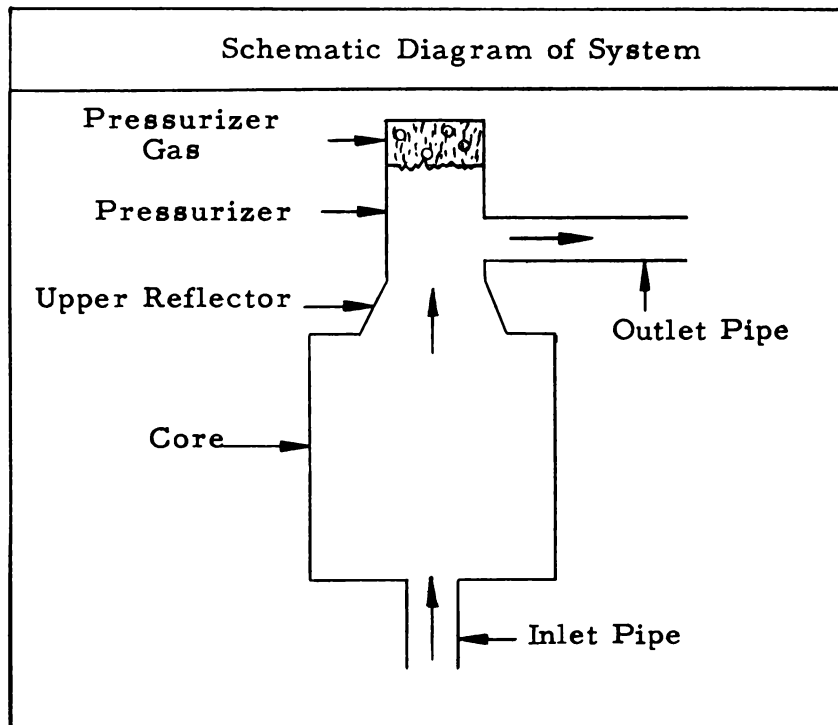
1. The System

a. The system contains three parts.

(1) The core consists of a graphite block through which equally sized and spaced fuel channels are bored. For graphite temperature calculation the core is divided into cells, each containing one fuel channel and the associated cylindrical graphite sleeve.

(2) The fuel in the upper reflector .

(3) The pressurizer, which contains fuel and gas components.



b. A complete kinetic description would require that the following properties be completely described as functions of time and position:

- (1) Power density in each component
- (2) Temperature of each component
- (3) Pressure of each component
- (4) Velocity of each component
- (5) Density of each component

c. Because, physically, the system contains components not included in the mathematical formulation, the rates at which material and energy enter and leave through the boundaries of the system must be described as functions of time and position.

d. All quantities are assumed to be in a steady state at time 0.

2. Simplifying Assumptions

The complete kinetic description is complicated and would require excessive amounts of time to obtain. As a result the following assumptions have been made.

a. Boundary Conditions

(1) The only material that enters or leaves the system is fuel. The fuel enters the core inlet at a constant density, velocity and temperature (and, therefore, a constant mass flow rate) and leaves through the pressurizer outlet at a rate dependent on the pressure in the pressurizer.

(2) Energy enters and leaves the system only in the forms of kinetic, potential, and internal energy of the fuel.

(3) Except for the core inlet and pressurizer outlet, the system may be considered enclosed in a rigid, perfectly insulating shell which prevents the movement of either mass or energy across the initial boundaries of the system.

b. Internal Processes

For the present study all quantities are assumed uniform in the radial direction (except the graphite temperature), and can vary only in the axial direction.

(1) The power density is time dependent and is assumed uniform in the core fuel. The power density in the graphite is a constant fraction of that in the fuel, but can vary radially about each fuel channel. All energy generated is converted to internal energy.

(2) The temperature of the graphite in a cell varies radially and is an unspecified function in the axial direction, and is a function of time. All other properties of the graphite are assumed to be independent of time and position.

(3) In the core the fuel temperature is time dependent and varies linearly in the axial direction. The temperature in the upper reflector and pressurizer is unspecified. The kinetic and potential energies of the fuel are assumed to be negligible.

(4) The density of the fuel in the core is time dependent and varies linearly in the axial direction. The density in the upper reflector and pressurizer is uniform and equal to that at the core outlet.

(5) The velocity of the fuel is time dependent, varies in an unspecified way in the core, and is constant and equal to the core outlet velocity in the upper reflector and pressurizer.

(6) The pressure drop in the core is negligible. The pressure drop in the upper reflector and the pressurizer is time dependent. The pressure drop from the core outlet to points in the upper reflector is an unspecified function of position.

(7) The gas in the pressurizer is assumed to be an ideal gas. It absorbs no energy from the fuel, and its temperature is unspecified. The amount of gas remains constant.

(8) Further assumptions are made when certain parameters are selected as constants, and in the derivation of the equations.

c. Variables

In view of the above assumptions, the following unknowns remain.

(1) Power Density

The quantity calculated is the total power $P(t)$, of which known fractions are assigned to the fuel and graphite.

(2) Core Fuel Temperature

The quantity calculated is $T_F(t)$, the average core fuel temperature. In conjunction with the known and constant inlet temperature T_i , and the assumed linearity in the axial direction, the fuel temperature at every point in the core is known.

(3) Graphite Temperature

The radial distribution of the graphite temperature in a cell (at the point axially where the final temperature is T_F) is calculated as a multi-region heat flow problem. The results give T_n , the temperatures at distances r_n from the center of the fuel channel.

(4) Core Fuel Density

The quantity calculated is $\rho(t)$, the mean density. In conjunction with the known and constant inlet density and the assumed linear variation in the axial direction, the density at any point in the core can be determined.

(5) Uniform Fuel Velocity in the Upper Reflector

This quantity, $U(t)$ is calculated directly.

(6) Pressure Drop in the System

The quantities calculated are $p_c(t)$ and $p_p(t)$, the pressures of the fuel at the core outlet and the gas in the pressurizer.

(7) Gas Volume

The gas volume $V_p(t)$ is calculated from the gas pressure and the expression for an adiabatic compression of an ideal gas.

(8) Flow Rate Through the Outlet From the Pressurizer

This quantity is expressed $q(t)$.

3. Power Equations

The power equation is

$$P = \frac{[k_{ex} (1 - \beta) - \beta] P}{\ell} + \frac{1 + k_{ex}}{\sum_{i=1}^I} \lambda_i C_i, \quad (1)$$

- where
- $1 - \beta$ = the fraction of fission neutrons which are prompt,
 - ℓ = the average neutron lifetime,
 - ϵ = the energy per fission,
 - V_F = the volume of the fuel in the core,
 - ν = the number of prompt neutrons + precursors produced by a fission,
 - λ_i = the decay constant of precursors of type i ,
 - $C_i = \frac{\epsilon V_F}{\nu} \times$ (precursor concentration),
 - and I = number of delayed neutron groups.

The excess multiplication factor is defined by

$$k_{ex} = \delta k(t) + \delta k(U) + \frac{\partial k}{\partial T_F} (T_F - T_{F,0}) + \frac{\partial k}{\partial T_G} (\bar{T}_G - \bar{T}_{G,0}), \quad (2)$$

where $\delta k(t)$ is an arbitrary function, $A + Bt$.

$$\delta k(U) = \frac{\sum_{i=1}^I \frac{\beta_i}{\lambda_i V_F / AU + 1}}{\sum_{i=1}^I \frac{\beta_i}{\lambda_i V_F / AU + 1}}$$

- where
- A = the cross-sectional area of the upper reflector,
 - and U = flow velocity through the upper reflector.

The partial derivatives are the temperature coefficients of reactivity of the fuel and graphite, and are assumed constant.

The subscript 0 indicates initial, steady state values.

$$\bar{T}_G = 1/2 \sum_{n=1}^{N-1} (T_{n+1} + T_n) \frac{V_n}{V_G}, \text{ the average graphite temperature,}$$

where $\frac{V_n}{V_G}$ = the volume fraction of the n^{th} graphite region.

C_i , which is proportional to the concentration of precursors of type i , is given by

$$C_i = -\lambda_i C_i + \beta_i P - \frac{AU}{V_F} C_i, \quad (3)$$

where β_i is the fraction of neutrons + precursors which are precursors of type i .

$$\sum_i \beta_i = \beta$$

In the derivation of the precursor equation, (3), it is assumed that the concentration is uniform throughout the core, and no precursors enter with the fuel.

4. Temperature Equations

a. Energy Balance in Fuel in the Core

The energy balance in the core states that the rate of change of energy in the core fuel is the sum of the energy generated by fissions, the internal energy entering with the fuel, and the heat transferred to the fuel from the graphite, less the internal energy carried out by the fuel.

$$\rho C_F V_F \frac{dT_F}{dt} = P(1-a) + A'U'\rho' C_F T' + \theta(T_1 - T_F) - AU(2\rho - \rho')C_F(2T_F - T') - C_F T_F (A'U'\rho' - AU\bar{\rho}), \quad (4)$$

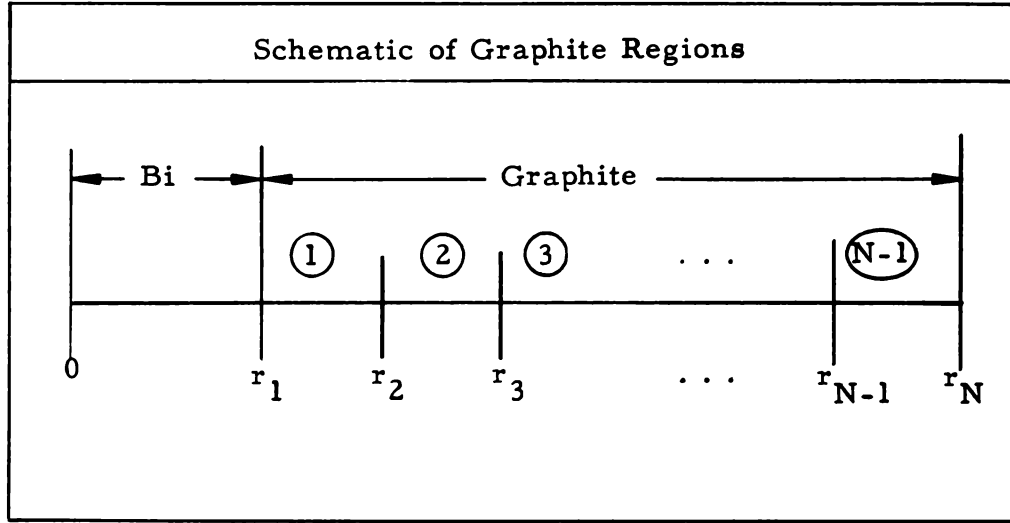
where C_F = the heat capacity of the fuel, (assumed constant),
 a = the fraction of the power generated in the graphite (constant),
 A' = the area of the core inlet,
 U' = the inlet velocity (constant),
 ρ' = the inlet density (constant),
 T' = the inlet temperature (constant),
 θ = the heat transfer coefficient from graphite to fuel (constant).

b. Energy Balance in the Graphite

The graphite temperature distribution is determined by solving a difference form of the time dependent heat equation

$$S(r) + \frac{1}{r} \frac{\partial}{\partial r} (r K \frac{\partial T}{\partial r}) = \rho C \frac{\partial T}{\partial t} \quad (5)$$

The difference equations are given below. The subscript n ($n = 1, 2, \dots, N$) refers either to the n^{th} region or the n^{th} interface, as shown schematically.



$$\dot{T}_N = \frac{a_{N-1}}{2M_{N-1}} P - \frac{(A_N + A_{N-1})(T_N - T_{N-1})}{2M_{N-1}(r_N - r_{N-1})} K_{N-1}, \quad (6)$$

$$\dot{T}_n = \frac{a_n}{M_n} P + \frac{A_{n+1}}{2M_n} Z_{n+1} - \frac{A_n}{2M_n} Z_n - \dot{T}_{n+1} \quad 2 \leq n \leq N-1, \quad (7)$$

$$\dot{T}_1 = \frac{a_1}{M_1} P - \frac{\theta}{M_1} [T_1 - T_F] + \frac{A_2}{2M_1} Z_2 - \dot{T}_2, \quad (8)$$

where $M_n = \frac{\rho_n C_n V_n N_c}{2}$,

T_n = the temperature at the n^{th} interface,

ρ_n = the graphite density of the n^{th} region,

C_n = the specific heat of the n^{th} region,

V_n = the volume of the n^{th} region of a single cell,

$$Z_n = K_n \left[\frac{T_{n+1} - T_n}{r_{n+1} - r_n} \right] + K_{n-1} \left[\frac{T_n - T_{n-1}}{r_n - r_{n-1}} \right],$$

$$\begin{aligned}
Z_n &= 0, \\
K_n &= \text{the thermal conductivity of the } n^{\text{th}} \text{ region,} \\
r_n &= \text{the inner radius of the } n^{\text{th}} \text{ region,} \\
A_n &= 2\pi r_n H N_c, \\
N_c &= \text{the number of cells in the core,} \\
a_n &= \text{the fraction of power produced in the } n^{\text{th}} \text{ graphite region,}
\end{aligned}$$

$$a = \sum_{n=1}^{N-1} a_n,$$

and $N-1$ = the number of graphite regions.

The temperatures found from the solution of these equations are averaged for the \bar{T}_G used in the reactivity equation, (2).

5. Hydraulic Equations

a. Equation of Continuity - Core Fuel

The equation of continuity states that the rate of change of fuel mass in the core is the difference between the amount that flows in and the amount that flows out.

$$V_F \dot{\rho} = A'U'\rho' - AU\bar{\rho}, \quad (9)$$

where $\bar{\rho} = 2\rho - \rho'$, is the average density at the core outlet.

b. Equation of Continuity - Pressurizer Gas

The equation of continuity represents the conservation of volume in the pressurizer, and states that the time rate of change of the volume gas in the pressurizer is equal to the outlet minus the inlet volume rates of flow of fuel.

$$V_P = -AU + q ; \quad \dot{q} = \frac{A_s}{L_s \bar{\rho}} (p_p - p_{p,0}) , \quad (10) \quad (11)$$

where V_P = the pressurizer gas volume
 q = the volume flow rate out of the pressurizer,
 A_s = the cross-sectional area of the outlet pipe,
and L_s = the length of the outlet pipe.

The pressure outside the system is assumed constant.

c. Force Balance in the Connector

The force balance expresses the fact that the unbalanced force on the fuel in the upper reflector is proportional to the acceleration of the fuel. The upward force is due to the pressure in the core. The downward forces are due to the gas pressure, the fuel mass, and tractive forces.

$$p_c - p_p = \left[\frac{Lf}{2D_e} + \mathcal{L} \right] (\bar{\rho} U^2) + \bar{\rho} Zg + \bar{\rho} L\dot{U} , \quad (12)$$

where L = the distance along the upper reflector from the core outlet to liquid level in the pressurizer (assumed constant),
 Z = the vertical distance from the core outlet to the liquid level (assumed constant),
 D_e = the hydraulic diameter in the upper reflector,
 f = the friction factor,
 \mathcal{L} = a term to account for pressure drops due to bends, contractions, etc., in the upper reflector,
 p_c = the pressure in the core,
 p_p = the gas pressure in the pressurizer,
and g = the acceleration due to gravity.

6. Equations of State

Equations of state relate temperature, density, and pressure.

a. Fuel in the Core

$$\rho - \rho_0 = \frac{\partial \rho}{\partial p_c} (p_c - p_{c,0}) + \frac{\partial \rho}{\partial T_F} (T_F - T_{F,0}) \quad (13)$$

The partial derivatives are known and assumed constant.

b. Gas in the Pressurizer

$$p_p = p_{p,0} \left[\frac{V_{p,0}}{V_p} \right]^\gamma$$

γ is a known constant, the ratio of the specific heats of the gas.

7. Summary

There are 19 equations in 19 unknowns. These are made up of 9 equations in P , T_F , ρ , V_p , q , U , k_{ex} , p_c , p_p , C_i ($i = 1, 2, \dots, I$), and T_n ($n = 1, 2, \dots, N$), such that $I + N = 10$. This system has been programmed for the Electrodata computer by J. G. Stein.

8. The Initial Steady State

It is assumed that initially, before the introduction of δk , the system is operating in a steady state. Under these circumstances, the time derivatives of Equation 1, 3, 4, 6, 7, 8, 9, 10, 11, and 12 are zero, and a set of consistent steady state values of the unknowns can be found.

a. Assume a value for ρ_0 , and calculate $\bar{\rho}_0 = 2\rho_0 - \rho'$

The steady state form of equation 9 is

$$A'U'\rho' = AU_0\bar{\rho}_0 \quad (15)$$

This can be solved for U_0 ,

$$U_0 = A'U'\rho' / A\bar{\rho}_0 \quad (16)$$

The steady state value of V_p is independent of the steady values of other quantities. The steady state value of q is

$$q_0 = AU_0 \quad (17)$$

b. The steady state form of equation 12 is

$$p_{c,0} - p_{p,0} = \left[\frac{Lf}{2D_e} + \mathcal{L} \right] (\bar{\rho}_0 U_0^2) + \bar{\rho}_0 Z_g \quad (18)$$

$p_{p,0}$ may be selected arbitrarily, and since $\bar{\rho}_0$ and U_0 are known $p_{c,0}$ may be calculated from

$$p_{c,0} = p_{p,0} + \left[\frac{Lf}{2D_e} + \mathcal{L} \right] (\bar{\rho}_0 U_0^2) + \bar{\rho}_0 Z_g \quad (19)$$

c. The steady state precursor equation (3) is

$$-\lambda_i C_{i,0} + \beta_i P_0 - \frac{A U_0}{V_F} C_{i,0} = 0 \quad (i = 1, 2, \dots, I). \quad (20)$$

P_0 is known and 20 may be solved for $C_{i,0}$,

$$C_{i,0} = \frac{\beta_i P_0}{\lambda_i + A U_0 / V_F} \quad (i = 1, 2, \dots, I). \quad (21)$$

d. The steady state form of the power equation (1) is

$$\left[k_{\text{ex}} (1 + \beta) - \beta \right] P_0 + (1 + k_{\text{ex}}) \sum_{i=1}^I \lambda_i C_{i,0} = 0. \quad (22)$$

Substituting 21 into 22 and solving for k_{ex} ,

$$k_{\text{ex},0} = \frac{\sum_{i=1}^I \frac{\beta_i}{\lambda_i V_F / A U_0 + 1}}{I - \sum_{i=1}^I \frac{\beta_i}{\lambda_i V_F / A U_0 + 1}} = k(U_0). \quad (23)$$

Although this relationship has been obtained in what may seem to be an arbitrary way, it is, in fact, the multiplication factor for a circulating fuel reactor.

e. The steady state temperatures are found as follows.

(1) The steady state forms of equations 6, 7, and 8 are

$$a_{N-1} P - (A_N + A_{N-1}) \frac{(T_N - T_{N-1})}{(r_N - r_{N-1})} K_{N-1} = 0, \quad (24)$$

$$a_n P + 1/2 A_{n+1} Z_{n+1} - 1/2 A_n Z_n = 0, \quad (2 \leq n \leq N-1), \quad (25)$$

and
$$a_1 P - \theta (T_1 - T_F) + 1/2 A_2 Z_2 = 0. \quad (26)$$

The "0" subscript is omitted throughout section e.

(2) Since $Z_N = 0$, Z_{N-1} may be found from 25, and in general,

$$Z_n = \frac{2 a_n P}{A_n} + \frac{A_{n+1} Z_{n+1}}{A_n} \quad (2 \leq n \leq N-1). \quad (27)$$

(3) Equation 24 may be solved for $T_N - T_{N-1} = -T_{N-1}^*$,

$$T_{N-1} - T_N = \frac{a_{N-1} P}{(A_N + A_{N-1})} \frac{r_N - r_{N-1}}{K_{N-1}} = T_{N-1}^* \quad (28)$$

(4) The definition for Z_n may be written

$$T_n - T_{n+1} = \frac{K_{n+1} (r_{n+1} - r_n) (T_{n+2} - T_{n+1})}{K_n (r_{n+2} - r_{n+1})} - \frac{Z_{n+1} (r_{n+2} - r_{n+1}) (r_{n+1} - r_n)}{K_n (r_{n+2} - r_{n+1})}, \quad (29)$$

when $n = N - 2$, 29 becomes

$$T_{N-2} - T_{N-1} = \frac{K_{N-1} (r_{N-1} - r_{N-2}) (T_N - T_{N-1})}{K_{N-2} (r_N - r_{N-1})} - \frac{Z_{N-1} (r_{N-1} - r_{N-2})}{K_{N-2}} \quad (30)$$

then

$$T_{N-2} - T_{N-1} - T_N + T_N = T_{N-2}^* - T_{N-1}^* = - \frac{K_{N-1} (r_{N-1} - r_{N-2}) (T_{N-1}^*)}{K_{N-2} (r_N - r_{N-2})} - \frac{Z_{N-1} (r_{N-1} - r_{N-2})}{K_{N-2}} \quad (31)$$

This process may be continued until T_1^* has been calculated.

(5) Equation 26 may be solved for $\theta (T_1 - T_F)$

$$\theta (T_1 - T_F) = a_1 P + 1/2 A_2 Z_2 \quad (32)$$

The steady state form of Equation 4 is

$$P (1-a) + A' U' C_F \rho' T' - A U C_F (2T_F - T') \bar{\rho} + \theta (T_1 - T_F) = 0. \quad (33)$$

Substituting 32 into 33 and solving for T_F

$$T_F = \frac{T_1}{2} + \frac{P(1 - a + a_1)}{2 AUC_F \bar{p}} + \frac{A_1 U_1 C_F T_1}{2 AUC_F \bar{p}} + \frac{A_2 Z_2}{4 AUC_F \bar{p}} \quad (34)$$

With T_F known, the value may be substituted into 32, and T_1 found

$$T_1 = \frac{a_1 P}{\theta} + \frac{A_2 Z_2}{2\theta} + T_F \quad (35)$$

(6) With T_1 and T_F known, T_N can be found

$$T_N = T_1 - T_1^* \quad (36)$$

Similarly all temperatures may be found from

$$T_n = T_n^* + T_N \quad (2 \leq n \leq N-1) \quad (37)$$

f. There is now available a consistent set of steady state values of the unknown functions.

In summary, the values of ρ_0 , P_0 , $V_{p,0}$, $p_{p,0}$ are picked arbitrarily in advance. The other quantities, U_0 , $T_{F,0}$, $p_{c,0}$, q_0 , $C_{i,0}$ ($i = 1, 2, \dots, I$), $T_{n,0}$ ($n = 1, 2, \dots, N$) are calculated.

9. The Final Steady State

The equations are such that a final steady state may be obtained for a constant reactivity change. This calculation is done by machine.

B. RESULTS OF CALCULATIONS

1. Introduction

A kinetic analysis of the 8.3 MW LMFRE has been carried out to study the transient effects of changes of reactivity.

The changes in reactivity were introduced as combinations of step and ramp changes in the effective multiplication constant.

The problem was solved using the Generalized Integration Program on the Datatron. The Runge-Kutta method was used.

In all cases run, the power level, delayed neutron precursor concentrations, fuel and graphite temperatures, and the excess multiplication were calculated. In most cases the additional properties of fuel velocity and density, pressure in the core, and gas pressure and volume were also calculated.

The constants used are given in section 5 a.

2. Ramp Inputs in Reactivity

a. Cases Investigated

Ramp inputs of up to 1.5 percent/sec were studied. These ramps were assumed to continue for 11.5 sec, for a total reactivity increase of approximately 17.25 percent.

In one case the effects of reversing the slope of the ramp at 11.5 sec were investigated.

The cases run were:

56, 60, 63	1.5 percent/sec ramp
57	1.0 percent/sec ramp
59	0.5 percent/sec ramp

b. Power

The characteristic response of the power to a ramp input is a series of damped oscillations followed by a nearly linear rise.

The maximum power level is reached on the first surge after the introduction of the disturbance, although higher powers might be obtained if the ramp input were continued for more than 11.5 sec.

The results are shown in Figure 19.

c. Fuel Temperature

The characteristic response of the fuel temperature to a ramp disturbance is a continuous rise. During the period of power oscillations there is considerable variation in the rate of rise, but during the linear power rise the temperature rises linearly.

The results are summarized in Figure 20.

FIG. 19: POWER VS. TIME FOR RAMP INPUTS

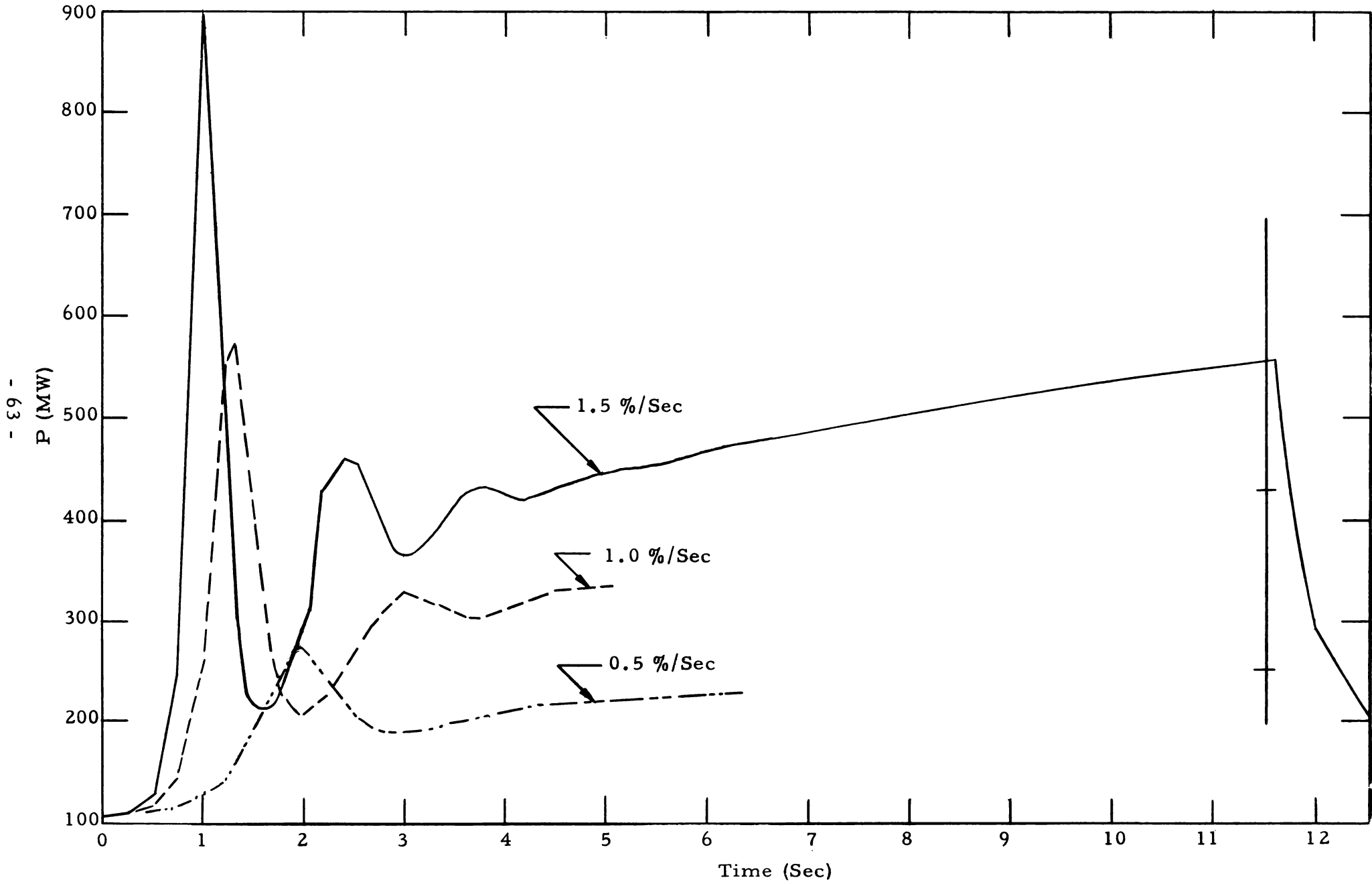
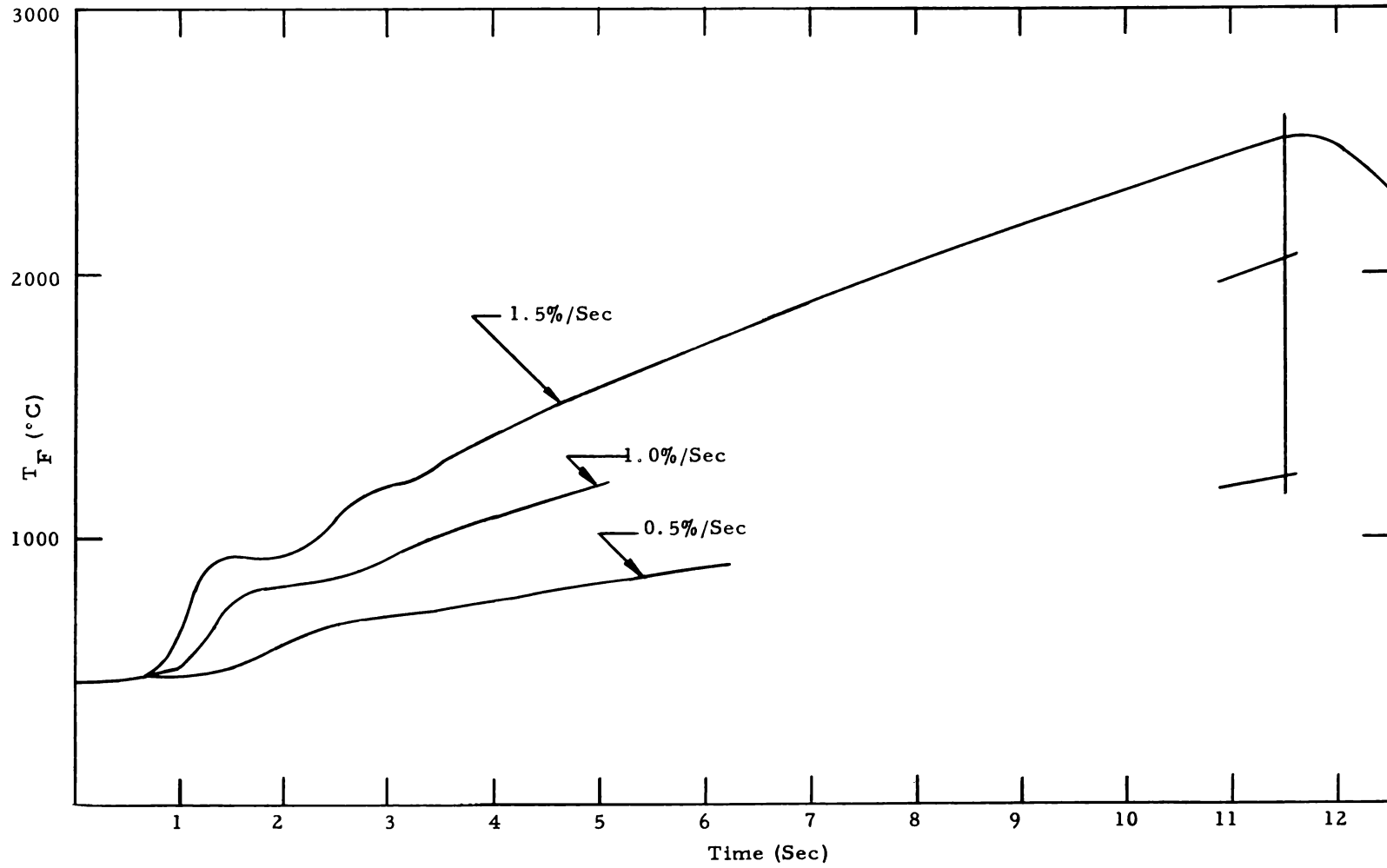


FIG. 20: MEAN FUEL TEMPERATURE VS. TIME FOR RAMP INPUTS



d. Core Pressure

The response of the core pressure to a ramp input is an initial surge, after which the pressure remains essentially constant.

The pressure was calculated only for case 63. The pressure effects were omitted in case 56, and in case 60 the gas pressure was assumed to be constant. No significant differences were found in the power and temperature values calculated by the three cases.

The behavior of the pressure is shown in Figure 21.

e. Other Properties of the Reactor

The behavior of the other reactor variables, for case 63, are plotted vs. time in Figures 21, 22, and 23 (Case 56, after 11.5 sec)

3. Step Inputs in Reactivity

a. Cases Investigated

Step inputs of up to 16 percent were studied.

The cases run were

53, 55	16 percent step
61	8 percent step
62	4 percent step

b. Power

The characteristic response of the power to a step input is an initial surge after which the power levels out and approaches the steady state value.

The results are shown in Figure 24.

c. Fuel Temperature

The temperature response is a sharp rise followed by a slow drop to a steady state value.

The results are shown in Figure 25.

d. Core Pressure

The core pressure was calculated for case 53 only. No significant differences in power and temperatures were found between cases 53 and 55.

FIG. 21: PRESSURE OF FUEL IN CORE (P_c) AND PRESSURE OF GAS (P_p)
VS. TIME FOR 1.5%/SEC RAMP

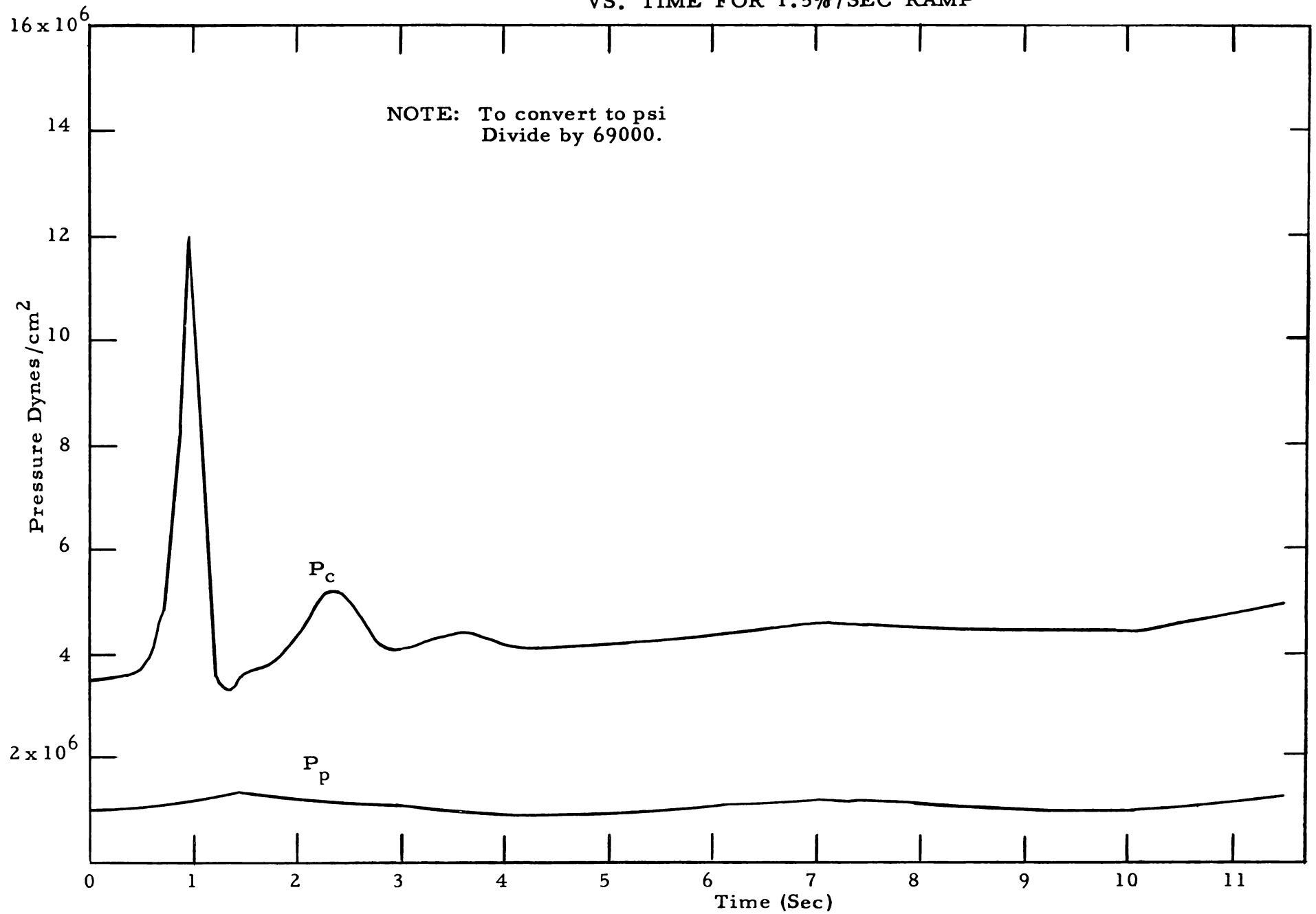


FIG. 22: EXCESS MULTIPLICATION VS. TIME FOR 1.5%/SEC RAMP

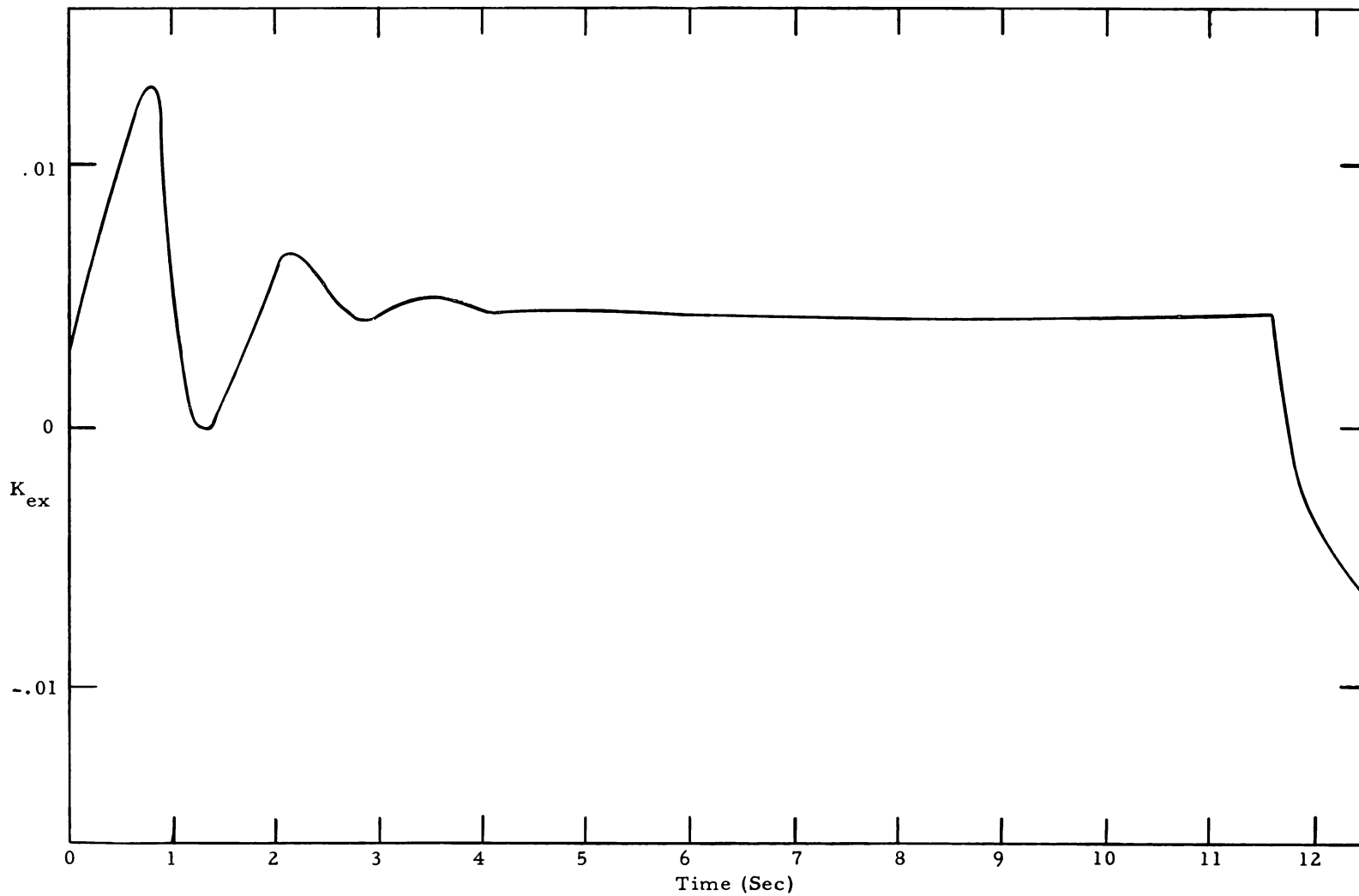


FIG. 23: GRAPHITE TEMPERATURES VS. TIME, FOR 1.5%/SEC RAMP

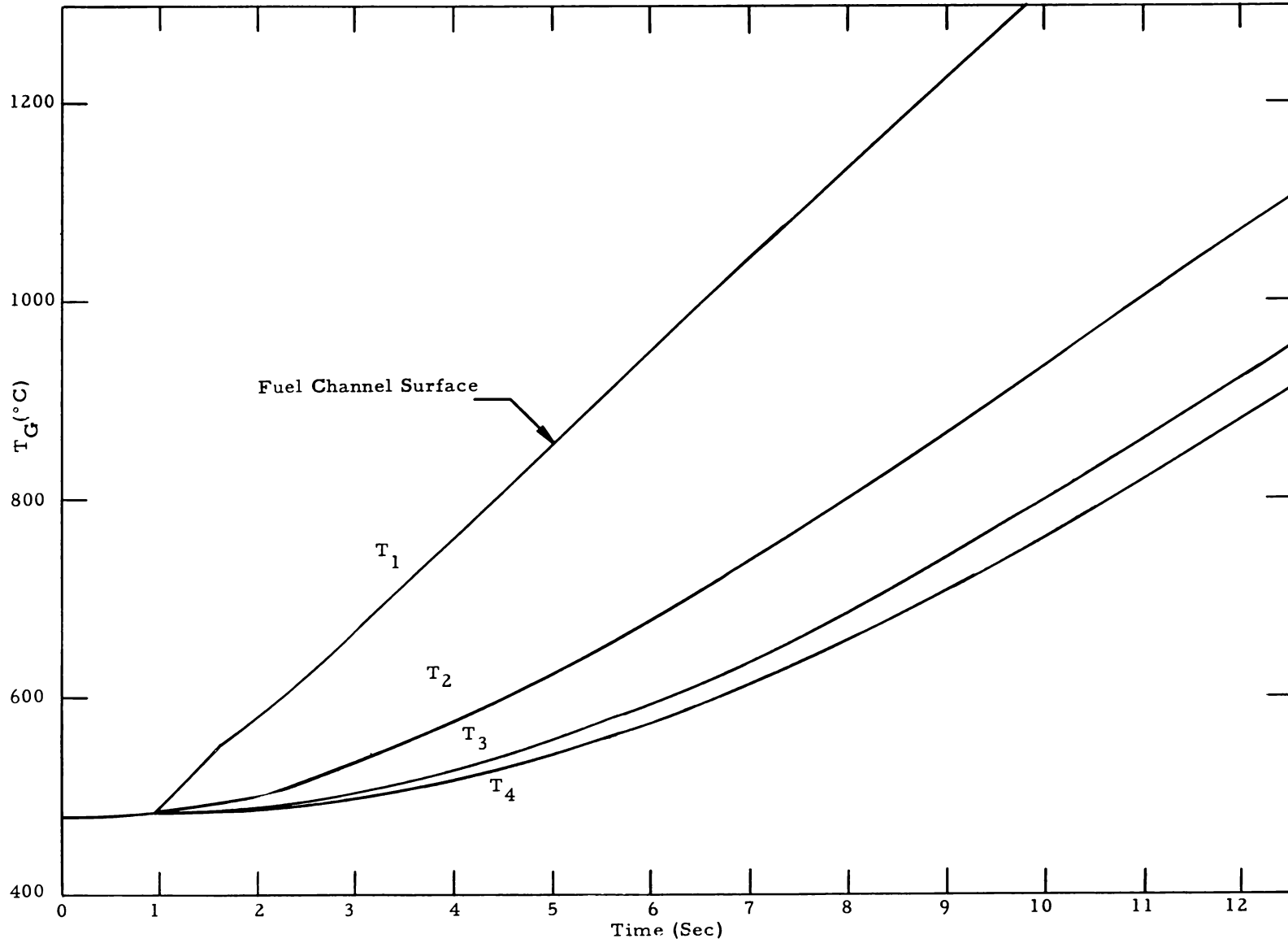


FIG. 24: POWER VS. TIME FOR STEP INPUTS

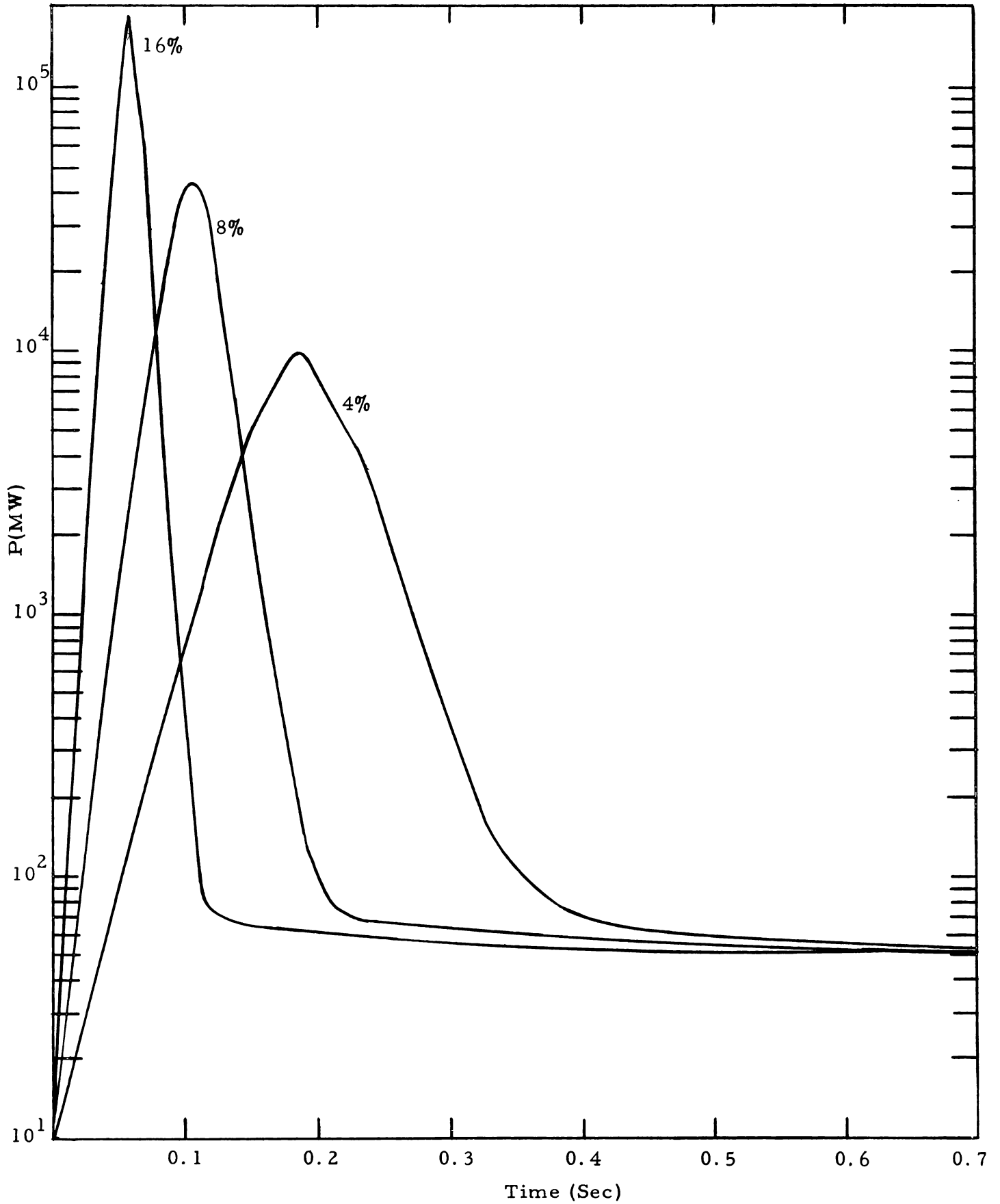


FIG. 25: MEAN FUEL TEMPERATURE VS. TIME FOR STEP INPUTS

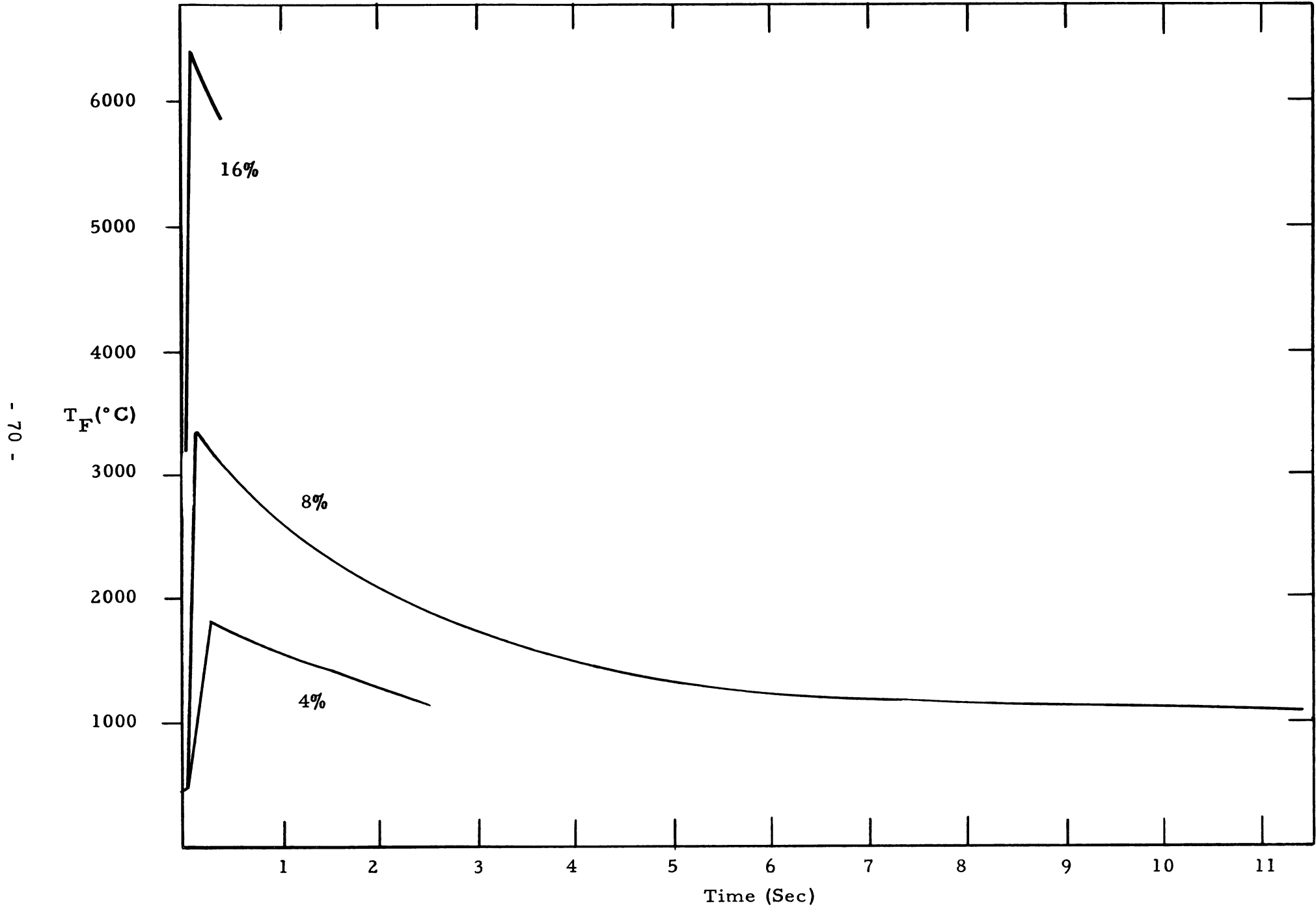


FIG. 26: GRAPHITE TEMPERATURES VS. TIME, 8% δk STEP INPUT

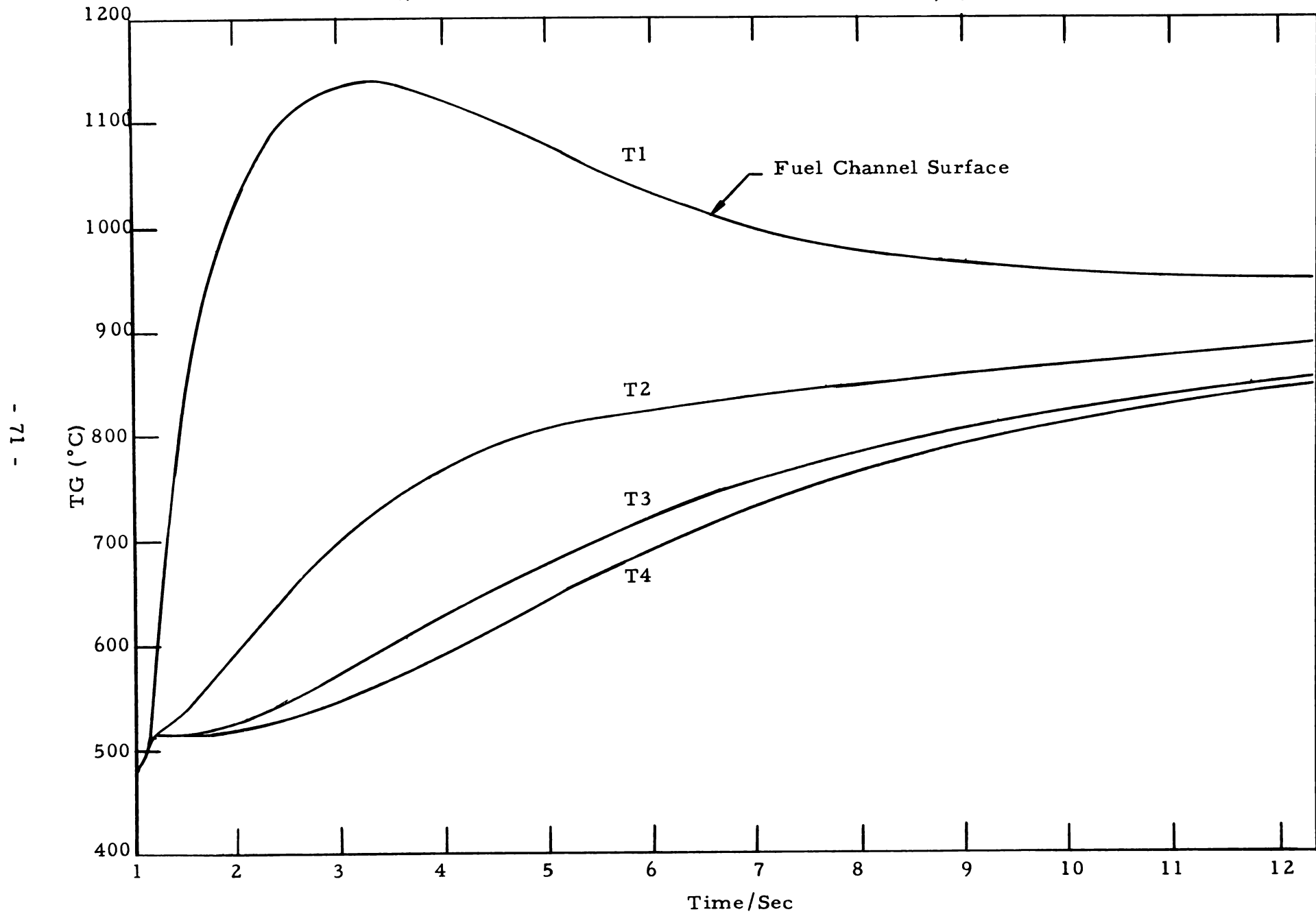


FIG. 27: EXCESS MULTIPLICATION VS. TIME, 8% δk STEP INPUT

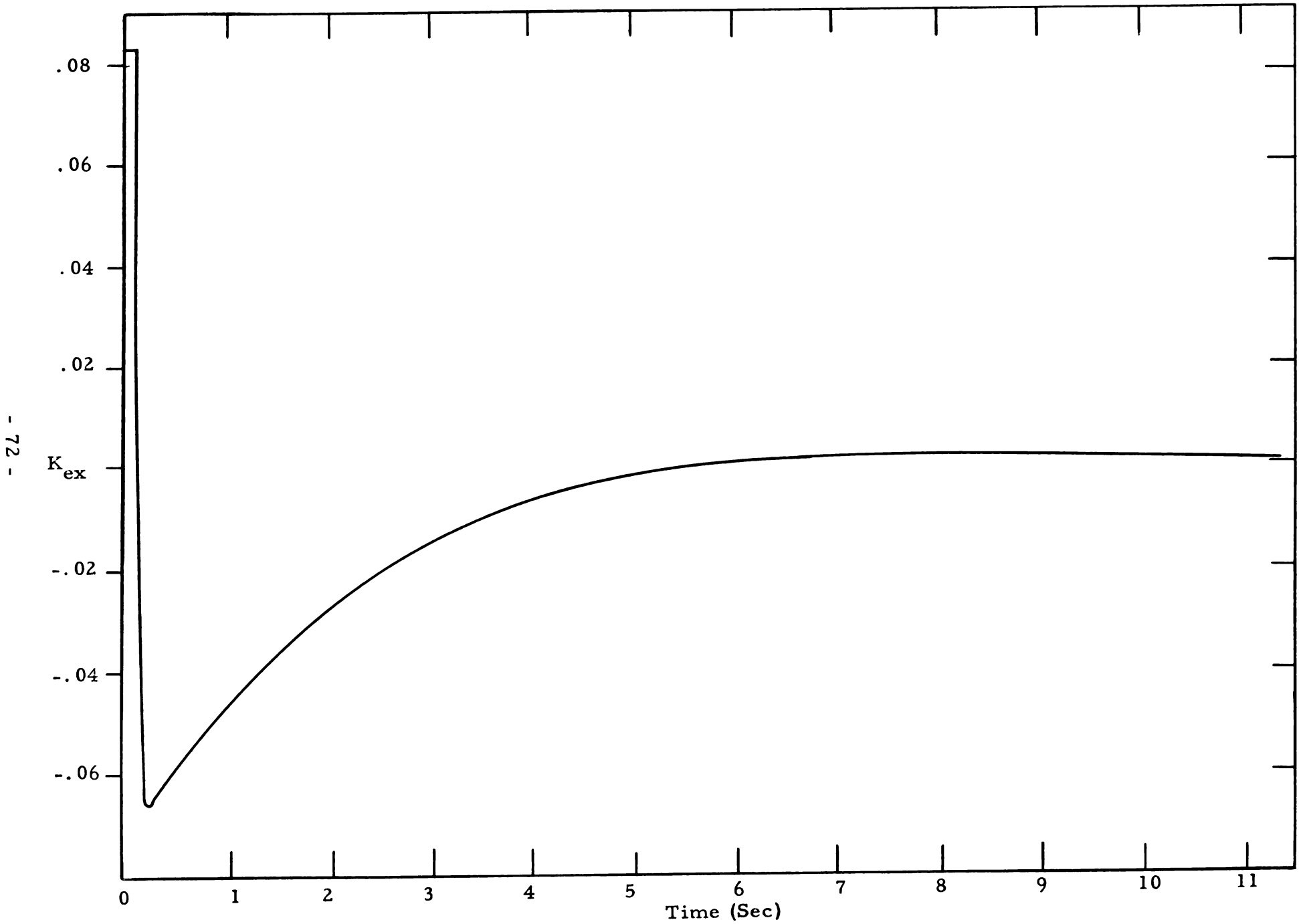


FIG. 28: POWER VS. TIME WITH CONTROL ROD OPERATION

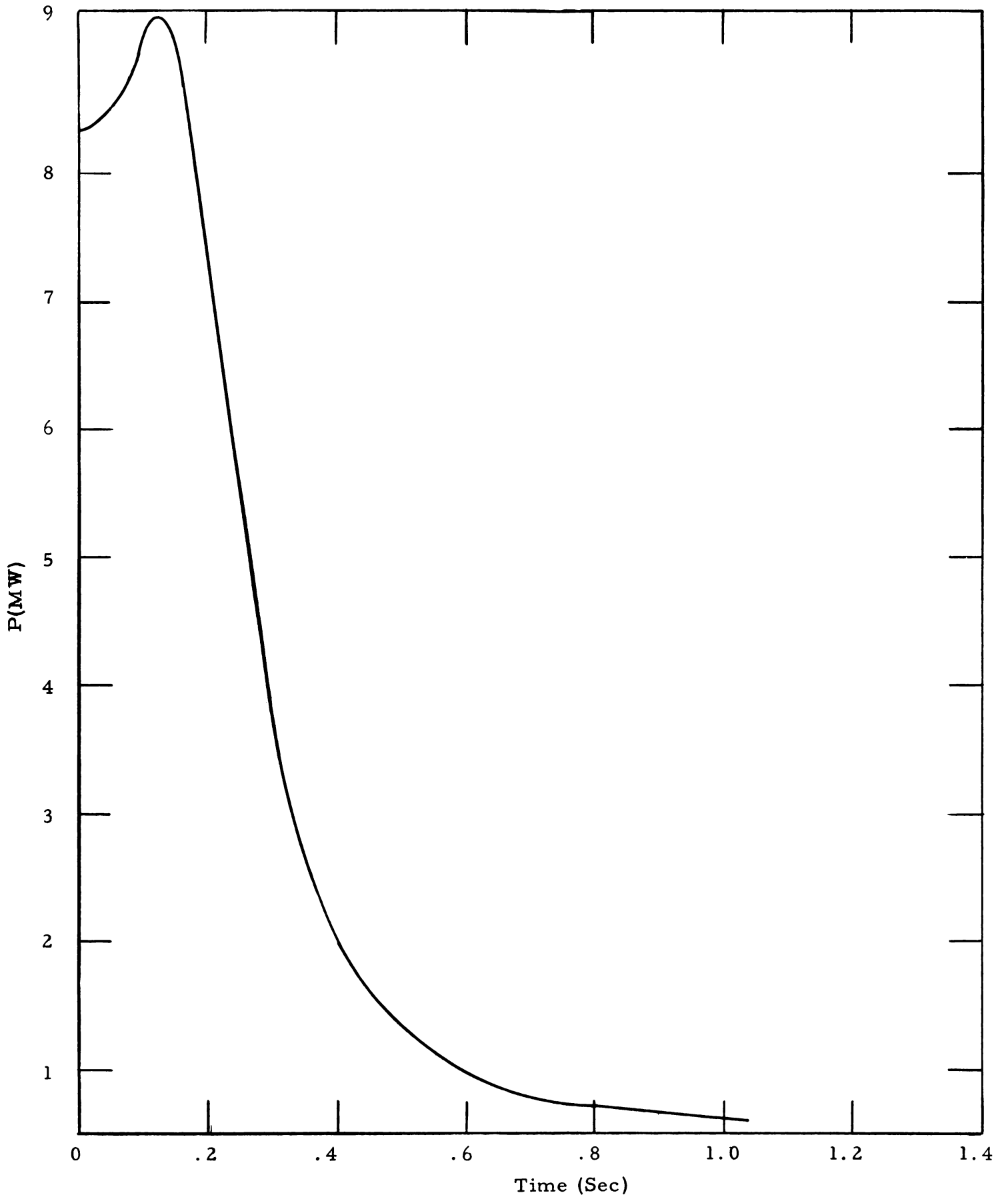
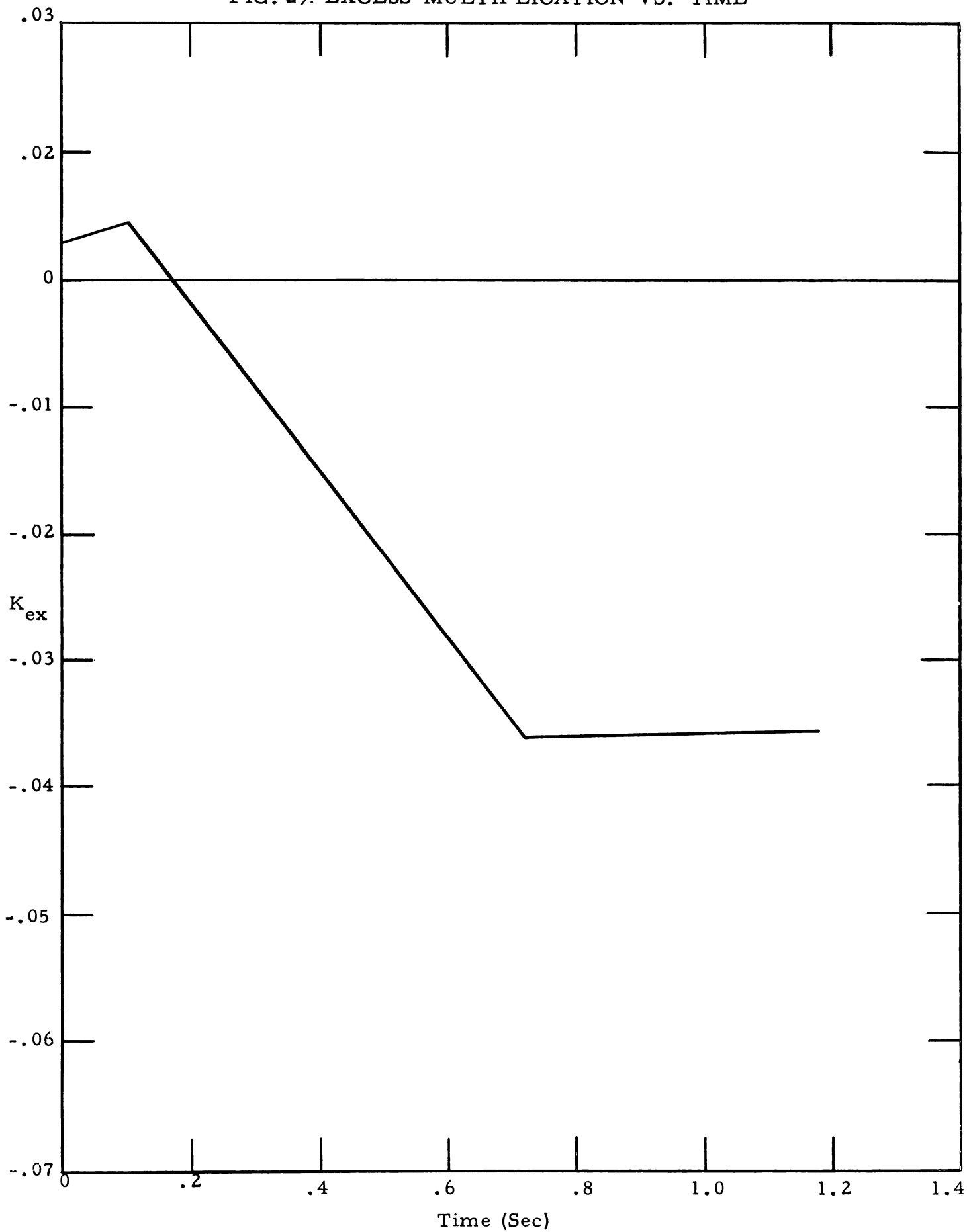


FIG. 29: EXCESS MULTIPLICATION VS. TIME



The pressure was found to rise very high, very rapidly, increasing by a factor of ~ 100 before the power reached its first maximum.

e. Other Properties

The other properties calculated are shown for case 61, in Figures 26 and 27.

4. Normal Operation

a. Case Investigated

In normal operation (case 54) it was assumed that 1.5 percent/sec ramp disturbance occurred for 0.1 sec, after which the control rods introduced a negative reactivity amounting to 4 percent during the following 0.6 sec.

b. Results

No serious fluctuations in any of the reactor properties occurred in case 54.

The power and excess multiplication as functions of time are plotted in Figures 28 and 29.

The changes in temperature, pressure, and other reactor properties were negligible.

5. The Computer Program

a. Input

A complete list of the input constants and the values used is given below.

C_n	$n = 1, 2, 3$	Product of specific heat in graphite and number of fuel channels in core: 465 joules/gm°C
ρ_n	$n = 1, 2, 3$	Density of graphite: 1.8 gm/cm ³
a_n	$n = 1, 2, 3$	Fraction of power generated in each graphite region: 0.014 This corresponds to a total of 4.2 percent of the power, generated in the graphite.

K_n	$n = 1, 2, 3$	Thermal conductivity of graphite: 0.2945 joules/sec-cm-°C
β_i	$i = 1, 2, \dots 6$	Fraction of fission neutrons which are of type i: 0.00027, .00158, .00144, .00307, .00101, .00014 There is a total delay fraction of .00751
λ_i	$i = 1, 2, \dots 6$	Decay constant of precursors of type i: .0128, .0319, .1181, .3180, 1.5068, 5.5012, sec ⁻¹
D		Core diameter: 115 cm
H		Core height: 115 cm
V_F/V_G		Ratio of bismuth volume to graphite volume in core: 0.5
T'		Bismuth temperature at core inlet: 400 C
$\partial k / \partial T_F$		Prompt temperature coefficient of reactivity: $-5 \times 10^{-5} / ^\circ\text{C}$
$\partial k / \partial T_G$		Delayed temperature coefficient of reactivity: $-1.3 \times 10^{-4} / ^\circ\text{C}$
θ		Film coefficient for transfer of heat from bismuth to graphite: 129500 joules/sec- °C
C_F		Specific heat of fuel mixture: 0.155 joules/gm-°C
ℓ		Prompt neutron lifetime: 8×10^{-4} sec
ρ'		Bismuth density at core inlet: 9.91 gm/cm ³
$\partial \rho / \partial T_F$		Change in bismuth density with temperature: -1.32×10^{-3} gm/cm ³ - °C
A'U' ρ'		Bismuth flow rate at core inlet: 353000 gm/sec
V		Velocity of sound in bismuth: 152400 cm/sec This item is 0 when pressure is not calculated
L		Flow distance from core outlet to free sur- face: 150 cm

Z Vertical distance from core outlet to force surface: 150 cm
This item is 0 when pressure is not calculated.

f Friction factor in upper reflector: .0205
This item is 0 when pressure is not calculated.

\mathcal{L} Head loss term in upper reflector: 1.26
This item is 0 when pressure is not calculated.

D_e Hydraulic diameter of flow channel in upper reflector: 3.8 cm

A Flow area in upper reflector: 147 cm²

g Acceleration due to gravity: 981 gm/sec²

N_c Number of fuel channels in core : 300

γ Ratio of specific heats of pressurizer gas: 1.67

θ_o Time required for fuel to flow through core:
11.4 sec

L_s Length of outlet pipe: 160 cm

r_1 Radius of fuel channel in core: 1.91 cm

A_s Cross sectional area of outlet pipe: 147 cm²
This item is 0 when pressure is not calculated.

P_0 Initial power: 8.3 MW

ρ_0 Initial mean density of bismuth in core:
9.84 gm/cm³

$V_{p, 0}$ Initial volume of gas above free surface:
170000 cm³

$p_{p, 0}$ Initial pressure of gas:
1.035 x 10⁶ dynes/cm² (15 psi)
This item is 0 when pressure is not calculated.

$T_{F, 0}$ Initial mean bismuth temperature in core.
(Calculated by machine program): 475.84757 C

$T_{n,0}$ Initial graphite temperatures in core. (Calculated by machine program):
 478.53947 C (at fuel surface)
 479.64958 C
 480.08120 C
 480.19541 C

U_0 Initial velocity of bismuth in upper reflector. (Calculated by machine program):
 245.78920 cm/sec

q_0 Initial rate of flow through outlet. (Calculated by machine program):
 36131.012 cm³/sec

$P_{c,0}$ Initial core pressure. (Calculated by machine program): 3.4551527 x 10⁶ dynes/cm² (50 psi)

$k_{ex,0}$ Initial excess multiplication (Calculated by machine program): .0027802655

b. Machine Operation

The program selected its own time interval based on a comparison of results with those obtained using half-and double-intervals.

The shortest intervals were required during the initial parts of the transient. Intervals of .003 - .006 sec were required when pressure was calculated. Without pressure, intervals of $\Delta t = .012 - .024$ sec were used.

After the initial disturbances, the program selected larger time intervals. Without pressure, these became as large as .384 sec.

An approximate calculation time is 2-3 sec of real time per hour of machine time.

c. Output

For all cases except 63, the output format was

t	Δt	T_F	P	ρ	V_f	U
C_1	C_2	C_3	C_4	C_5	C_6	T_{G1}
T_{G2}	T_{G3}	T_{G4}	p_c	p_p	k_{ex}	-

For case 63, the output format was

t	Δt	T_F	P	ρ	V_P	U
C_1	C_2	C_3	C_4	C_5	C_6	T_{G1}
T_{G2}	T_{G3}	T_{G4}	q	p_p	k_{ex}	p_c

It is only the three lines which are of interest. Occasional fourth and fifth lines are due to time interval testing and changes in program parameters.

Caution must be exercised because of the time interval testing. The program sometimes decides it is using too large a time interval, and goes back, repeating some calculations with a smaller interval. When these repeated time steps are found, the second set is more accurate.

PART TWO
RESEARCH AND DEVELOPMENT PROGRAM

I. CHEMISTRY

A. CHEMICAL METHODS OF ANALYSIS

1. Wet Chemical Analysis

Major efforts have been directed toward sample preparation for spectrographic analysis to simplify operation and speed up analysis. This emphasis will aid present analytical work and develop methods more applicable to radioactive samples and handling problems.

Preparation of standards for the detection of corrosion products in bismuth samples were based on the need for high purity bismuth. Chromium levels were reduced to negligible amounts by reprecipitating the bismuth as the nitrate and oxy-nitrate. For removing iron, an electrochemical separation using a mercury cathode cell was used successfully to amalgamate the bismuth. At the amperage used, the iron remained in solution and was decanted from the mercury. The bismuth metal was in turn separated from the mercury and was tested spectrographically for purity using the oxide form. An iron content, barely detectable by spectrographic means was obtained. Contacts were made for high purity bismuth and material was received which was reported to contain <0.1 ppm iron. This material appeared to have approximately the same iron level as that prepared in B&W's research laboratory.

More recent efforts were directed toward determining fission products in conjunction with projected corrosion product solubility studies. Spectrographic and colorimetric procedures are in progress using cerium as representative of rare earth elements. Yttrium has been used as the rare earth carrier, and bismuth separation is effected by sulfide precipitation.

The ester halogen method for determining aluminum nitride was used successfully, and the chemical zirconium method for possible fission product interferences was tested. Nominal concentrations of fission products indicated no interference.

2. Spectrographic Determination of Corrosion Products in Bismuth

Chemical methods have been worked out for determining the corrosion products iron, chromium, manganese, and molybdenum in bismuth. To save time, emphasis has been placed on determining these elements by spectroscopic methods. Since the chemical chromium determination was the most time-consuming, its determination spectrographically was considered most important.

The method of Owens and Webb, British Atomic Energy Research Establishment, was followed using cobalt as an internal standard and d. c. arc excitation of the bismuth oxide sample. Three independent sets of standard samples were prepared - one set by dry grinding, recommended by Owens and Webb; the other two sets by a wet method, using different bismuth base material. The latter two working curves were practically identical and are considered valid. About 50 chromium determinations have been carried out. Accuracy is considered about ± 10 percent of the amount present in the 1-25 ppm range.

A similar program was initiated with the manganese determination but has not been completed. Manganese determinations on loop samples are carried out currently by wet chemical methods.

Determination of iron in the 1-25 ppm range is being attempted by this method. Until recently the difficulty of obtaining a sample of bismuth with very low (less than 1 ppm) iron content has rendered spectrographic determination of this element quite difficult. However, a sample of very high purity bismuth was acquired, and work has been resumed.

3. Spectrographic Determination of Synthetic Fission Products in Bismuth

A study was initiated to find out what elements comprising the synthetic fission product mixture might be determined spectrographically.

The initial approach was to decide which, if any, of these elements might be determined by the rotating disc-solution technique. It was found that this method would probably be sensitive enough to determine barium and strontium, but none of the proposed rare earth fission products. Ytterbium was easily detected, and it is suggested that the difficulties of determining rare earth fission products would be markedly reduced if ytterbium could be substituted for the proposed lanthanum-enriched misch metal.

Because the rotating-disc method lacks sensitivity, emphasis was shifted to investigating the possibility of gaining more sensitivity through use of d. c. arc techniques. Preliminary investigations showed that probably all synthetic fission elements except samarium and ruthenium can be determined by suitable adaptations to the basic d. c. arc method.

4. Determination of Thorium in Bismuth by X-ray Fluorescence

During studies on bismuth-thoria slurries, it became necessary to determine whether magnesium was reducing thoria to thorium. Thoria is relatively insoluble in nitric acid and may be determined as an insoluble residue, but the thorium metal dissolves and goes along with the bismuth-nitric acid solution. To determine the thorium metal, the solution was made alkaline and the precipitate ignited and examined by X-ray fluorescence for the thorium $L\alpha$ radiation. Synthetic standard samples gave a working curve over the range of 0.5-3.0 percent Th in which the corrected line intensity of the Th $L\alpha$ was linear with concentration. By using this technique, it was possible to demonstrate quickly that thorium metal was formed in the thoria-bismuth mixture.

5. Further Analytical Development

A preliminary description of the analytical R&D required for the LMFRE was released for publication in BAW-1104.⁵ The R&D needs include:

- a. Further analytical methods for "cold" experiments
- b. Corresponding methods for irradiated samples
- c. FPV analysis of fuel solution and off gas
- d. Polonium analysis in several media

- e. Isotopic analysis of fuel solution
- f. Thorium and slurry analysis
- g. Fission product analysis
- h. Electrolytic analytical methods

Liaison with several design groups has continued for the purpose of obtaining satisfactory design of sampling mechanisms, laboratory arrangements, and hot cell arrangements.

A subcontract has been awarded to Nuclear Science and Engineering Corporation for developing analytical methods and apparatus for volatile fission products both in the fuel solution and in the off gas. These methods will be used in the fission gas study to be conducted as a part of Radiation Loop No. 2 (ETR). The scope of this subcontract calls for developing a means of measuring xenon, krypton, and iodine. NSEC will develop a chromatographic method for the separation of the gaseous elements. The separated gases will be assayed using specialized counting equipment.

After the annual LMFR analytical symposium at BNL, it can be concluded that the basic analytical techniques for analyzing unirradiated fuel solutions are well in hand. These techniques must be refined for use with highly irradiated samples. Work is well under way to develop more efficient and integrated methods of analyzing several constituents simultaneously.

It has been decided to adopt the BNL analytical methods as a basis for the control analysis for Radiation Loop No. 2. These methods and sample handling procedure will be used by BNL for the control of Radiation Loop No. 1. Loop No. 1 fuel solution will be analyzed for uranium, magnesium, zirconium, and corrosion products in the presence of about 1 curie/cc of mixed fission products and about .01 curie/cc of polonium. The initial steps in BNL's universal sample preparation technique are believed to remove most of the mixed fission product activity along with practically all of the polonium activity. These steps also remove the bismuth, which is an interfering agent in many analytical techniques.

B. CHEMICAL CLEANING AND DECONTAMINATION

Two sumps and pumps from the bismuth test loops were cleaned with mercury vapor. The sumps were filled slightly less than half

full with mercury, then the pumps were sealed. The mercury was heated to near the boiling point; mercury vapor, produced in the air space above the mercury level, then condensed on the upper section of the sump and pump.

The bismuth was completely removed from the first pump. However, a deposit of additives plus iron, which the mercury could not remove, had built up during loop operation. A deposit remained on the second pump lid after mercury treatment. A sample of this deposit taken for chemical analysis, has been analyzed for mercury only, which is present in excess of 90 percent. The analysis shows that the mercury is amalgamating with the bismuth and that it would be only a question of time until this deposit would be dissolved completely.

Preliminary bench scale tests are being conducted to investigate the removal of bismuth by mercury vapor in a loop. These tests are to investigate methods of driving the mercury vapor in a tubular system and then condensing it where desired to remove bismuth. It appears that this may be accomplished by proper temperature control of the tubes.

C. FUEL SOLUTION STABILITY (Alliance Research Center)

The determination of uranium solubility in bismuth with and without additives in the "pot-type" apparatus has been completed. The tentative conclusions from this test are as follows:

1. The solubility curve of uranium in bismuth, as indicated by the present method, is almost identical with that drawn from the data of D. G. Schweitzer of BNL.

2. The effects of additives (zirconium, magnesium and fission products) on the solubility of uranium in bismuth was within the experimental limits of the method at the additives level used.

A technical report covering this work is being prepared.

D. URANIUM SOLUBILITY (Armour Research Foundation)

Experimental equipment was constructed and checked out. Two methods for obtaining solubilities are being used - the standard method, to which most effort is devoted, and the resistivity method. Development of the resistivity measurements has reached a stage where the method is reliable but slower than the standard method.

During preliminary runs, it was discovered that hydrogen refining of the bismuth produced no noticeable lowering of the trace impurities and did nothing to affect the experimental results. Therefore, this preliminary step has been discontinued.

Preliminary data on the U-Bi binary system have been obtained. Unlike prior published data for the system (but similar to BNL's recent interpretation of its own data), the solubility data appear as two straight line segments when plotted against reciprocal temperature. This deviation from van't Hoff's relationship (the straight line relationship expected) probably results from a change in the heat of solution because of a phase change.

There is good internal agreement of the U-Bi preliminary solubility data since both cooling and heating runs, in addition to those using refined and unrefined bismuth, appear to lie on the same curve. Analyses are performed by standard wet chemical methods.

A comparison of some preliminary data obtained by the resistivity and the standard method follows.

<u>Weight Percent U</u>	<u>Liquidus Temperature, °C</u>	
	<u>Resistivity</u>	<u>Direct Sampling</u>
0.47	505	510
0.10	362	355

Referring to concentration levels, the results by the two different methods are within 20 ppm of each other, well within limits of experimental error.

E. FUEL PREPARATION

1. Armour Subcontract

Armour Research Foundation has been selected to investigate methods of introducing additives to the fuel stream. This effort has been approved by the AEC as an amendment of their solubility subcontract. The study is to be completed by the end of the year.

2. Possible Means of Uranium Addition

a. General

The uranium addition problem falls into two distinct phases: (1) additions as initial criticality is approached, and (2) additions to make up for burnup.

b. Approach to Initial Criticality

The best information now available is that the primary loop will be operated initially at 25 percent of the anticipated critical concentration. This means that, subsequently, about 45 lb of uranium must be added in increments, the size of the permissible increment depending on the predicted distance from criticality.

During normal reactor operation it will be desirable to add uranium in about 50-gram increments. If the same size additions are made prior to criticality, a uniform addition slug can be used for both purposes. This means that about 400 slugs would be required to reach criticality (assumes 1000 ppm critical) after the initial loading, or 530 slugs would be required for the total initial loading. A remote control mechanism drops these slugs down a tube into the primary loop piping. This mechanism would be best located between the reactor and pump in the hot leg of the system. The end of the slug chute should be a cage to minimize the danger of slug movement through the primary loop before dissolution.

c. Additions to Replace Burnup

The slugs will be 5 percent U-Bi alloy and contain 50 grams of uranium; the total slug will weigh 1000 grams. The dimensions of such a slug would be 1 1/4 in. diameter by 5 in. long. The slugs will be canned in magnesium or some high magnesium alloy. The can will be gas tight; thus oxidation of the U-Bi slug prior to dissolution will be minimized. The slug will remain intact throughout the handling operation prior to introduction into the fuel. (Uncanned bismuth slugs would be subject to abrasion and breakage in the loading mechanism)

If the slugs are canned in .016-in. thick magnesium jackets, a total of about 5700 grams of magnesium would be added from this source, including the initial loading and 1 year's burnup. In 100 ft³ of fuel this amounts to 206 ppm magnesium. This concentration increase in magnesium could be tolerated over the life of the experiment. A logical procedure would be to pretreat the primary loop at a magnesium concentration of 150 ppm. After the initial loading the magnesium concentration would be about 356 ppm.

The 5 percent U-Bi alloy will contain uranium as UBi_2 in finely divided form. Once the magnesium jacket is dissolved through, the finely divided uranium that is liberated when the bismuth alloy melts is expected to go into solution rapidly. (The rate of dissolution of magnesium is rapid and dissolution will take place from both the outside and inside of the can.)

3. Theoretical Consideration of Rates of Dissolution

A study of the kinetics of dissolution was made with the following objectives in mind: to present a mathematical model for the definition of a rate constant, to facilitate interpretation of experimental results, and to reduce the quantity of experimental data required.

The theoretical equations were set up for a general case, and the solutions are presented in graphical form as a function of dimensionless parameters. The final equations derived from the assumed mathematical model are functions of saturation concentration, initial concentration, final concentration after all the material has dissolved, particle size and geometry, time, degree of dissolution, and the rate constant. No attempt has been made to predict the effect of agitation and other such variables on the rate constant itself. This information must be obtained from experimental data.

In this study, the process of dissolution of a solid in a liquid phase has been assumed to follow the Fick's Law model, where, for this case, the driving force is the concentration difference between the concentration of the saturated film assumed to be surrounding the solid at all times and the concentration of that particular specie in the solution.

For the case of a solid being dissolved in an infinitely large solution, the concentration of which remains constant at its initial concentration throughout the dissolution, the rate equation is:

$$\frac{dw}{dt} = -kA(w) [P_{eq} - P_s] \quad (1)$$

where w = weight of solid present at time t - grams
 $A(w)$ = surface area of solid (or solids) when total weight of solids present is w - cm^2
 P_{eq} = saturation concentration of specie at given temperature and solution composition - ppm
 P_s = original concentration of specie in solution - ppm
 k = rate constant - $grams/sec\ cm^2\ ppm$

The solution to the above equation is

$$k\tau = 1 - \left(\frac{w}{w_o}\right)^{1/3} \quad (2)$$

$$\text{where } \tau = \left[\frac{1.61 (P_{eq} - P_s)}{\Psi \rho^{2/3} w_o^{1/3}} \right] t \quad (3)$$

and where Ψ = sphericity of solids

w_o = original weight of solids added - grams. However, for substitution into equation (3) for τ , the original weight of a single, representative particle or solid should be substituted, in case more than one is being dissolved.

ρ = density of solid - gms/cm^3

The more general case of dissolving a solid in a solution of finite size (where the concentration of the specie in question increases as the solid dissolves and thus further reduces the potential driving force) is expressed by the following differential equation.

$$\frac{dw}{dt} = -kA(w) [P_{eq} - p] \quad (4)$$

where p is the specie concentration of the solution at any time t . Naturally, p is a function of the original solution concentration, the amount of solid dissolved, and the weight of the original solution. In

this derivation, the weight of the solid is assumed small compared to the total weight so that the change in weight of the liquid phase is negligible during the dissolution process.

In the solution of equation (4) it becomes convenient to define a parameter (w_o/w_q) where w_o is the original weight of solid added and w_q is the grams of specie the solution is still capable of absorbing after complete dissolution of the w_o grams originally added; i. e., it is the amount that still must be added to saturate the solution.

The final solution of equation (4) is of the form $k\tau = f\left[\frac{(w/w_o)}{(w_o/w_q)}\right]$, where the actual function is

$$k\tau = \frac{1+(w_o/w_q)}{3(w_o/w_q)^{1/3}} \left\{ \frac{1}{2} \ln \frac{\left[1+(w_o/w_q)^{1/3}\right]^2}{\left[1+(w_o/w_q)^{1/3} (w/w_o)^{1/3}\right]^2} \times \frac{\left[1-(w_o/w_q)^{1/3} (w/w_o)^{1/3} + (w_o/w_q)^{2/3} (w/w_o)^{2/3}\right]}{\left[1-(w_o/w_q)^{1/3} + (w_o/w_q)^{2/3}\right]} + \sqrt{3} \left(\tan^{-1} \frac{2(w_o/w_q)^{1/3}-1}{\sqrt{3}} - \tan^{-1} \frac{2(w_o/w_q)^{1/3} (w/w_o)^{1/3}-1}{\sqrt{3}} \right) \right\} \quad (5)$$

In the calculations performed by the methods above, k for a given system is assumed to have a fixed value, independent of concentrations, temperature, or surface area. However, k may be, and in all probability will be, a function of some additional variables such as degree of agitation. These relationships must be gleaned from additional experimental data. For experimental work performed with the same system and under conditions of equal agitation, the k value should be applicable to the design of equipment operating under varying conditions of particle size and shape, temperature, and concentrations.

Values of $k\tau$ as a function of (w/w_o) and (w_o/w_q) have been calculated and are presented graphically. Back calculation of (w/w_o) for known values of $k\tau$ is also facilitated since an implicit solution of equation (5) by trial and error is not needed.

FIG. 30: FRACTION OF WEIGHT REMAINING AS A FUNCTION OF $k\tau$ FOR VARIOUS VALUES OF w_o/w_q

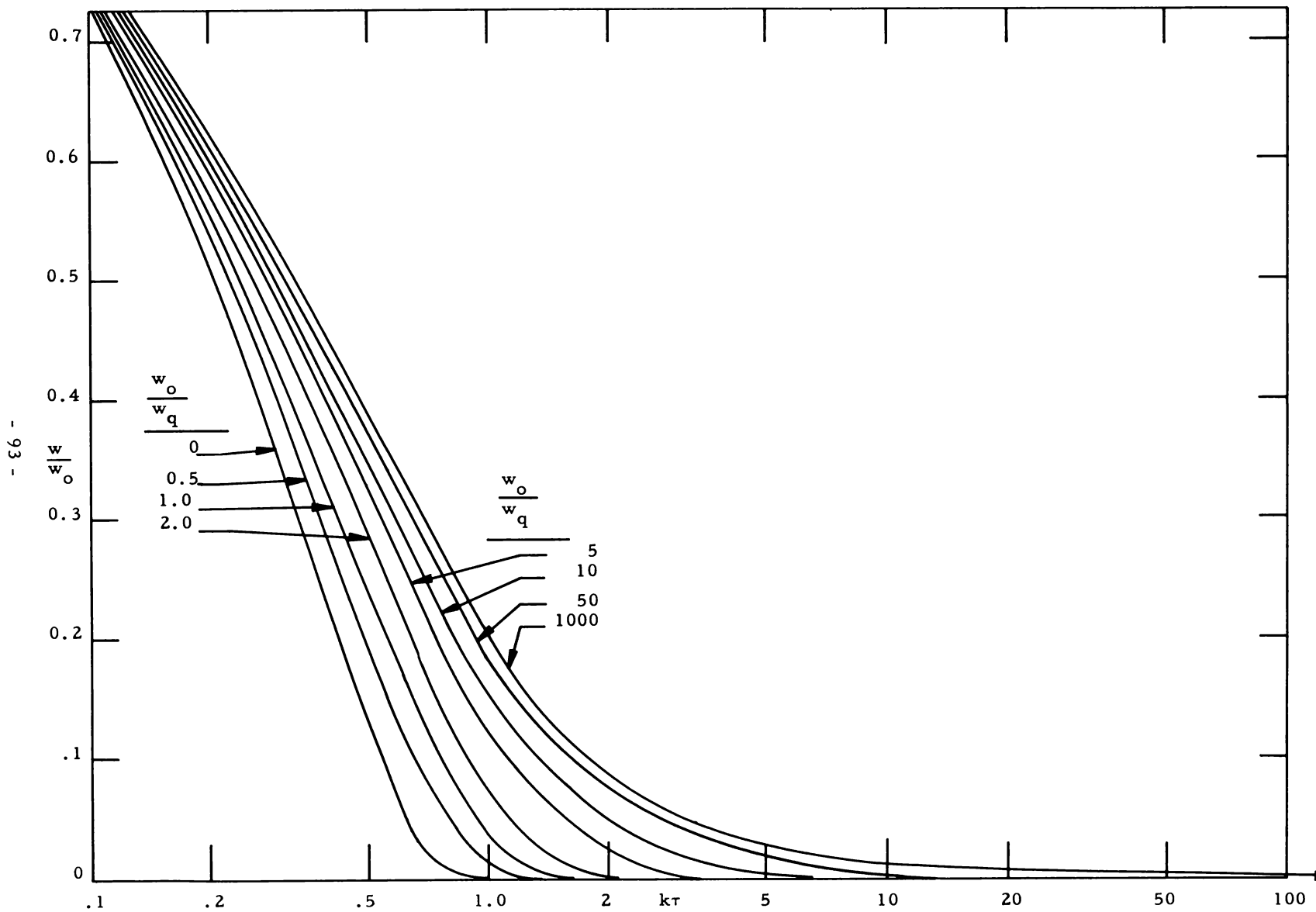


FIG. 31: $k\tau$ FOR COMPLETE DISSOLUTION VS. w_o/w_q
 (i. e. CROSSPLOT FOR $w/w_o = 0$)

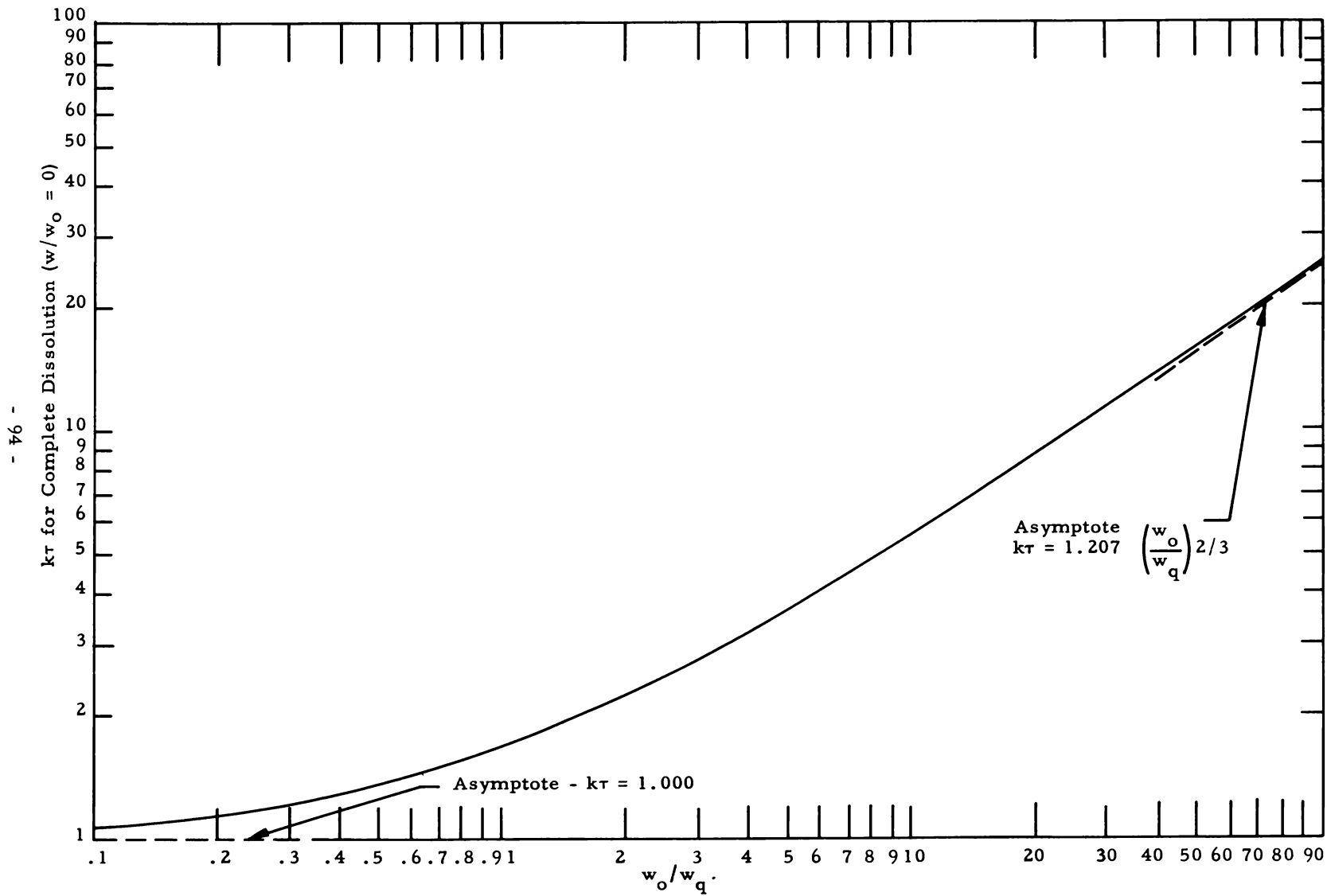


Figure 30 is a graphical presentation of equation (5) where $k\tau$ is given as a function of (w/w_o) and (w_o/w_q) .

The following empirical equation was derived for the range above that given in Figure 30 and is felt to express the values of $k\tau$ to within ± 5 percent over the indicated range of interest:

$$\text{For } 1 > (w/w_o) > 0.7$$

$$k\tau \cong \left[1 - (w/w_o)^{1/3} \right] \left[1 + 0.0023 \tan^{-1} \frac{w_o/w_q}{3} \right] \quad (6)$$

where $\tan^{-1} \frac{(w_o/w_q)}{3}$ is in degrees (not radians!).

Figure 31 is a cross-part of $k\tau$ vs. (w_o/w_q) for $(w/w_o) = 0$; i. e., the values $k\tau$ extant at the time of complete dissolution. From this plot, the values of $k\tau$ for complete dissolution at any given operating condition (w_o/w_q) may be ascertained. This value may be directly used for computing the time required for dissolution if the rate constant is known or, conversely, the rate constant may be ascertained if the time for complete dissolution is known. For values of (w_o/w_q) greater than 100, the following asymptotic expression for the $k\tau$ at complete dissolution was found to hold:

$$k\tau = 1.207 (w_o/w_q)^{2/3} \quad (7)$$

In essence, the graphs presented permit the experimenter to compute values of the rate constant, k , from integral data without having to solve the complex equations that account for concentration changes during the course of dissolution. As an alternative, differentially obtained rate data - which may have been obtained to check the true constancy of the rate constant k for various operating conditions, may be conveniently applied to actual situations by use of the curves shown here. Once a rate constant has been determined, the time required for any degree of dissolution (or, conversely, the degree of dissolution at any given time) can be obtained by using the curves presented.

The functional relationships that have been derived and their implications are

Basic Relationships:

$$\tau = \left(\frac{1.61 [P_{eq} - P_s]}{\Psi \rho^{2/3} w_o^{1/3}} \right) t$$

$$k\tau = f \left[(w/w_o, (w_o/w_q)) \right] \quad (\text{See Fig. 30})$$

$$(w_o/w_q) = f \left[(w_o, W, (P_{eq} - P_s)) \right]$$

A convenient relationship for determining w_o/w_q is

$$\frac{w_o}{w_q} = \frac{P_i}{P_{eq} - P_s - P_i} \quad (8)$$

where

P_{eq} = saturation concentration in ppm of specie in question at given temperature and solvent composition

P_i = increase in ppm due to addition and complete dissolution w_o gms of material; i.e., $P_i = 10^6 (w_o/W)$, where W is the weight of solution in gms.

P_s = original concentration of specie in solution - ppm

Implications:

The following table shows the effect of the parameter in question on the time required to attain any desired degree of dissolution (including complete dissolution):

<u>Parameter</u>	<u>Effect of Time to Reach a Given Degree of Dissolution</u>
Density of solid - ρ	t varies directly proportional to $\rho^{2/3}$
Sphericity of solid - Ψ	t varies directly proportional to Ψ
Weight of a single representative particle of solid - w_o	t varies directly proportional to $w_o^{1/3}$
Initial driving force - $[P_{eq} - P_s]$	t varies as an inverse function of $[P_{eq} - P_s]$, but not linearly since a complex dual effect is present. An increase in $[P_{eq} - P_s]$ reduces the required τ for a given degree of dissolution. Then, t is inversely proportional to $[P_{eq} - P_s]$ for the new, reduced value of τ , so that the net effect is for t to be reduced more than the simple inversely proportional relationship.

The preceding table should be helpful in estimating the effect of changing various pertinent parameters.

The value of the rate constant can be determined using Figure 30 for data obtained at partial degrees of dissolution, and from Figure 31 for the case of complete dissolution. The procedure to be used is

- a. From a knowledge of initial and equilibrium conditions for the case under consideration, determine (w_o/w_q) . (See Equation 8)
- b. For the given value of (w_o/w_q) and the degree of dissolution, (w/w_o) , consult the appropriate figure and read off the value of $k\tau$.
- c. Now $k = \frac{k\tau \text{ (from the graphs)}}{\tau}$.

Substitute the experimentally obtained time and the other pertinent parameters into the equation defining τ ; using the τ thus obtained, evaluate the above equation for k .

Once the rate constant is known, calculations for any other initial and operating conditions can be computed. Times required for given degrees of dissolution at different operating conditions may be obtained without explicit knowledge of the rate constant k .

Figures 30 and 31 indicate how much longer it takes to attain a given degree of dissolution when the final concentration approaches the saturation concentration; i. e., as (w_o/w_q) increases.

The theory and the resulting curves presented here must be confirmed by experimental data and, therefore, must be considered tentative.

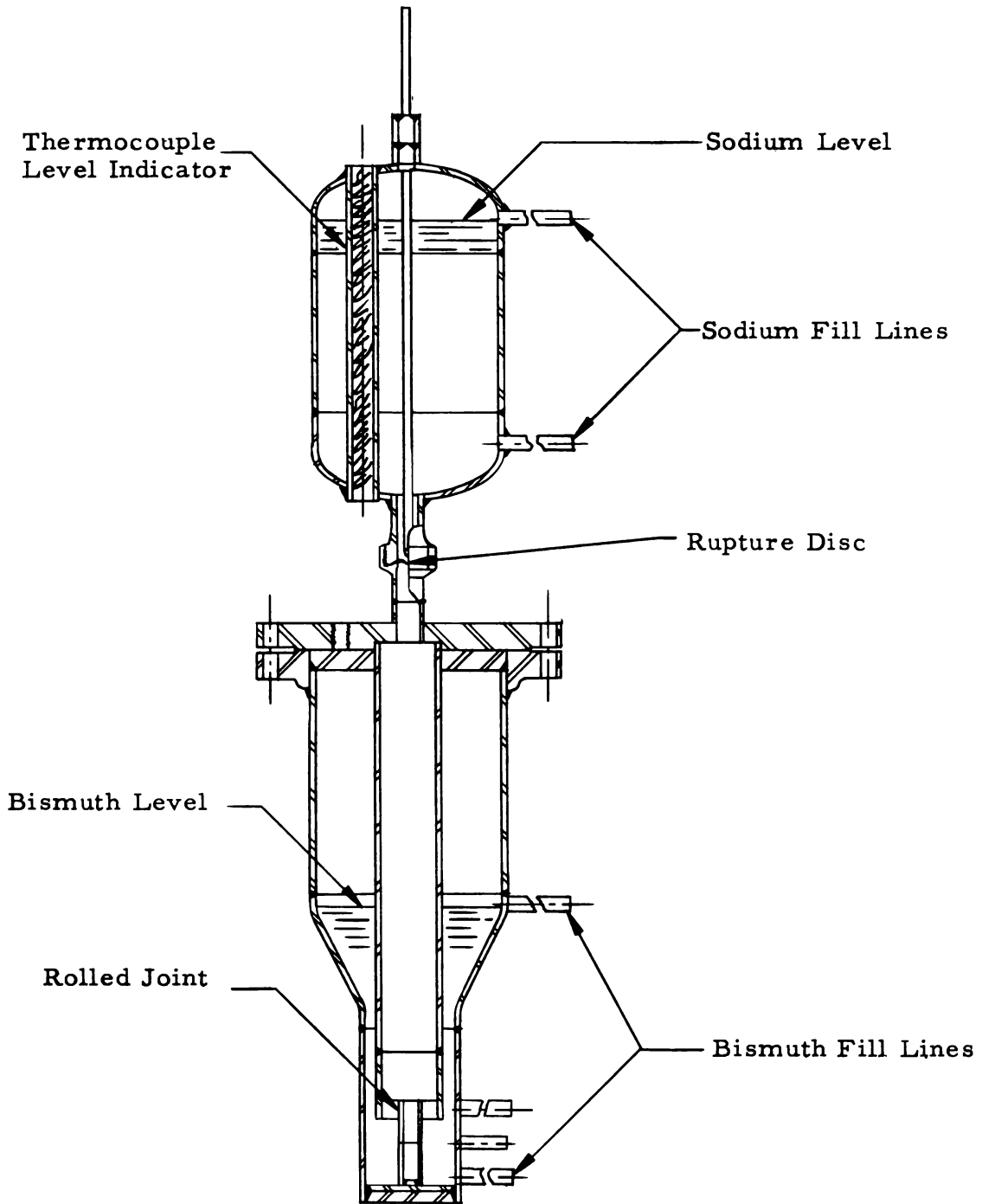
F. SODIUM BISMUTH LEAK TEST

The test apparatus (Fig. 32) has been constructed; the upper tank was charged with sodium, the lower with bismuth. The electrical wiring was completed recently leaving only instrumentation and insulation work.

A water test was run on the tube and tube sheet arrangement to adjust the leak so that a 500-hr test could be accomplished with the 20-lb sodium capacity of the unit. The unit used showed a leak rate of .0036 cc/sec.

The first run of this apparatus should begin within the next few weeks.

FIG. 32: SODIUM BISMUTH LEAK TEST



G. SLURRY DEVELOPMENT

1. Introduction

In November, 1957, the AEC directed both BNL and B&W to accelerate their effort on slurry development aimed at the long-range objective of establishing the technical feasibility of a converter or breeder LMFR. B&W immediately started work on slurries, and BNL accelerated the work that was already in progress. Concurrently, BNL and B&W initiated preparation of an overall slurry program. A preliminary report, representing the combined thinking and recommendations of these two organizations, was issued.

Slurries are attractive for reactors because of their fluid properties at concentrations greater than can be achieved with solutions. Fluid fuels or blankets promise simplification of fuel preparation, concentration adjustment, and reprocessing. The major problems in applying slurries to reactor heat removal systems are associated with stability, homogeneity, and corrosion or erosion.

The metal carriers under consideration for this study are bismuth, lead, and alloys that contain these as principal constituents. The slurries under consideration for an LMFR are grouped as soluble or insoluble. This distinction is made because the difficulties associated with mass transport are characteristic only of suspended particles that have an appreciable solubility in the vehicle. In general, insoluble slurries are dispersions of non-metals in a liquid metal. Thorium and uranium have limited solubility in bismuth and lead and, if added in excess of their solubility, form solid intermetallic compounds in the melt. The resulting dispersions are under consideration as LMFR fluids and comprise the soluble slurries.

Some problems encountered with soluble slurries are increasing particle size, accumulation of solids on cold surfaces, agglomeration of particles, and recrystallization of particles to a less desirable structure. These difficulties with soluble slurries have been attacked by (a) controlling the size and shape of particles forming the initial dispersion, (b) adding other metals which may either modify particle formation or decrease the solubility of the particular slurry particle in the liquid phase, (c) processing the slurry to restore fluidity lost by particle growth or (d) providing insoluble seeds to act as nuclei during crystal formation.

The selection of metals that may be added to modify particle formation is limited because of thermal neutron absorption considerations. Small amounts of high absorption cross section materials may be used; relatively large amounts of low cross section materials may be used.

The elements combined with uranium or thorium for insoluble slurries must have low thermal neutron cross sections. Uranium and thorium compounds with oxygen, fluorine, carbon, and sulfur are possibilities. The hydrides are probably too unstable to be considered. Sulfur, which has the highest cross section of the elements mentioned, has some nuclear limitation and may present processing and reconstitution problems.

Solid compounds of uranium and thorium with oxygen, fluorine, carbon and sulfur probably can be dispersed in the heavy metal carrier if proper wetting agents are added. These additives must meet the same nuclear restrictions imposed on the soluble slurry additives.

Possible slurries for use as nuclear fuels or breeder blankets must be critically examined in the following categories:

- a. Dispersion stability (with thermal cycling)
- b. Additives to insure stability
- c. Methods of initial preparation including solids work
- d. Fluidity of slurry
- e. Pumpability
- f. Effect of radiation on dispersion stability and general properties
- g. Effect of fission products on dispersion stability and general properties
- h. Chemical processing
- i. Reconstitution of slurry
- j. Mass transfer, corrosion, and erosion in dynamic systems
- k. Component development and testing
- l. Operational characteristics sufficient to design reactor blanket

Slurries are under consideration for both the single- and two-fluid LMFR. In the latter, they will be the fertile blanket in a two-fluid reactor. In this instance, a bismuth system should contain at least 10 weight percent thorium. A slurry for a single-fluid reactor would contain about 3 weight percent thorium as the fertile material and about 0.15 weight percent uranium as the fuel if a bismuth vehicle is employed.

The two-fluid arrangement has potential as a breeder reactor. The one-region reactor has lower thorium conversion but can be operated for long periods without chemical processing. These two concepts were evaluated recently and appear equally attractive. The eventual selection of a slurry for use in an LMFR concept must be based upon economics as well as all the categories mentioned. Some of this evaluation can be done on paper, but most will require experimental work. Of utmost importance are the physical characteristics of the dispersions themselves.

The sequence of work to develop possible slurries is important. The categories to be studied are listed in section b in the general order in which developmental work should proceed.

2. Research Program for Development of LMFR Slurries

The slurry development program planned for this work will cover about 6 years. The program is divided into five major phases, covering the 12 items presented in section 1. The suggested order for carrying out the program is such that slurry types are continuously screened so that the more expensive tests will be performed with, at most, two slurry types. The five phases are

Phase I: SCREENING TESTS

- a. Dispersion stability (with thermal cycling)
- b. Additives to insure stability
- c. Methods of initial preparation including solids work
- d. Fluidity of slurry
- e. Corrosion and erosion screening studies
- f. Pumpability

Phase II: RADIATION PROPERTIES

- a. Effect of radiation on dispersion stability and general properties
- b. Effect of fission products on dispersion stability and general properties

Phase III: SMALL LOOP TESTS

- a. Mass transfer, corrosion, and erosion in loops with between 100 and 225 F ΔT .
- b. Small component testing

Phase IV: PROCESSING

- a. Chemical processing
- b. Reconstitution of slurry

Phase V: LARGE LOOP TESTS

- a. Component development and testing
- b. Operational characteristics to the extent that sufficient information is available for design

Phase I, which is the preliminary screening stage, should eliminate at least 50 percent of the suggested slurries. Phase II may possibly eliminate some more of the slurries, since stability of the slurry in a neutron flux will be examined. Phase III will study the most promising slurries in larger dynamic systems and will reveal any difficulties associated with the larger circulating systems. Phase IV will examine processing methods for the most promising slurry. After the feasibility has been demonstrated in the earlier phases, development of full-scale components, Phase V, can proceed for the best slurry.

The program is planned so that the various phases overlap to some extent. It is estimated that Phase I will take about two years; Phase II, 1 1/2 years; Phase III, 1 1/2 years; Phase IV, 1 1/2 years; and Phase V, 2 years.

3. Progress During Reporting Period

a. Slurry Test Loop

Bismuth has been dumped back into the pump sump where it is being kept in a molten condition. This test will be restarted when the results of the basic slurry work have provided sufficient information to justify loop startup.

b. Slurry Technology

Efforts to disperse thoria in molten bismuth continue.

Indications are that magnesium is the only agent used in this series of tests that will promote dispersion of thoria in molten bismuth. Neither selenium nor zirconium were successful, although zirconium used with magnesium seems to increase the stability of the dispersion.

Results were unsuccessful when thorium metal was used as the dispersing agent; however, sufficient time may not have been allowed.

Good dispersion was obtained with less than 0.1 micron size thoria by using 1000 ppm magnesium and 1000 ppm zirconium at 750, 900, and 1200 F. These dispersions were in no case stable for more than one hr. In general much poorer results were obtained with 1-10 micron size thoria.

It was discovered that thoria is reduced by magnesium. This phenomenon casts doubt on the usefulness of magnesium as a dispersing agent. Since magnesium reduces ThO_2 there can be little doubt that in systems containing UO_2 , reduction to uranium metal will result and the magnesium will be oxidized. Therefore, it seems that if soluble quantities of uranium will disperse ThO_2 in bismuth, the use of magnesium is not necessary. This point is being further investigated.

While it was possible to disperse ThO_2 in bismuth, the poor stability achieved seems to indicate that agglomerates, rather than individual particles, may have been wet by the bismuth.

In an attempt to achieve wetting of individual particles, tests were made in which thorium metal in solution in bismuth was oxidized to ThO_2 . Bismuth trioxide was used as an oxidizing agent, but the test results showed no improvement over dispersions formed from ThO_2 .

A steel ball mill with tantalum balls has been used to break up the agglomerates and/or particles containing voids in the molten bismuth plus 1000 ppm magnesium and zirconium. The milling was done at 1200 F for approximately 40 hr. The melt is being examined.

H. URANIUM CARBIDE FORMATION (Michigan Research Institute)

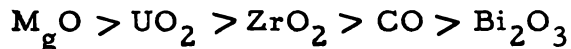
The subcontract with the University of Michigan for a study of carbide formation on graphite walls in contact with simulated LMFRE fuel solution has been approved by the AEC. Experimental equipment is under construction, and batches of uranium carbide for studying the thermodynamics of formation are being prepared. An all-out effort is under way to provide preliminary design information by the fourth quarter of 1958.

I. ELECTROLYSIS

Discussions were held with several research and development institutions concerning the possible application of electrolysis in the fuel processing systems under consideration. This activity has been discontinued at B&W, but the national laboratories will perform some studies as a part of their LMFR programs.

J. FUEL OXIDATION

A thermodynamic study of oxidation reactions occurring in liquid bismuth was carried out. The purpose was to determine (1) the relative stability of the oxides formed in the liquid bismuth in the event of air in-leakage, and (2) the relative effectiveness of the metal additives in the fuel as oxygen getters. Experimental data regarding solubility of oxygen and carbon (graphite) in bismuth were incorporated into the study. The results, when compared on an equivalent oxygen basis, indicate the order of stability of the oxides to be



Oxidation of carbon (graphite) apparently does not become competitive with magnesium until temperatures of 800 C or higher are reached. The effectiveness of magnesium as an oxygen getter seems to be supported by the experimental kinetics work at Brookhaven. Further work along these lines will determine the optimum magnesium concentrations for the LMFRE fuel.

K. ETR LOOP OFF-GAS HANDLING

The method of handling off gas from this loop, eliminating radioactive exhaust to the stack, has been accepted by the ETR staff. The operation is a modification of the reactor sweep gas system described in the last quarterly report (BAW-1107). A charcoal bed has been included in the gas loop to conserve space. Thermocouples placed radially and longitudinally in the charcoal bed are expected to provide data useful in future design calculations.

The feasibility of placing graphite blocks in the pump sump to evaluate fission product pick-up is under consideration.

II. INSTRUMENTS AND CONTROL

A. NON-NUCLEAR INSTRUMENTATION

1. Temperature Sensing Devices

Two sets of thermocouples have been received. One set is tantalum sheated; the other is Croloy 2-1/4 sheated. The tantalum sheated thermocouples have been calibrated and a test to determine their response rate (Fig. 33) will be run before they are installed in the utility loop.

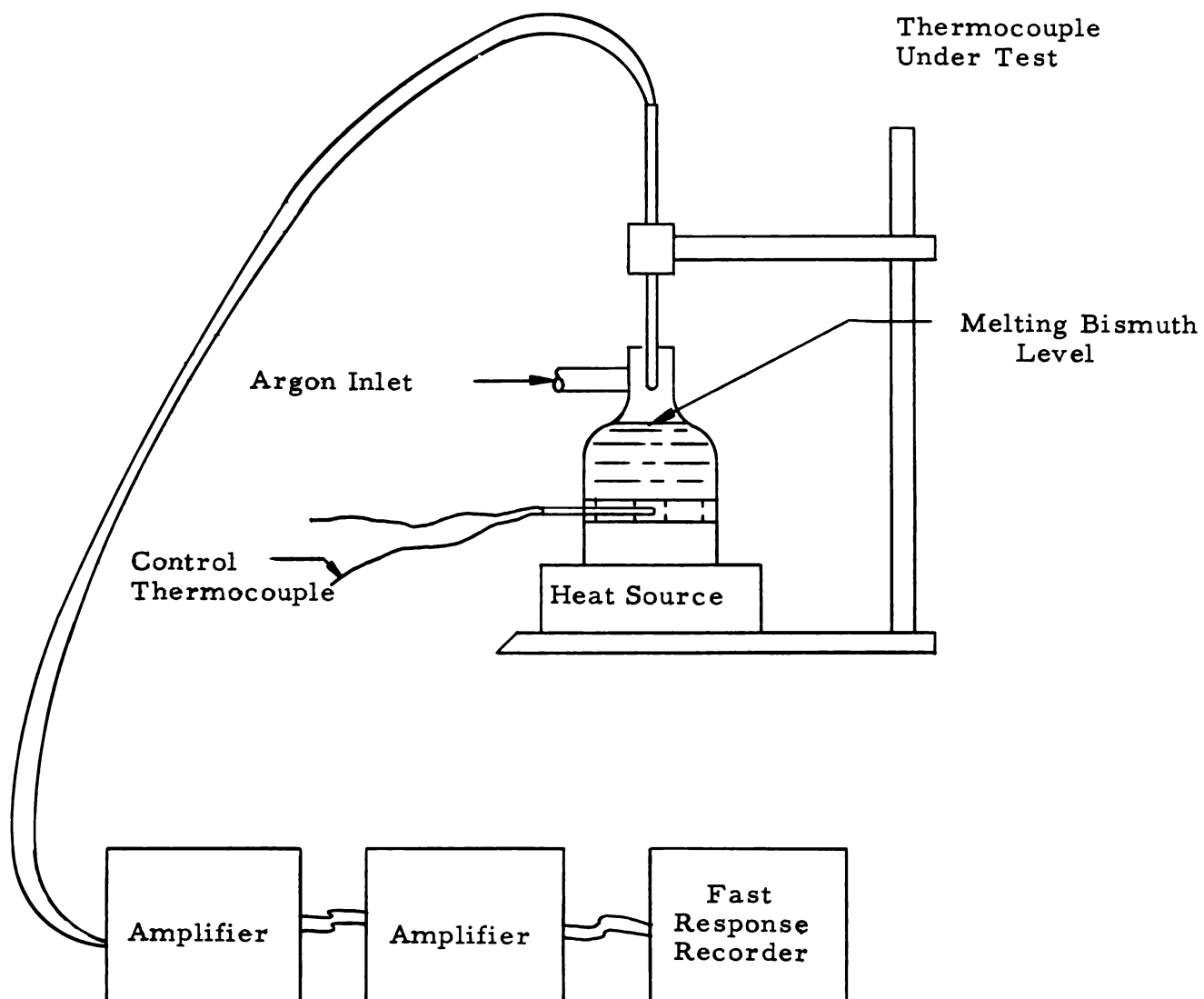
2. Pressure Sensing Devices

Two pressure sensing devices have been purchased for testing by the AED. Both units use a NaK filled slack diaphragm as the sensing element. Delivery of one instrument is expected within the next two months, the other later.

Apparatus necessary for calibration tests will be a bismuth filled tank that can be heated to various temperatures and pressurized to the maximum range required. Response time will be tested by applying gas pressure suddenly to the vessel and determining by a motion photographic technique the time required for the gauge to read line pressure. Accuracy will be checked by comparing the gauge under test with a precision test gauge that can be accurately calibrated on a standard dead weight tester. Sensitivity will be determined on the same device by varying the pressure slightly to determine the dead band.

Following these tests, gauges will be installed on the utility loop for a period of operation. Then, the tests will be repeated.

FIG. 33: THERMOCUOPLE RESPONSE TIME
TEST APPARATUS SCHEMATIC



3. Level Sensing Devices

Four indicators were purchased for testing by the AED. Two gauges employ a NaK filled diaphragm with a Statham strain gauge. The third uses a float linked to a magnetic core of a differential transformer, and the fourth is a "J" probe which operates on an electrical resistance principle.

These indicators will be tested by attaching them to a tank (Fig. 34) and varying the level by pumping the bismuth into an auxiliary tank. The indicated level will be compared to the level determined by an electrical conductivity probe for accuracy and sensitivity determinations. The response rate will be determined by suddenly forcing a known volume into a bismuth tank. This will change the level quickly and the response time can be recorded. After testing, the instrument will be removed from this apparatus and placed on a 2 1/2-in. loop for a period of operation, after which the earlier test will be rerun.

4. Flowmeters

Three prototype flowmeters have been purchased for testing by the AED: (1) an electromagnetic meter with a Croloy 2-1/4 lined stainless flow tube, (2) a flowrator type meter connected to an electronic transmitter, and (3) a calibrated elbow arrangement with differential pressure transmitters. All these meters are for the 3/4-in. pipe. They will be installed in the 2 1/2-in. loop just downstream of the pump for testing (Fig. 35) The upper tank of the loop will be used as a calibration tank with two conductivity probes to determine the flow per unit time. The flow will be varied by a control valve located downstream of the flowmeter. This should supply the necessary accuracy and sensitivity information required on the flowmeters. Following these tests, the flowmeters will be installed on the utility loop for an operational period. The tests on the 2 1/2-in. loop will be repeated (following the utility loop run) to determine the instruments reproducibility.

FIG. 34: TEST FOR LIQUID LEVEL INDICATORS
(SCHEMATIC)

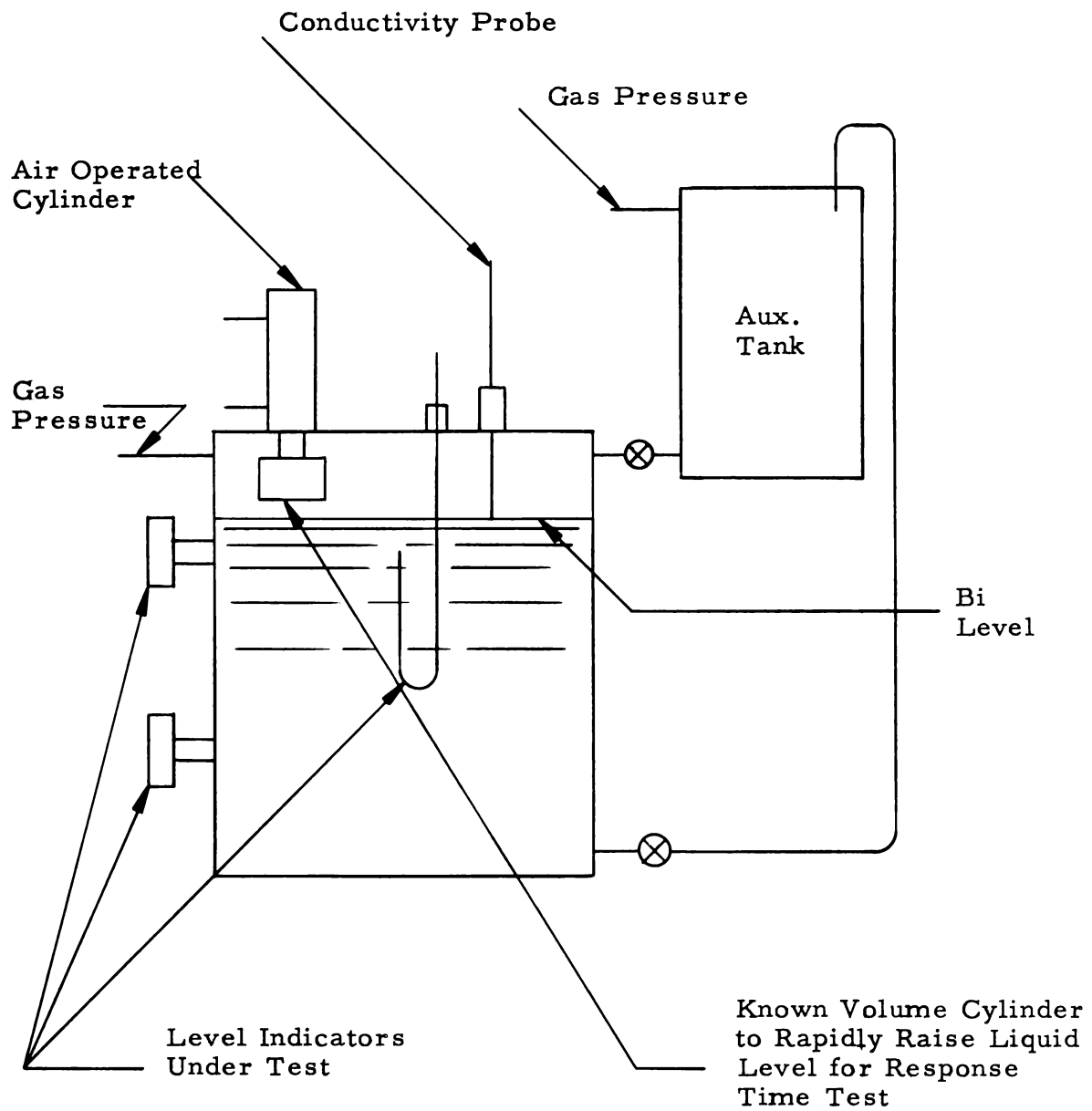
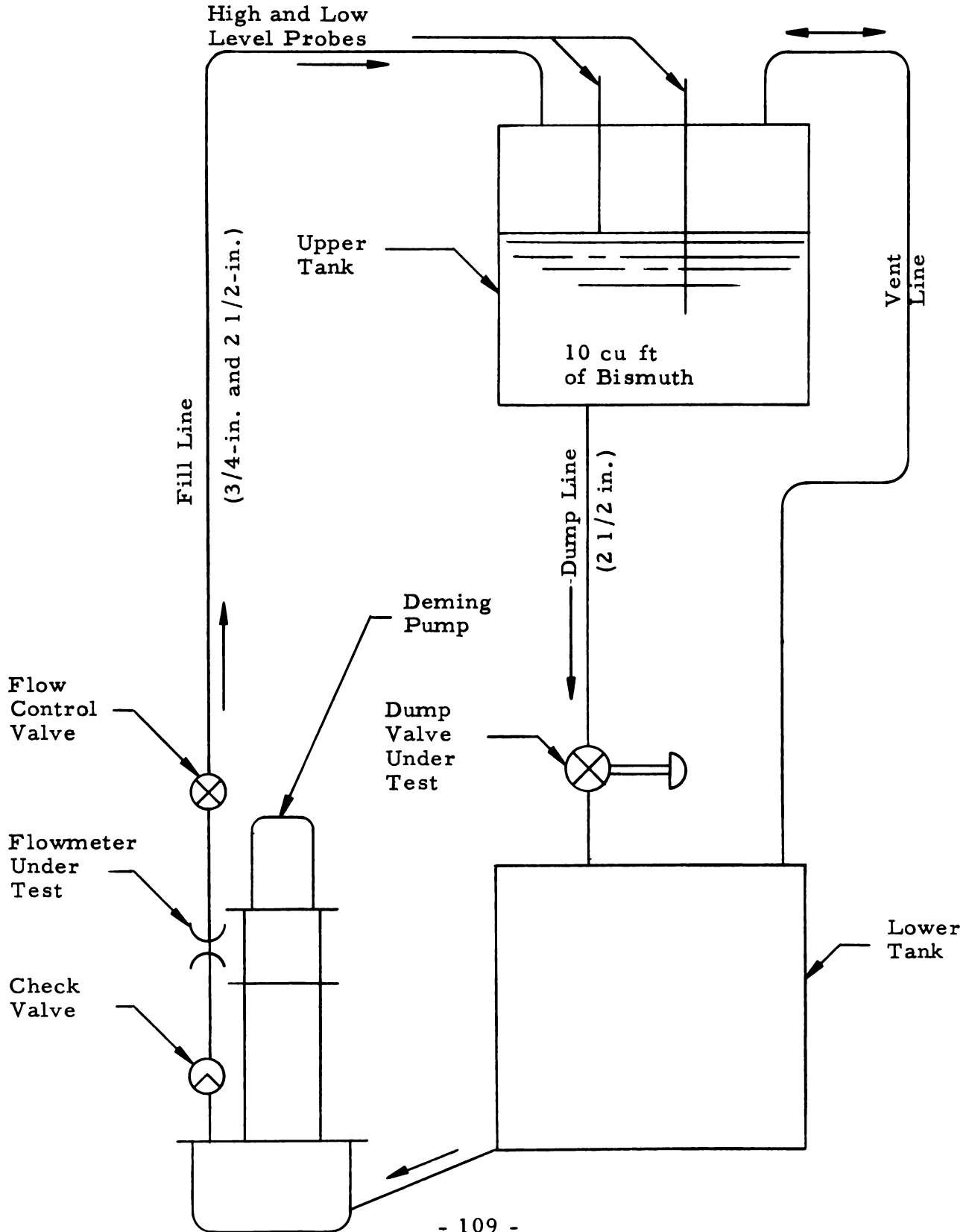


FIG. 35: 2-1/2-IN. LOOP FOR 3/4-IN. FLOWMETER TESTING (SCHEMATIC)



B. NUCLEAR INSTRUMENTATION

Uranium (Reactivity) Monitor

The second phase of the A. D. Little contract was initiated. This feasibility study will determine whether a method of monitoring for uranium (reactivity) in the primary system fuel stream is practical. The primary purpose of the instrument is to protect the reactor from serious over-concentrations of fuel and to initiate reactor scram and/or dump if dangerous conditions are detected. A variation of the slow/slow neutron measuring scheme as proposed in C-61041⁷ has been extensively investigated over a range of uranium concentrations from 0 to 1600 ppm by weight. The calculations are encouraging and indicate that this method may be adaptable to an LMFRE monitor.

The study covers a 5-month period and will be completed near the end of August. The final recommendation made at that time will indicate the cost of a monitor and the direction of development most likely to succeed.

III. MATERIALS TESTING

A. DYNAMIC TEST LOOPS

The dynamic loop test program was revised because information on 225 ΔT operation is not needed to specify material for LMFRE-I. The loop test schedule was revised to make available all data from the 135 ΔT tests of both Croloy 2-1/4 and Croloy 1-1/4 before material for the LMFRE-I is selected. Testing of steel at 225 ΔT will begin after completion of the 135 ΔT test program. Data from the latter program will be available before the reactor is operated at a 225 ΔT .

Table I shows the current status of the dynamic corrosion testing loops. Those shown operating with uranium are 885 F at the hot end and 750 F at the cold end. Metallographic examination of the components from Loop 4 (no zirconium) revealed severe intergranular or intercrystalline attack on all areas except the cold leg and the dash pot line. The weldment taken from the hot leg showed extreme porosity and appeared to have had a faulty root pass. The corrosive attack in the weld was intercrystalline. The attack was intergranular adjacent to the weld and there was an acicular structure of the heat zone. The dash pot line shows transported metal which caused partial plugging. The cold leg shows slight corrosive attack where the bismuth adhered to the leg. There was a metallic deposit of what appeared to be grains that had been partially taken into solution and carried by the bismuth stream. The attack on the corrosion specimen and specimen holding clips is intergranular.

Test 4A had a NaK leak in the inlet to the cooler. The NaK oxidized through the pipe and a small bismuth leak occurred. The combination of NaK and bismuth oxide sealed off the leak, before it was discussed and the test ran the scheduled time.

TABLE I
STATUS OF TEST LOOPS JUNE 25, 1958

<u>Test No.</u>	<u>Loop Mat'l</u>	<u>Heat Treat.</u>	<u>Operating Time With Uranium</u>	<u>Total Operating Time in Hr</u>	<u>Status of the Loops as of June 25, 1958</u>
2	2-1/4	Annealed	2161	2584	Under test
3	2-1/4	Annealed	1484	1719	Under test
Loop 4*	2-1/4	Annealed	None	1015	Secured and examined
4A	2-1/4	Annealed	1515	2187	Secured and examined
4B	2-1/4	Annealed	2780	3280	Secured and examined
5A	2-1/4	N&T	204	2723	Secured
5A2	2-1/4	N&T	165	328	Under test
5B	2-1/4	N&T	None	3001	Secured
5B2	2-1/4	N&T	452	672	Under test
5E	2-1/4	Annealed	None	None	Installing loop in test station
Slurry	2-1/4	Annealed	None		Bismuth being kept molten, in the sump
10	1-1/4	Annealed	2110	3300	Under test
11	1-1/4	Annealed	None	None	Installing loop in test station
12A	1-1/4	Annealed	1512	1724	Secured and examined
12B	1-1/4	Annealed	793	1970	Under test
12C	1-1/4	Annealed	3385	3530	Under test
13A	1-1/4	N&T	None	1297	Preconditioning (replaced pump)
13B	1-1/4	N&T	676	1170	Under test
13E	1-1/4	Annealed	None	None	Wiring station for test loop
13F	1-1/4	Annealed	None	None	Wiring station for test loop

*Test without zirconium

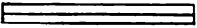
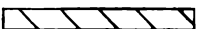
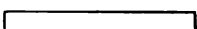
The metallurgical summary of Test 4A indicates that the loop was susceptible to intergranular attack and probably the attack was accelerated by the low zirconium concentration. A selective intergranular penetration took place in the welds. Transported metal was deposited at the colder section of the loop. Visual examination of Test 4A showed holes (apparently caused by erosion) through several of the 1/2-in. OD tubes where the bismuth enters the shell side of the heat exchanger from the main heaters. The internal surface of the 3/4-in. connecting piping was severely pitted.

Test 4B completed a total test time of 3280 hr, 2780 at the 135 F temperature difference. The average zirconium concentration during the test was approximately 157 ppm. Corrosion rates of the weighed specimens from the hot and cold legs of Test 4B are shown in Figures 36 and 37 respectively. The maximum average corrosion rate is a metal loss of .6 mil/yr. This test has the lowest bismuth corrosion rate of all the tests completed to date and had the highest average zirconium concentration during testing.

Tests 5A2 and 5B2 are reruns of tests 5A and 5B respectively. Test 5A completed only 204 hr at the specified 135 F temperature difference. After the last forced shutdown, circulation could not be started since some specimens from the cold leg got loose and became lodged across the outlet of the cold sample pot. Test 5B was secured because of difficulty in obtaining filtered bismuth samples and dissolving the additives in the loop. This was caused by contamination of the bismuth. Tests 5A and 5B were secured and started numerous times mainly because of mechanical failures of the test apparatus. Both tests contained mixed Croloy 2-1/4 and 1-1/4 tubes in the heat exchanger and were invaluable for obtaining operating experience on the corrosion loops.

Test 12A operated for a total of 1724 hr, 1512 at the 135 F temperature difference. The average zirconium concentration during the test was approximately 122 ppm. The corrosion rates of the weighed specimens from the hot and cold legs of Test 12A are shown in Figures 38 and 39 respectively. The maximum average corrosion rate was a metal loss of 3 1/2 mils/yr.

FIG. 36: CORROSION RESULTS - DYNAMIC TEST LOOP NO. 4B
HOT LEG

Key: MeOH Rinse 
 Sand Blasted 
 Bi Plated 

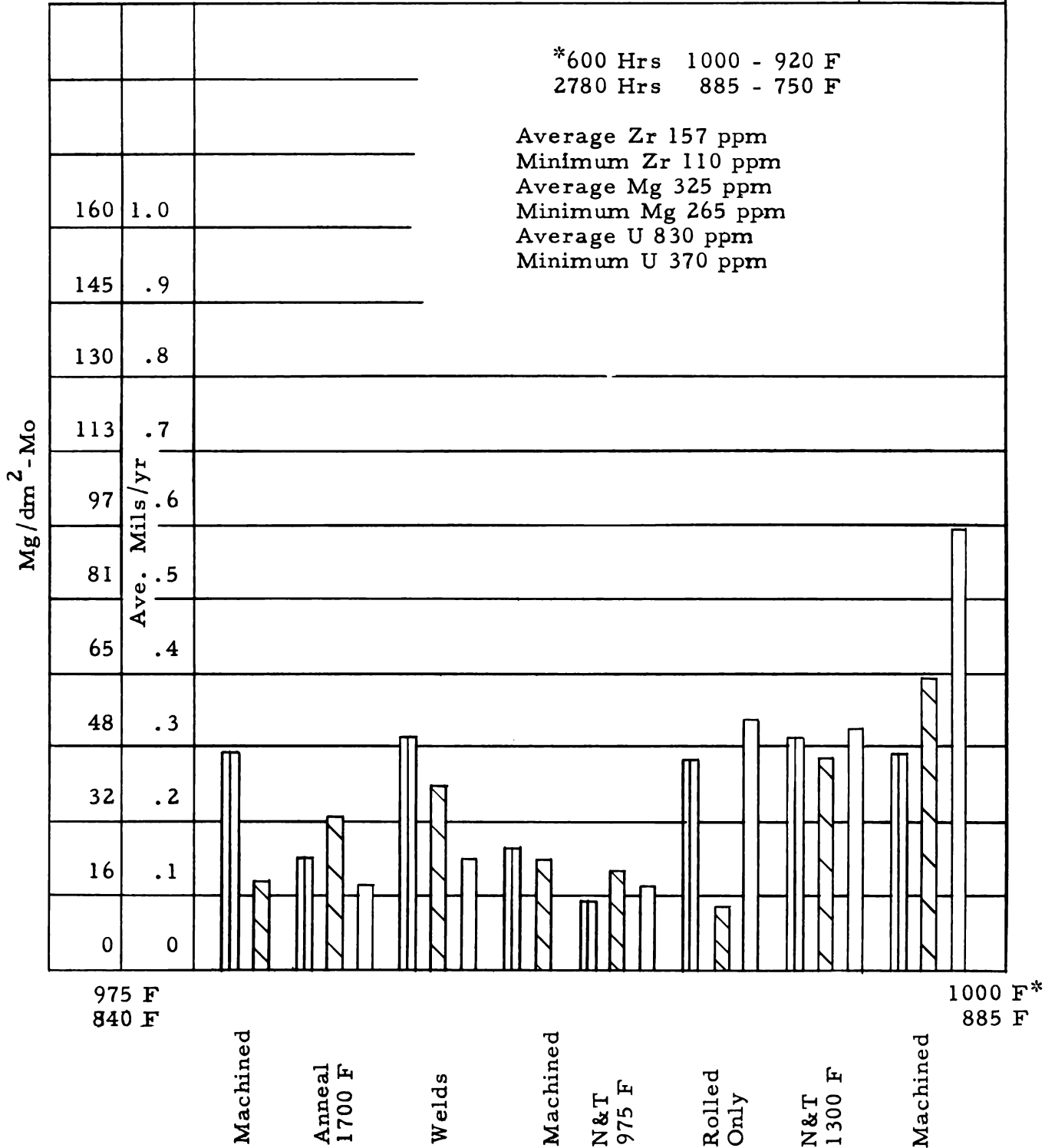


FIG. 37: CORROSION RESULTS - DYNAMIC TEST LOOP NO. 4B

COLD LEG Key: MeOH Rinse 
 Sand Blasted 
 Bi Plated 

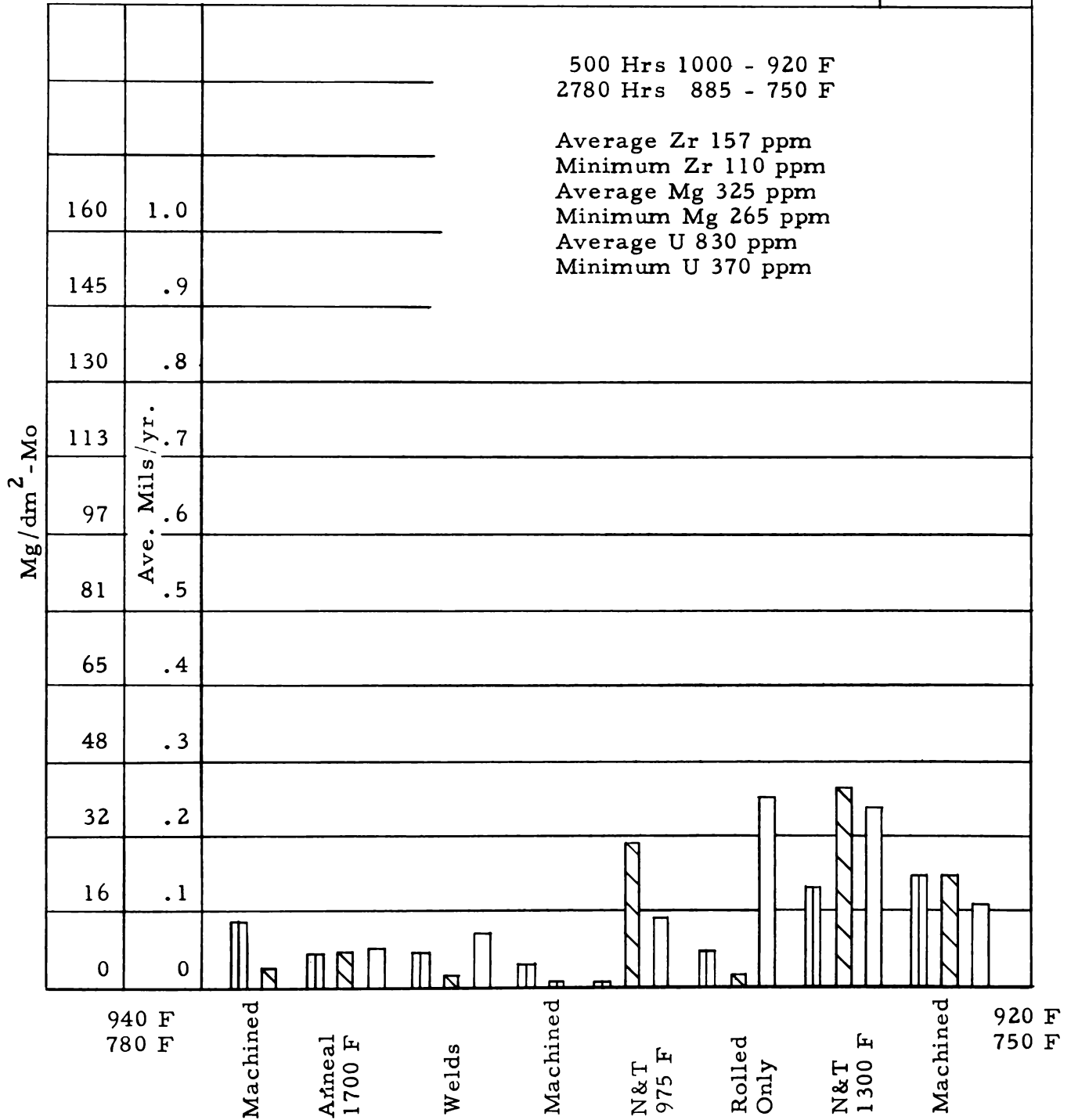


FIG. 38: CORROSION RESULTS - DYNAMIC TEST LOOP NO. 12A
HOT LEG

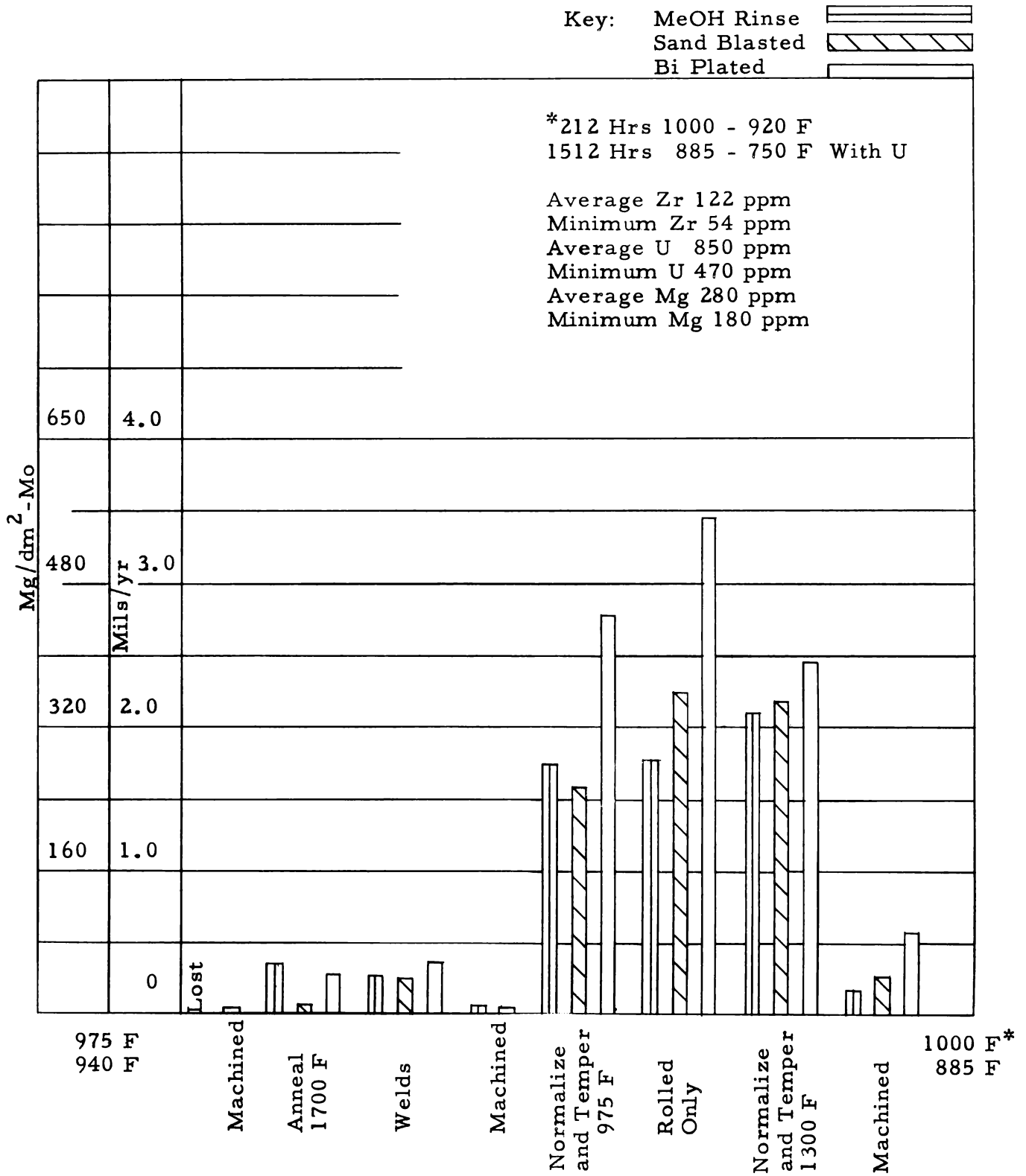
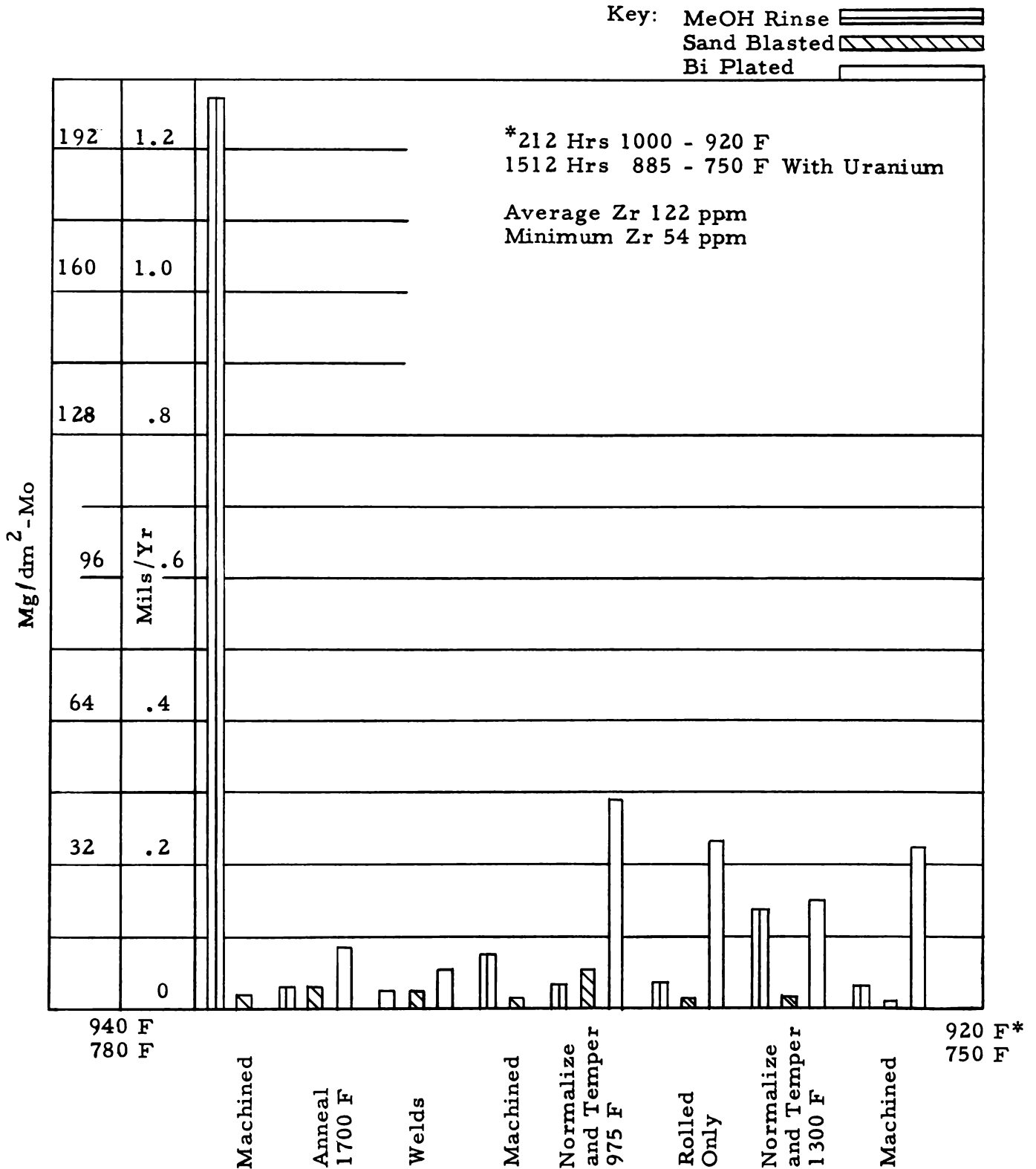


FIG. 39: CORROSION RESULTS - DYNAMIC TEST LOOP NO. 12A
COLD LEG



The pump on Test 13A froze during a plantwide power failure, necessitating replacement. The first attempt to start bismuth circulation with the new pump was unsuccessful. The loop was radiographed and a graphite sample boat was located in the piping. When this was removed, the test was started without additional trouble.

During the past three months, efforts have been centered around keeping the uranium concentration in the test loops up to the specified value of 1150 ppm. Three test loop critical areas are the pump sump head, the fill line on the sump, and the cold sample pot. The uranium concentration in the pump fill line was at normal levels, although there is a solid-to-liquid interface in that location.

Definite changes in the uranium concentration in the loops have been effected by changing the operating condition of the pump sump and the cold sample pot. No significant change was detected by maintaining the bismuth in the pump fill line at a minimum of 750 F. Changes that have been incorporated on the loops have not had sufficient operating time for their result on uranium concentration to be fully evaluated.

Attempts were made to determine whether there was a concentration of uranium in the fill line on Test 4A. A capsule was made up from a piece of pipe and attached to the valve on the end of the sump fill line. The line was heated and about one third of the total line volume was drained. Another capsule was attached and another one-third drained. The third capsule was attached and the last one-third of the line volume was obtained. None of the three bismuth samples analyzed were significantly different in uranium concentration from the concentration in the loop.

B. STATIC AND CAPSULE TESTS

The 2000- and 3000-hr capsules have been completed since the last quarterly report. The findings are reported in Tables II and III. These units used the standard fuel charge of 1150 ppm uranium, 350 ppm magnesium, and 175 ppm zirconium and operated at a temperature difference of 225 F with surface preparations and heat treatments as noted.

TABLE II

SUMMARY OF TILTING CAPSULE TEST
 MATERIAL-CROLOY 2 $\frac{1}{4}$, Δ T-225 F
 FLUID-BISMUTH WITH ADDITIVES-
 1150 PPM URANIUM, 350 PPM MAGNESIUM, 175 PPM ZIRCONIUM

Test No.	Test Time Hrs.	Heat Treatment			Cap- sule Prep.	Spec. Prep.	Specimen Wt. Change in Mg 975 F	Average Pene- tration Mils/Yr	Specimen Wt. Change in Mg 750 F	Average Pene- tration Mils/Yr	Remarks
		N-1700	N-1700	A.R.							
		T-975	T-1300								
288	2000	-	-	X	S.B.	S.B.	-856.6 -759.8	12.0	-34.0 -49.4	.62	
292	2000	-	-	X	A.C.	A.C.	- 39.4 - 51.7	.67	-10.9 -18.2	.21	
296	2000	X	-	-	S.B.	S.B.	-1189.7 -1277.4	18.37	-23.6 -34.7	.43	
300	2000	X	-	-	A.C.	A.C.	-322.3 -352.0	5.02	-16.1 -15.7	.23	
304	2000	-	X	-	S.B.	S.B.	-1713.7 - 685.4	17.0	-18.0 -14.9	.24	
308	2000	-	X	-	A.C.	A.C.	- 378.3 - 44.5	3.14	-23.1 -18.0	.30	
312	2000	-	-	X	Honed	Electro Pol.	-1510.5 Met	22.5	Met -1.0	.014	
326	2000	Hydrogen Fire	-	-	S.B.	S.B.	- 401.8 - 334.4	5.48	-21.1 -22.1	.32	
328	2000	-	Hydrogen Fire	-	S.B.	S.B.	- 726.0 - 818.7	11.5	-16.8 -19.7	.27	
330	2000	-	-	Hydrogen Fire at 975 F	S.B.	S.B.	-1503.3 -1886.2	25.2	-33.5 -29.2	.46	

TABLE III

SUMMARY OF TILTING CAPSULE TEST
 MATERIAL-CROLOY 2 $\frac{1}{4}$, Δ T-225 F
 FLUID-BISMUTH WITH ADDITIVES-
 1150 PPM URANIUM, 350 PPM MAGNESIUM, 175 PPM ZIRCONIUM

Test No.	Test Time Hrs.	Heat Treatment			Cap- sule Prep.	Spec. Prep.	Specimen Wt. Change in Mg 975 F	Average Pene- tration Mils/Yr	Specimen Wt. Change in Mg 750 F	Average Pene- tration Mils/Yr	Remarks
		N-1700	N-1700	A.R.							
		T-975	T-1300								
222	3000	-	-	X	S.B.	S.B.	- 687.5 - 382.9	5.31	- 1.3 - 5.4	.03	Specimen Holder Failure
226	3000	-	-	X	A.C.	A.C.	- 20.1 - 13.8	.167	- 2.3 - 1.8	.019	
230	3000	X	-	-	S.B.	S.B.	-5186.3 -5285.1	51.99	- 7.3 - 1.2	.04	Temperature Excursion
234	3000	X	-	-	A.C.	A.C.	- 111.9 - 156.4	1.33	- 4.5 -12.5	.08	
238	3000	-	X	-	S.B.	S.B.	- 28.7 - 39.4	.33	- 1.6 - 0.3	.009	
242	3000	-	X	-	A.C.	A.C.	- 12.7 - 592.6	3.0	-12.3 - 6.2	.09	
254	3000	-	-	X	Honed	Electro- Pol.	Met -4266.2	42.36	Met - 7.6	.07	Temperature Excursion
258	3000	Hydrogen Fire	-	-	S.B.	S.B.	-3103.2 -3070.0	30.64	- 1.0 - 1.0	.009	
262	3000	-	Hydrogen Fire	-	S.B.	S.B.	-5739.8 -5685.2	56.72	- 1.8 - 1.2	.014	
281	3000	-	-	Hydrogen Fire at 975 F	S.B.	S.B.	-2199.3 -2434.8	23.0	- 9.7 - 2.3	.05	

The results obtained in this group of tests show the same general trend as previously encountered; i. e. , losses sustained on the honed and hydrogen fired units were higher than those on capsules with sand-blasted or acid-cleaned surfaces. The honed capsules have shown unusually high corrosion losses when tested in the presence of the U-Bi fuel for over 2000-hr durations. Unit 313 used the honed capsule body and electropolished specimens and was scheduled to operate 4000 hr; however, after 2800 hr, it was noted that the 975 F end tended to creep over the set temperature, and the 750 F end failed to show the normal temperature rise immediately after furnace tilt.

These temperature fluctuations were controlled until the capsule attained 3202 hr, when the cold end failed to show any temperature change during cycling.

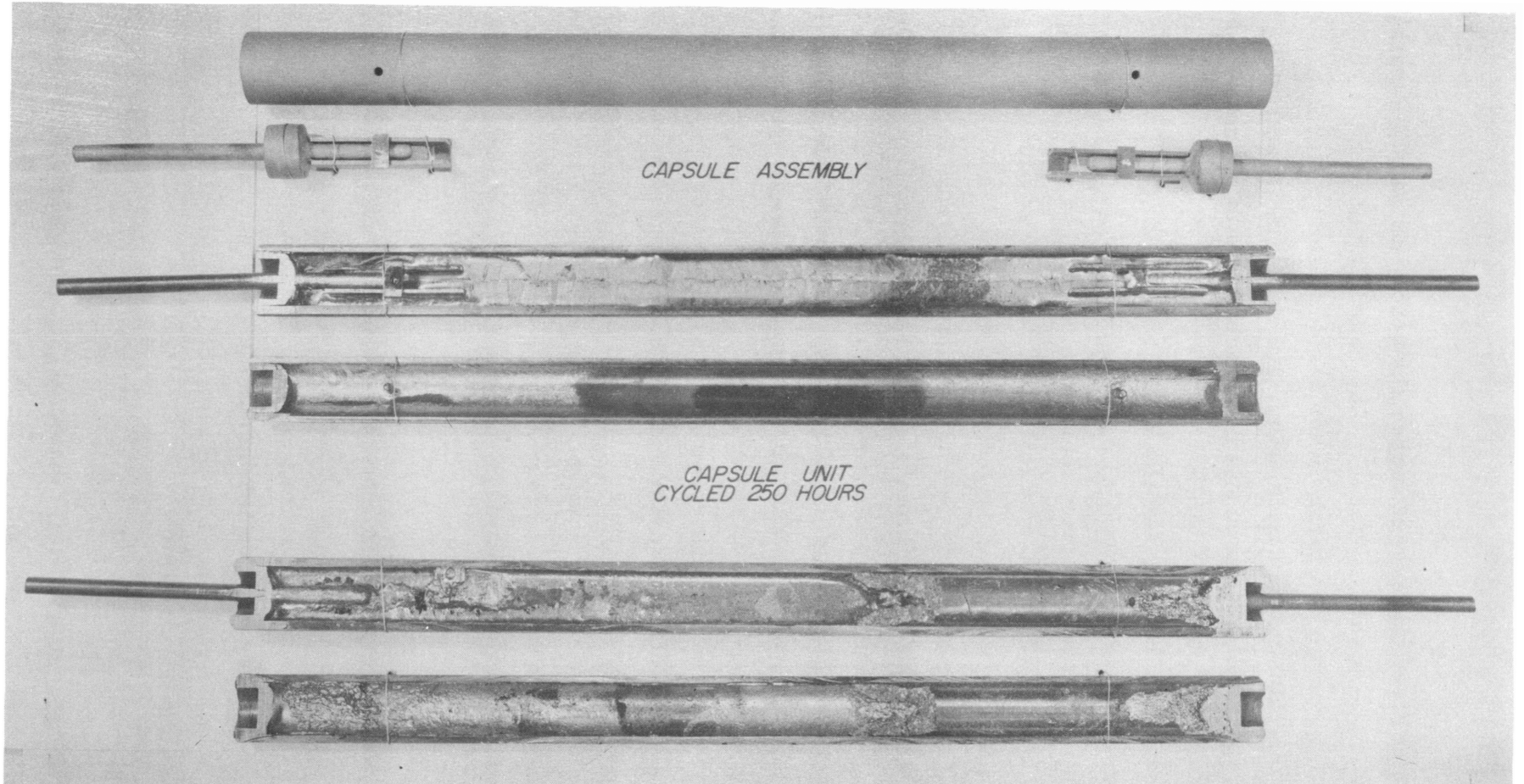
The unit was, therefore, removed and sectioned. Figure 40 shows the capsule interior. Complete plugging had occurred on the cold end even though the thermal gradient never exceeded the set 225 F difference.

The solution attack and metal dissolution thinned the specimen holder on the hot end and permitted the test coupons to be dislodged from their fixed positions in the holder.

This mass transfer that takes place within the capsule unit has been prevalent in all units cycled for over 2000 hr. The degree of plugging that resulted is a function of time and surface preparation.

The 2000-hr findings reported in Table II show that corrosion losses varied with surface preparations tested. It is felt that these variations in attack are caused by possible surface oxides and films that reduce liquid attack for the time periods under study. Corrosion usually starts at susceptible areas. These may be spots of non-uniformity in protective films or surface defects that break down, permit localized corrosion and selective attack, and result in the inconsistent losses that sometimes occur. These conditions are not present to such an extent on the honed surfaces where direct attack undoubtedly takes place but are minimized by films that may form because of additive variations.

FIG. 40: MASS TRANSFER AND FINAL PLUGGING
OF CAPSULE CYCLED 3203 HR



Three units using honed capsule bodies and electropolished specimens have been assembled to study mass transfer rates further. It is planned to establish the time at which this metal carry-over affects capsule work by checking any temperature fluctuation and by periodic gamma ray inspection of cold end sections.

Capsules 390, 391, and 392 have now been cycling 1587 hr with no apparent changes. However, unit 351, similarly prepared and scheduled to operate 3000 hr, has been cycling for 2471 hr. Figure 41 shows a gamma graph of the mass transfer starting to deposit in the cold end section.

Figure 42 shows a gamma graph of capsule 329 with a sandblasted surface, hydrogen fired at 1700 F, and tempered at 1300 F. The unit operated for 3714 hr before final plugging caused it to be removed. All capsule units scheduled for 4000 hr have had to be removed before completion because of plugging.

Work is being conducted on the original program, which consisted of varying additive levels, heat treatment, and surface preparations. After the first work on this program was reported it was decided to omit the bismuth plating preparation, as findings were very inconsistent. The final work in the program will delete this surface preparation from the series of tests. A statistical study has been started on this series to compare the effects of metallurgical preparations, additive levels, and cleaning methods. An "analysis of variance" will be used in evaluating the effects received by the different levels of the conditions under test.

All work has been completed on the beryllium, tantalum, and molybdenum -0.5 titanium metals. The findings from this group of auxiliary tests are shown in Tables IV, V, and VI. Results indicate little or no metal loss after 1000 hr in the LMFRE fuel solution.

Twelve capsules have been assembled, and part of the group is under test. Each uses Croloy 1-1/4 material and considers the 1150 ppm uranium, 350 ppm magnesium, and 175 ppm zirconium level of additives.

FIG. 41: GAMMA GRAPH OF CAPSULE NO. 351 AFTER 3000 HR

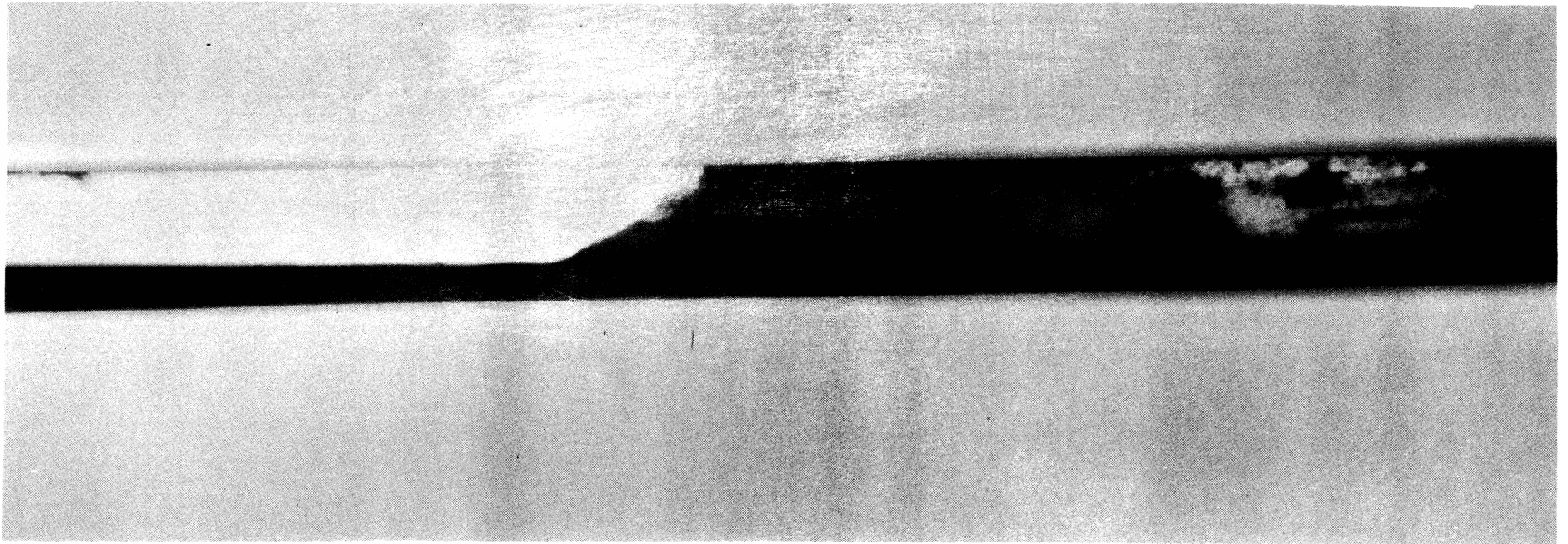


FIG. 42: GAMMA GRAPH OF CAPSULE NO. 329 AFTER 3714 HR

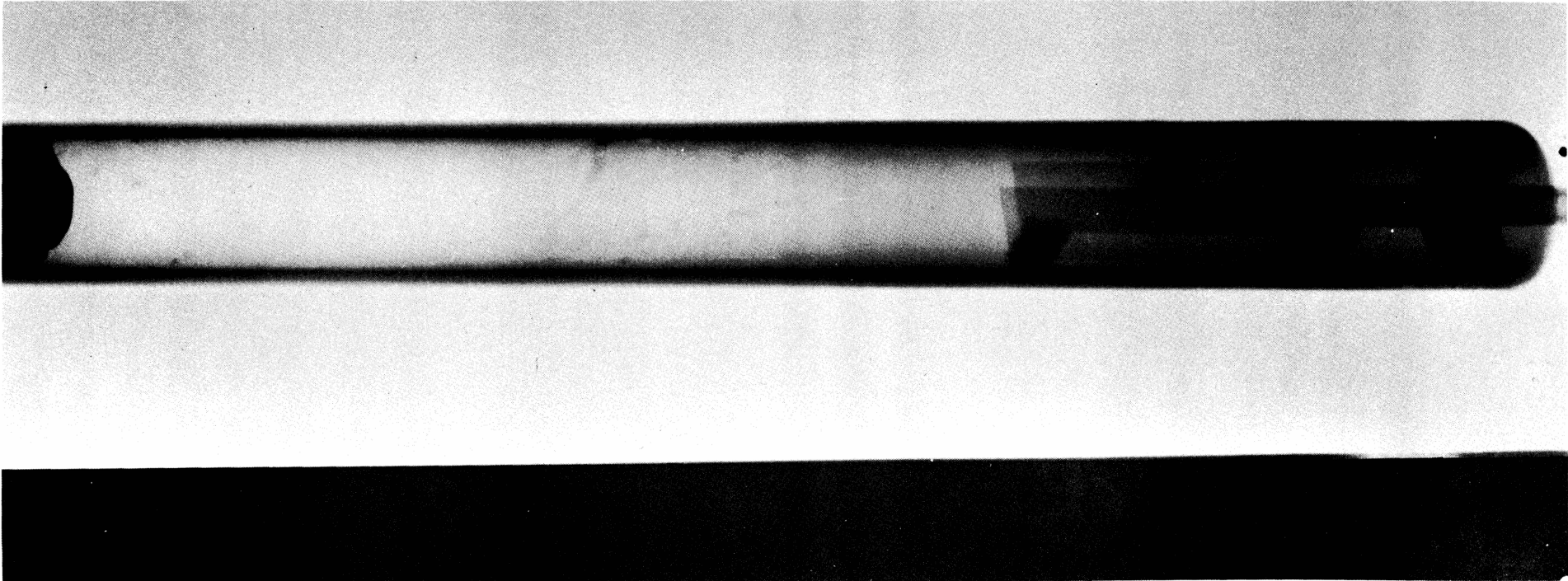


TABLE IV

TILTING CAPSULE TEST
 MATERIAL - MOLYBDENUM, 0.5 TITANIUM COUPONS, CROLOY 2-1/4 CAPSULES
 ΔT 225 F - FLUID, BISMUTH, 1150 PPM URANIUM,
 350 PPM MAGNESIUM, 175 PPM ZIRCONIUM

Test No.	Test Time Hrs.	Heat Treatment			A.R.	Capsule Prep.	Spec. Prep.	Specimen Wt. Change in Mg 975 F	Average Penetration Mils/Yr	Specimen Wt. Change in Mg 750 F	Average Penetration Mils/Yr	Remarks
		T-1700	N-1700									
		T-1300	T-975									
352	1000	-	-	X	S.B.	S.B.	+ 0.2 + 0.1	-	- 0.6 - 1.4	.029	Minor adherence of bismuth to specimen surfaces	
353	1000	-	-	X	S.B.	S.B.	+ 0.2 + 0.2	-	- 0.1 - 0.1	.002		
354	1000	-	-	X	S.B.	Fine Polish	- 3.5* - 1.0	.067	- 0.6 - 0.4	.014	No visual attack on specimen surfaces.	
355	1000	-	-	X	Honed	Electro Polish	- 2.7 - 2.2	.073	- 0.9 - 2.6	.051		
356	1000	-	-	X	AR	AR	Met - 0.1	- .002	- 0.5 - 0.7	.017	Capsule walls were wetted and appeared attacked.	

*Small piece broke off in removing specimen holder.

TABLE V

TILTING CAPSULE TEST
 MATERIAL - BERYLLIUM COUPONS, CROLOY 2-1/4 CAPSULES
 ΔT 225 F - FLUID, BISMUTH 1150 PPM URANIUM
 350 PPM MAGNESIUM, 175 PPM ZIRCONIUM

Test No.	Test Time Hrs.	Heat Treatment			Capsule Prep.	Spec. Prep.	Specimen Wt. Change in Mg 975 F	Average Penetration Mils/Yr	Specimen Wt. Change in Mg 750 F	Average Penetration Mils/Yr	Remarks
		N 1700	N 1700	A.R.							
		T 1300	T 975								
399	1000	-	-	X	S.B.	AR	- 1.5 - 0.9	.035	- 4.4* + 0.5	.056	Capsule Walls showed attack and were wetted with bismuth.
400	1000	-	-	X	S.B.	AR	- 3.6 - 4.3*	.117	- 5.1* + 0.1	.075	
401	1000	-	-	X	AR	AR	Met Met	-	-45.7** - 2.7	.721	Specimens had adhering bismuth but no wetting
402	1000	-	-	X	Honed	AR	- 5.6* - 5.1*	.159	- 0.3 + 0.4		No visual attack apparent on specimen surface

* Small particles of specimen adhered to specimen holder upon removal.

** A portion of specimen broke off during cleaning.

TABLE VI

TILTING CAPSULE TEST
 MATERIAL - TANTALUM COUPONS, CROLOY 2-1/4 CAPSULES
 ΔT 225 F - FLUID, BISMUTH, 1150 PPM URANIUM
 350 PPM MAGNESIUM, 175 PPM ZIRCONIUM

Test No.	Test Time Hrs.	Heat Treatment			Cap- sule Prep.	Spec. Prep.	Specimen Wt. Change in Mg 975 F	Average Pene- tration Mils/Yr	Specimen Wt. Change in Mg 750 F	Average Pene- tration Mils/Yr	Remarks
		N 1700	N 1700	A.R.							
		T 1300	T 975								
361	1000	-	-	X	S.B.	S.B.	+ 0.4 - 0.4	-	- 0.7 - 0.8	.022	No visual attack apparent.
362	1000	-	-	X	A.R.	A.R.	Met + 0.9	-	- 0.2 - 0.2	.005	
363	1000	-	-	X	S.B.	Rough Polish	+ 0.1 + 0.1	-	- 0.1 0	-	
364	1000	-	-	X	Honed	Fine Polish	- 0.3 - 0.1	.005	- 0.2 - 1.1	.017	
411	1000	-	-	X	S.B.	Welded S.B.	- 0.7 - 0.4	.014	- 0.3 + 0.1	.002	
412	1000	-	-	X	A.R.	Welded A.R.	Met + 1.1	-	0 - 0.7	.008	
413	1000	-	-	X	S.B.	Welded Rough Polish	+ 0.1 0	-	- 0.1 0	-	
414	1000	-	-	X	Honed	Welded Fine Polish	+ 0.4 + 0.4	-	+ 0.1 + 0.1	-	

Six capsules with honed surfaces and electropolished specimens have been prepared and are operating. These units contain the standard fuel charge and will be cycled from 250 to 4000 hr. This group of tests will be conducted at the lower temperature difference of 135 F to secure comparative data on similarly prepared capsules.

C. MISCELLANEOUS METALLURGICAL INVESTIGATIONS

The test procedure developed for creep-rupture testing of Croloy 1-1/4 and 2-1/4 material in a liquid metals atmosphere at 885 F and 975 F has been very satisfactory. Since the last quarterly report, one Croloy 1-1/4 specimen tested in the liquid metal atmosphere and one Croloy 1-1/4 specimen tested in an air atmosphere have ruptured. The status of specimens under test, test results of completed specimens, and conclusions follow.

1. Status of Tests in Progress

a. Liquid Metal Atmosphere

<u>Type of Material</u>	<u>Test Temp. F</u>	<u>Stress psi</u>	<u>Hours in Progress</u>	<u>Tentative Min. Creep Rate %/1000 hr</u>
Croloy 1-1/4	975	27,500	824	--
Croloy 1-1/4	975	23,500	5,930	0.093
Croloy 1-1/4	885	46,000	5,760	0.123
Croloy 1-1/4	885	40,000	5,344	0.089
Croloy 2-1/4	975	22,500	5,590	0.155
Croloy 2-1/4	975	19,500	5,337	0.093
Croloy 2-1/4	885	30,500	5,270	0.075
Croloy 2-1/4	885	26,500	5,079	--

b. Air Atmosphere

Croloy 1-1/4	975	36,000	997	--
Croloy 1-1/4	885	46,000	3,152	0.163

2. Test Results

The following Croloy 1-1/4 tests have been completed since the program was initiated:

a. Liquid Metal Atmosphere

<u>Test Temp. F</u>	<u>Stress psi</u>	<u>Rupture Time-Hr</u>	<u>Elong. % in 1.5-in.</u>	<u>Red. of Area %</u>	<u>Min. Creep Rate %/1000 Hr</u>
975	36,000	1430.7	*	*	3.33
975	33,000	2779.7	16.6	14.7	1.44

*Specimen has not been examined

b. Air Atmosphere

975	33,000	2584.3	8.0	9.1	1.38
-----	--------	--------	-----	-----	------

The stress-rupture test points are plotted in Figure 43 and the creep curves are shown in Figures 44 and 45.

3. Conclusions Drawn on Completed Tests

Croloy 1-1/4 comparison tests conducted in air and a liquid metals atmosphere for 2500-hr duration indicate that the liquid metals atmosphere has not had a harmful effect. The rupture results in Figure 43 and the creep rates in Figure 45 show

- a. Approximately the same rupture time
- b. Approximately the same minimum creep rates
- c. The test in an air atmosphere had lower rupture ductility than the test in a liquid metal atmosphere. The lower ductility is associated with the oxidation that occurs on exposure at 975 F in an air atmosphere.
- d. The high temperature strength of Croloy 1-1/4 is greater than that of Croloy 2-1/4 over this temperature range (indicated by the tentative minimum creep rates).

The results of low temperature impact testing of Croloy 1-1/4 and 2-1/4 in the annealed and the normalized and tempered conditions after long-time exposures to the LMFRE operating temperature were reported in the last quarterly technical report.⁶ During the current report period, high temperature impact testing was completed on the two materials with the same heat treatment, both in aged and unaged conditions.

FIG. 43: COMPARISON OF CREEP-RUPTURE PROPERTIES

(1.25 Cr - .50 Mo Tested in Air
and Liquid Metal Atmospheres)

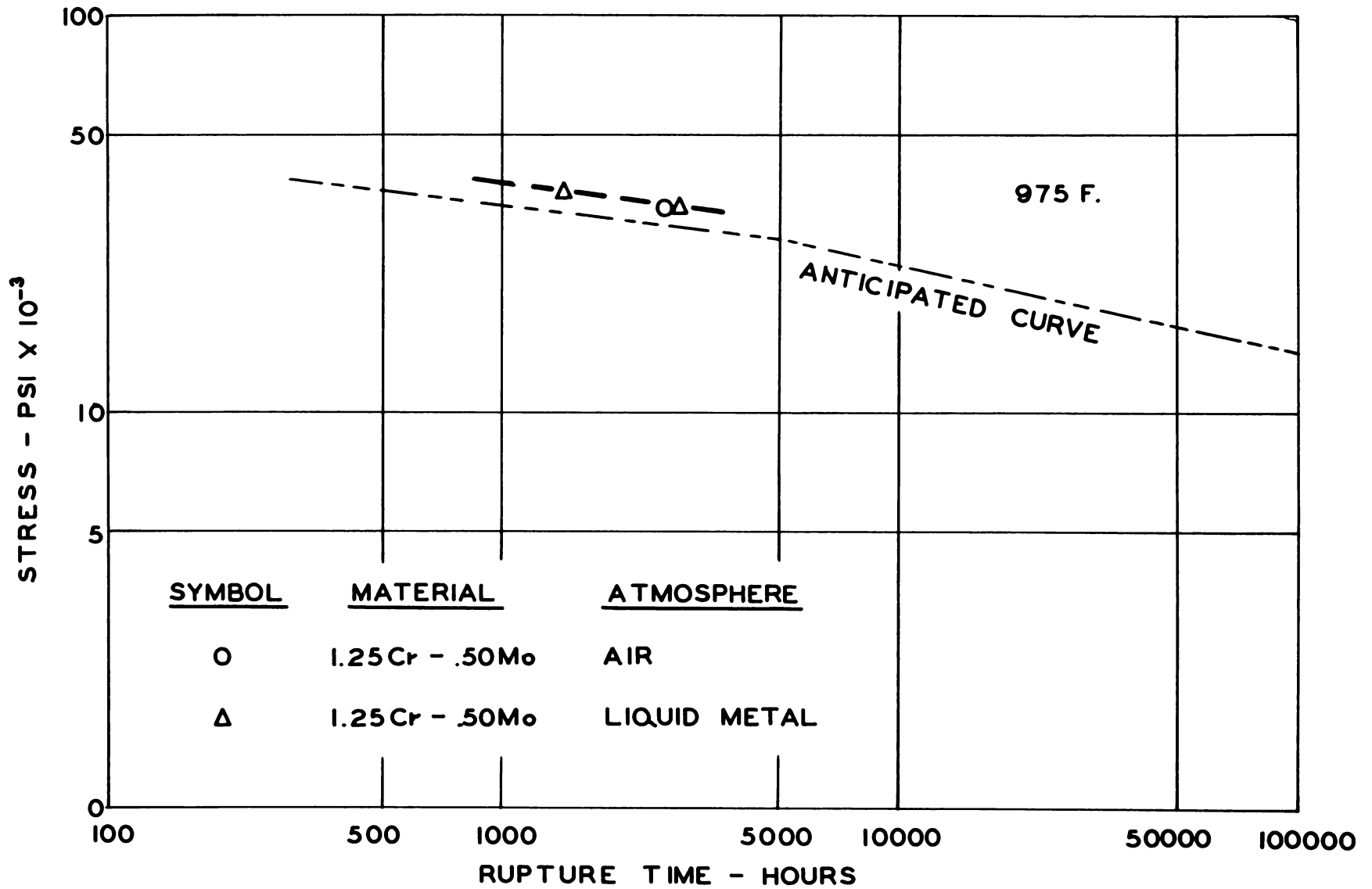


FIG. 44: CREEP CURVE FOR 1.25 Cr - .50 MO ALLOY TESTED
IN A LIQUID METAL ATMOSPHERE AT 975 F

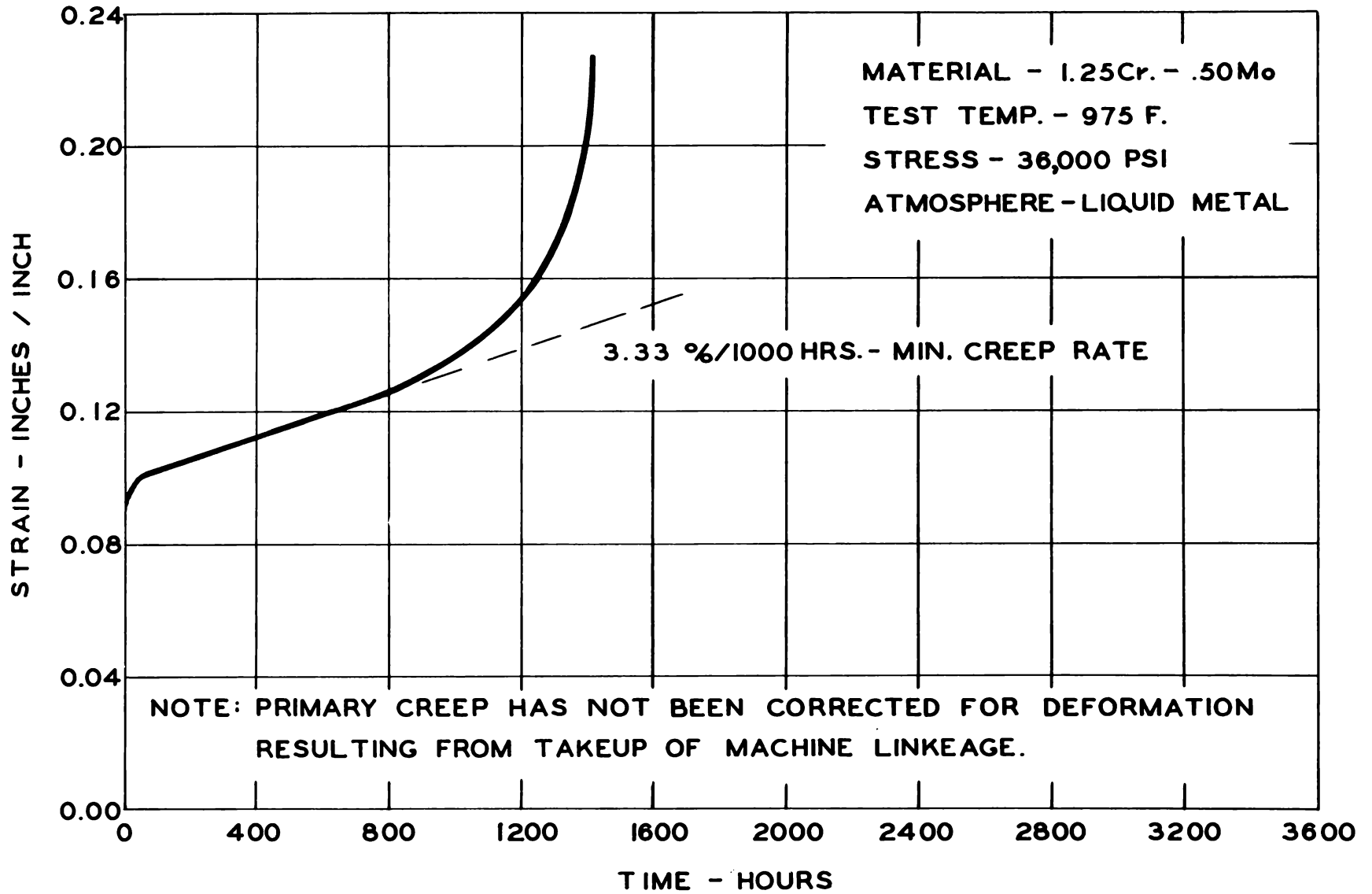


FIG. 45: COMPARISON OF THE MIN. CREEP RATES OF 1.25 Cr - .50 MO ALLOY TESTED IN AIR AND LIQUID METAL ATMOSPHERES

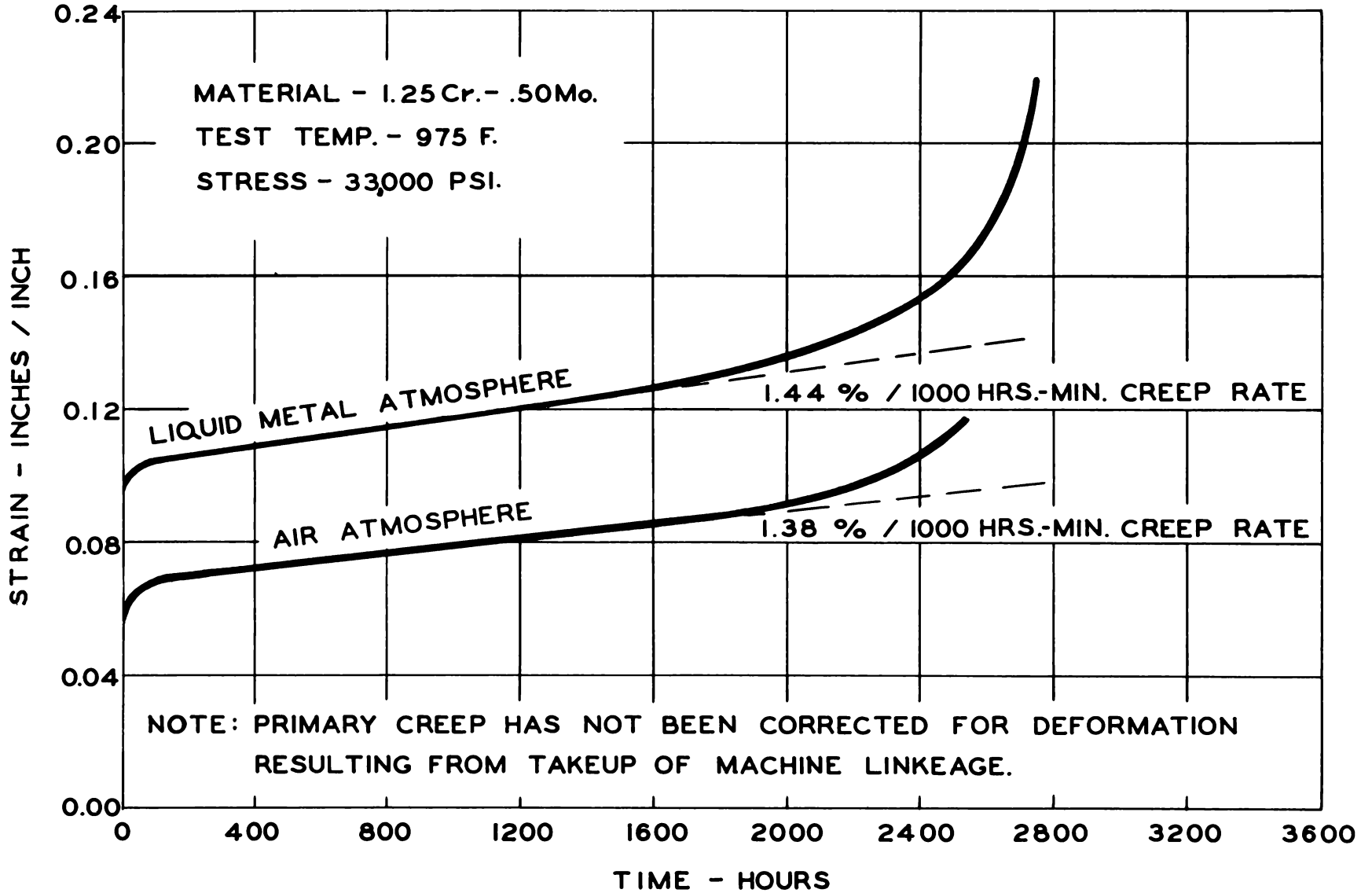


TABLE VII

IMPACT STRENGTH, FT-LB AT 885 F

<u>Condition</u>	<u>Croloy 2-1/4</u>	
	<u>Annealed</u>	<u>Normalized & Tempered</u>
Unaged	87.5, 93.0, 89.0	100.5, 115.0, 101.5
Aged 2000 hrs at 885 F	6 at 120.0	6 at 120.0

<u>Condition</u>	<u>Croloy 1-1/4</u>	
	<u>Annealed</u>	<u>Normalized & Tempered</u>
Unaged	120.0, 106.0, 120.0	108.0, 106.5, 116.5
Aged 2000 hrs at 885 F	6 at 120.0	6 at 120.0

At the contemplated operating temperature of LMFRE (885 F), the impact strengths of the unaged material were slightly lower than the values obtained at room temperature. After aging, the impact strength increased at the 885 F test temperature. It would seem, therefore, that exposure to operating temperatures is beneficial to the impact strength of the two materials at elevated temperatures.

The results of these tests are shown in Table VII.

D. GRAPHITE-TO-METAL SEAL

There have been many occasions to use seals between chrome steel and various grades of impervious graphite. There have been no significant problems in maintaining a leak tight seal against molten bismuth. The bulk of the seal testing took place on small 3 1/4-in. OD cylinders, and on 4 in. by 4 in. by 1 in. flat plates of graphite. One test is in progress on a large 12-in. OD graphite pot, and the seal appears to be holding very well. From the numerous tests run, involving a chrome steel-to-graphite seal, it appears that the data are conforming to the findings in the initial screening work on seals described previously.⁸

1. Weepage Tests

Tests are confined to the information from the seal tests and from some preliminary screening tests performed on small 3 1/2-in. diameter cylinders. The graphite for the actual tests will be selectively cut from the large 40-in. block when it arrives from the vendor.

A 12-in. graphite pot was tested in the Croloy-to-graphite seal testing apparatus. The material was H3LM with a density of 1.79 g/cc. Since this grade of graphite is not planned for use in the LMFRE, the results obtained in these tests should be used to indicate trends rather than quantitative data.

From the test, the following basic observations were made:

a. The temperature of the bismuth has an effect on the weepage rate, which depends on the fluid viscosity. (The small screening tests have been discontinued until a temperature controller can be added to the existing equipment).

b. The weepage rate appears to be linear with pressure difference. No threshold effects have been observed.

c. The bismuth could be driven from the interior of the graphite pot by reversing the pressures.

d. The H3LM pot increased in weight from 49 to 64.5 lb, or 31.6 percent. The specific weight of the graphite at the end of the test was 2.36 gm/cc. This is not the maximum amount of bismuth that could be absorbed, based on the capacity of the theoretical voids in the graphite.

2. Outgassing Tests

Instrumentation was obtained for the outgassing apparatus and a test was made on a 12-in. cube of MH4LM graphite. No significant change was detected in the data after evacuating and checking for three weeks. Leak testing of the system disclosed no leaks. The apparatus is being modified so that data can be obtained at 1000 F with the pot empty and again at 1000 F with the pot containing a 2-in. by 2-in. by 2-in. block of impervious graphite.

E. ALTERNATE IMPREGNANTS FOR GRAPHITE

The graphite alternate impregnants testing program, a preliminary investigation aimed at determining the feasibility of graphite impregnation with some material other than carbon, is being developed:

1. To determine if a metal were mixed in with the graphite during impregnation or by other means, whether or not that metal could be converted to the oxide without undue damage to the graphite. This is actually a test of the relative oxidation rate of the metal vs. the graphite.

2. To test the physical stability of graphite samples containing a metal oxide for the effects, if any, of the different coefficients of thermal expansion.

3. To demonstrate the feasibility of firing metal-graphite samples in the controlled atmosphere carbon tube furnace to form carbides and to determine whether the process of carbide formation is beneficial for reducing graphite permeability.

Graphite samples containing the additives as metals or as oxides were made by dry pressing methods using a small hydraulic press (Fig. 46) and a hardened steel die set (Fig. 47). These samples were 1/2-in. diameter by 1/2-in. length with a graphite density of 1.75 to 1.8 g/cc, or approximately 75 percent of theoretical density. The graphite was 44 micron particle size. The metals and oxides were 99 percent or better purity and under 325 mesh size.

Graphite samples containing 10 weight percent of Al, Mg, and Si have been fired in an air atmosphere furnace (Fig. 48) to determine whether the metal can be oxidized faster than the graphite. Firing a series of 5 samples for 1 hr at 1000 F and 1 hr at 1500 F have shown that the metal-graphite samples have a higher oxidation resistance than 100 percent graphite samples. However, the X-ray analyses showed no oxide present in the samples. Figure 49 is a photograph of pure graphite and graphite 10 weight percent Al after being fired for 1 hr at 1500 F. Additional samples fired for 4 hr and 12 hr at 1000 F show severe oxidation, evidenced by measurements of weight loss and volume change. Figure 50 shows graphite 10 weight percent Al samples as pressed and after 12 hr at 1000 F. Graphite-10 weight percent Mg samples completely disintegrated after 12 hr at 1000 F. None of the samples analyzed after 4 hr at 1000 F showed oxide to be present.

Data representing the measurements of average percent weight loss and average percent volume change for samples fired for 1 hr, 4 hr, and 12 hr at 1000 F are plotted in Figures 51 and 52 respectively. The analysis of volume change and weight loss data is complicated by the fact that during the firing of dry pressed samples there is a significant volume expansion even though the sample undergoes a weight loss. This expansion does not occur on samples cut from a graphitized carbon rod. This expansion will partially occlude any expansion caused by oxidation of metals and, at the same time, present a greater graphite surface area to be acted upon by the air atmosphere, causing an inconsistent change in the sample weight loss. However, the conclusion can be drawn from these oxidation tests that it would be unpractical if not impossible to convert a metal situated within the pores of a graphite shape to the oxide because of the higher oxidation rate of the graphite itself.

FIG. 46: HYDRAULIC PRESS USED TO FORM GRAPHITE SAMPLES
(1/4 ACTUAL SIZE)

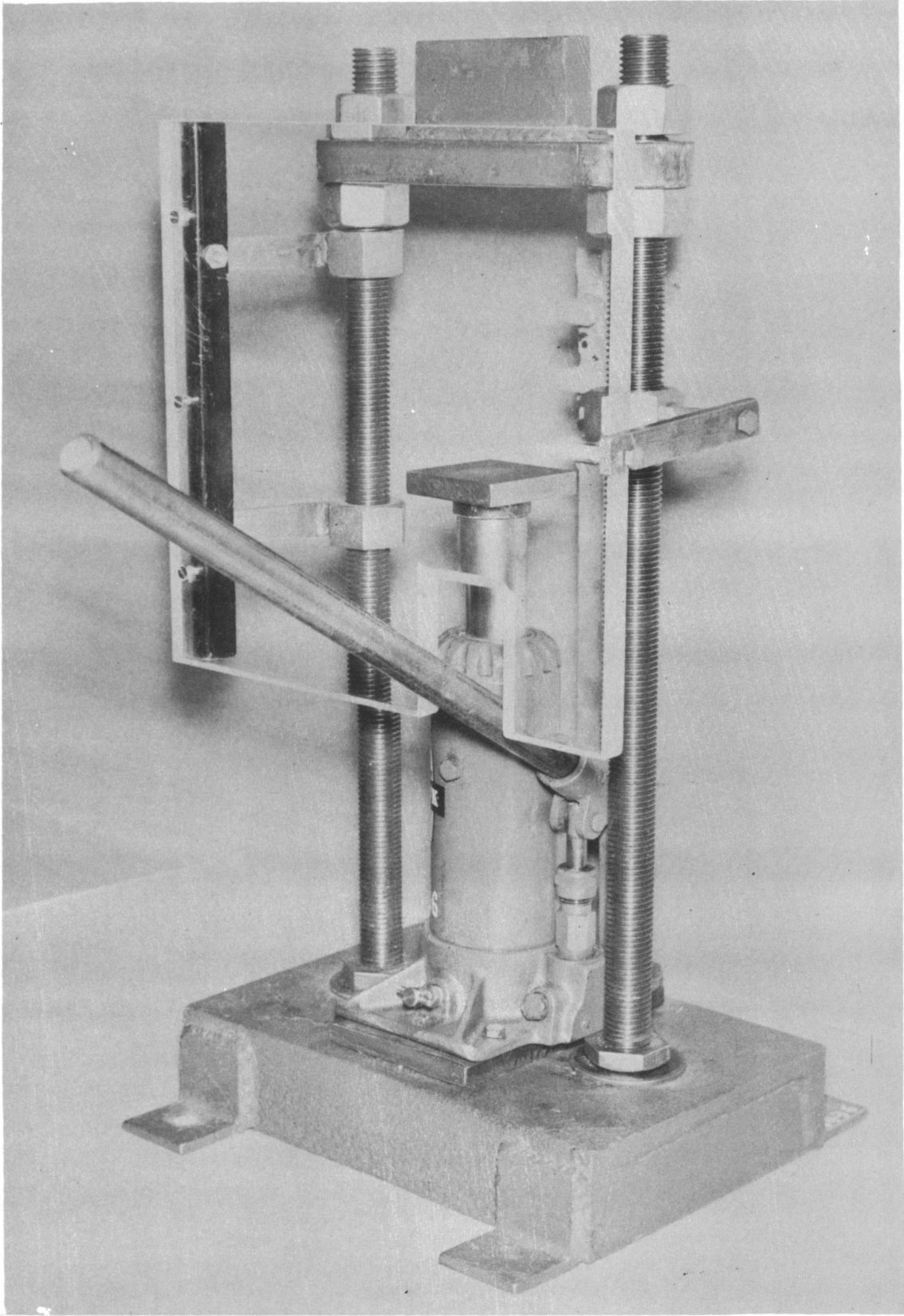


FIG. 47: PUNCHES AND DIES USED FOR DRY PRESSING SAMPLE PELLETS

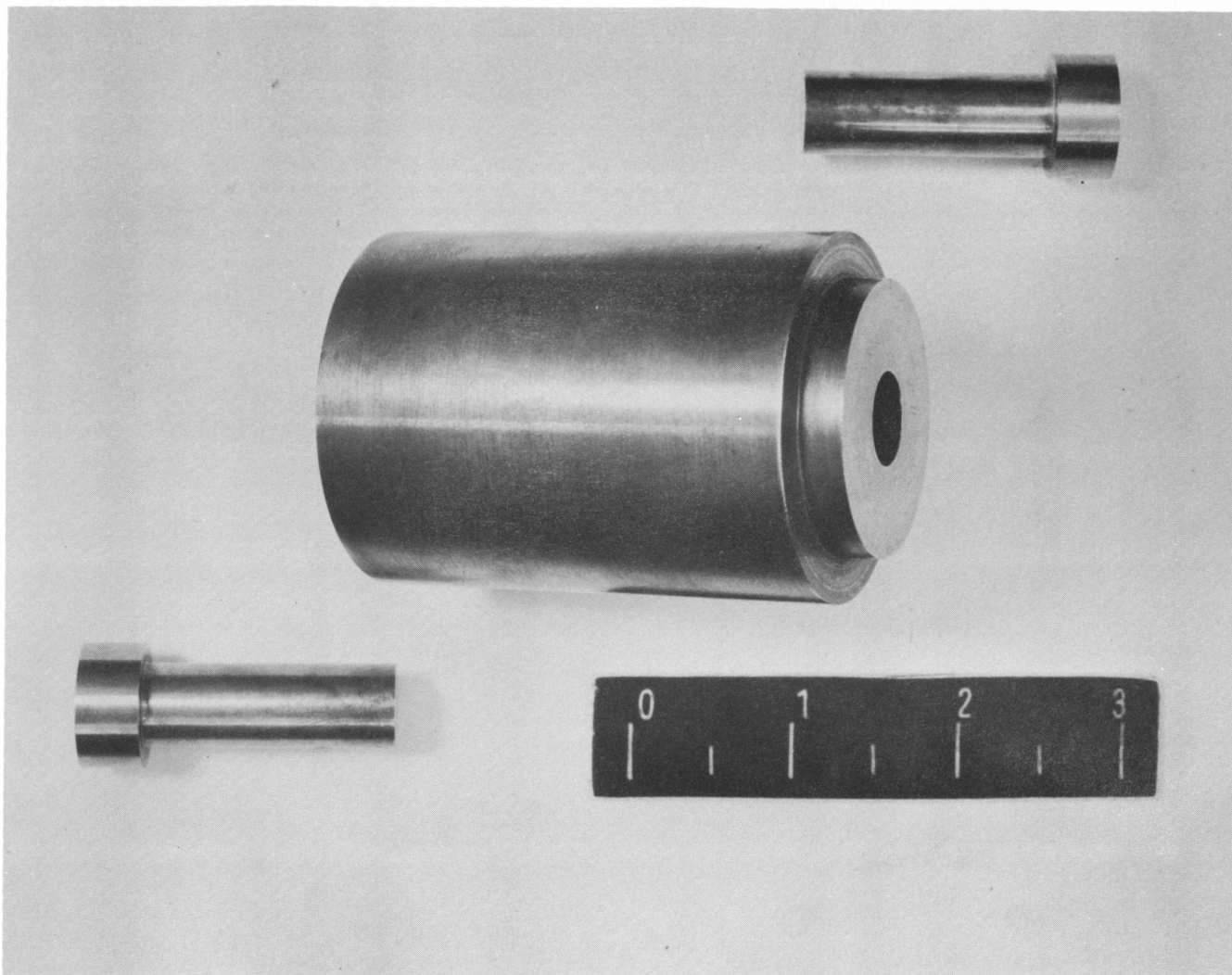
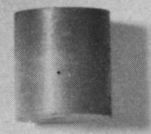
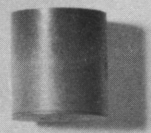
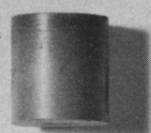


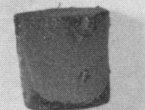
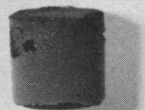
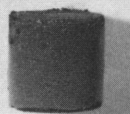
FIG. 48: ELECTRIC FURNACE AIR ATMOSPHERE



FIG. 49: GRAPHITE-ALUMINUM SAMPLES AFTER FIRING



(10% Al, 90% Graphite Samples after Firing at 1500 F)



(100% Graphite Fired for One Hr at 1500 F)

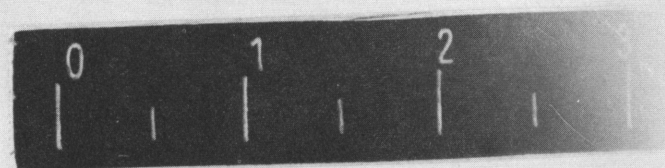


FIG. 50: GRAPHITE ALUMINUM SAMPLES AFTER FIRING

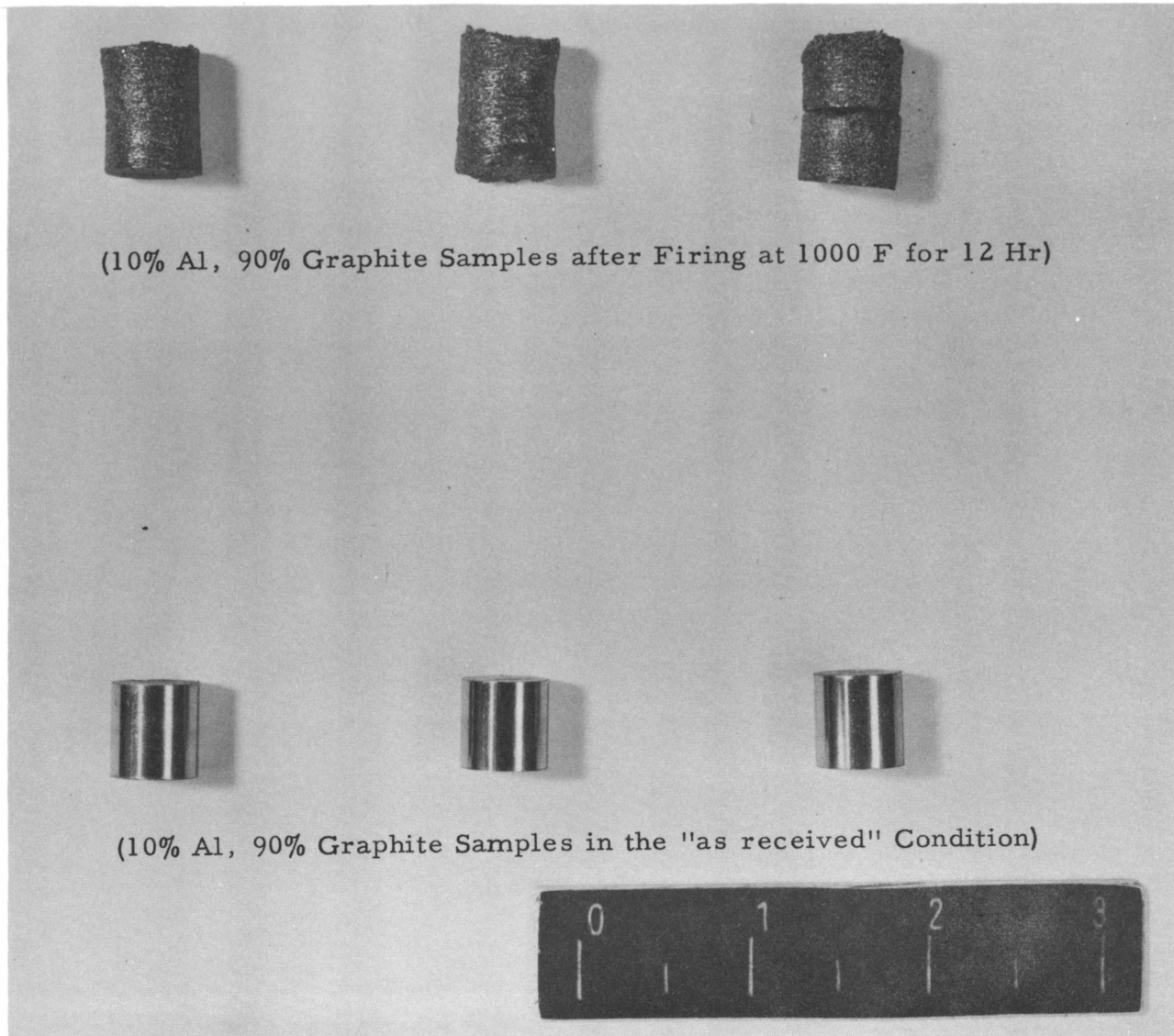


FIG. 51: PERCENT WEIGHT LOSS VS. TIME AT TEMPERATURE FOR VARIOUS GRAPHITE PELLETS

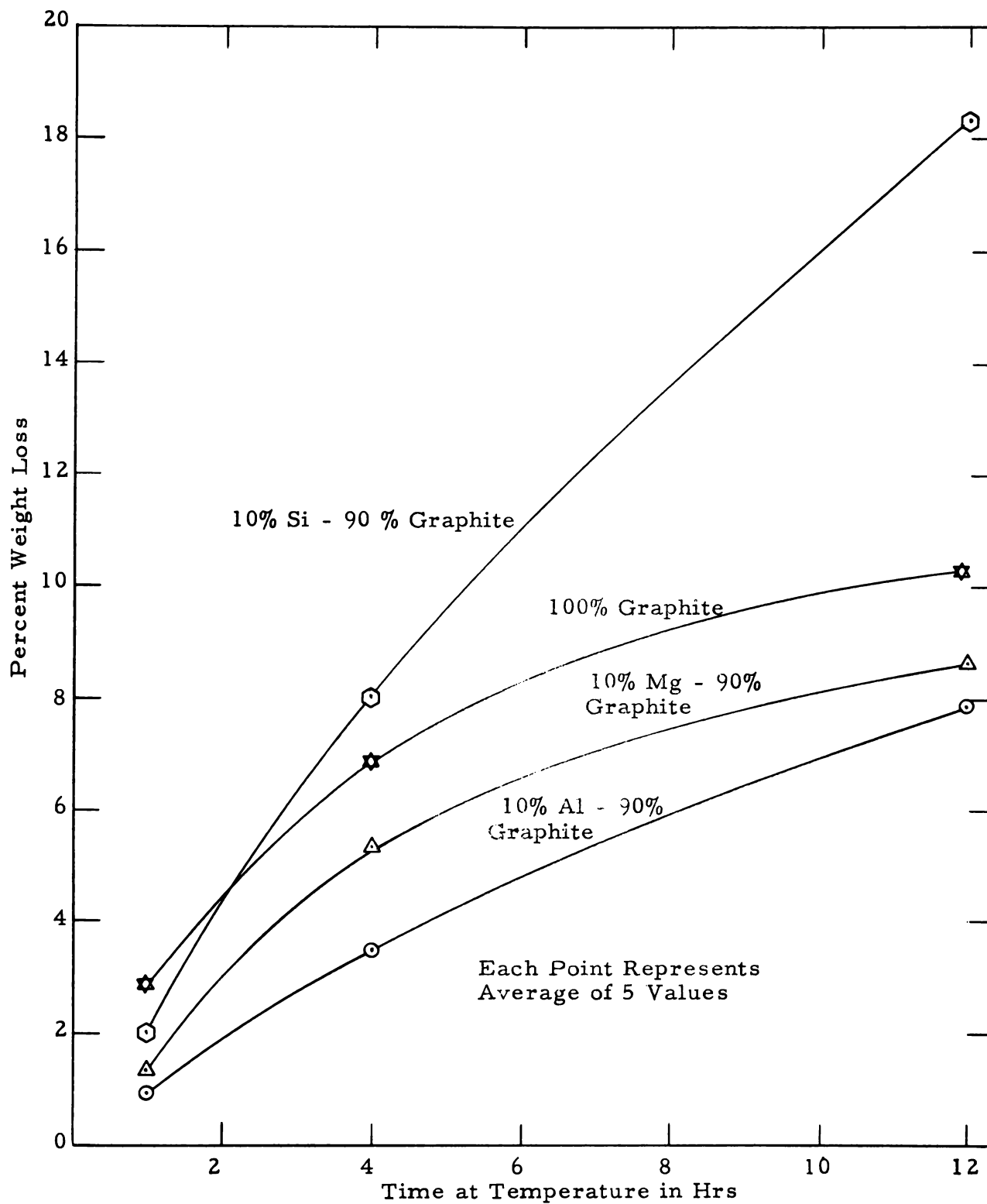
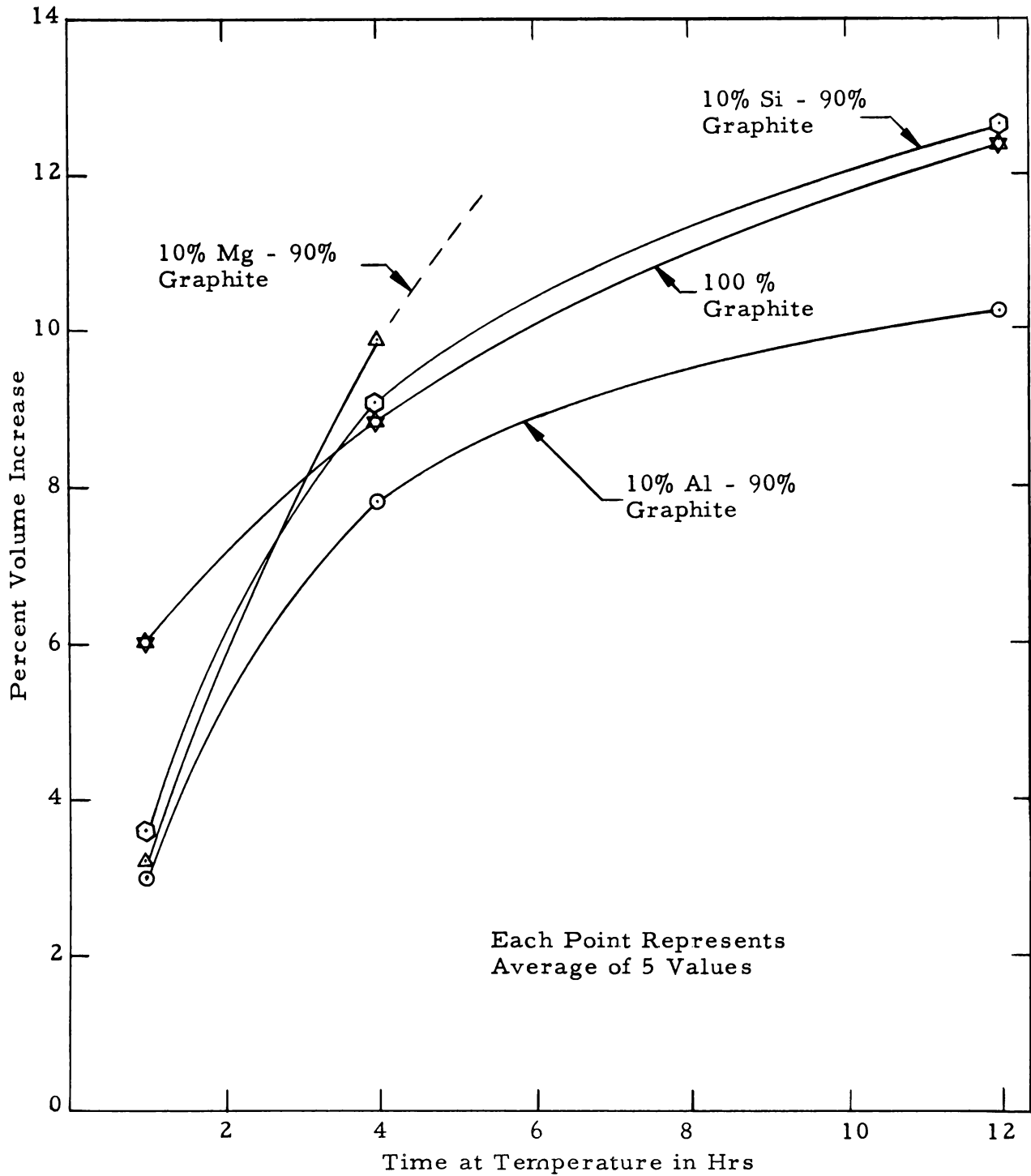


FIG. 52: PERCENT VOLUME INCREASE VS. TIME AT TEMPERATURE FOR VARIOUS GRAPHITE PELLETS



Pressed graphite samples containing 10 weight percent Al_2O_3 , MgO , SiO_2 , and ZrO_2 were fired in air at 1000 F for 1 hr, 4 hr, and 12 hr to detect any changes in sample stability caused by the different coefficients of thermal expansion. All these samples had large volume expansions, which made it impossible to determine the effects of the differing coefficients of thermal expansion. This volume expansion is attributed to the lack of bonding in the dry pressed graphite samples. There was no indication of any chemical reaction between the graphite and the oxides.

Graphite samples containing 10 weight percent of Al and Si have been fired in a controlled atmosphere carbon tube furnace (Fig. 53) to investigate the feasibility of forming Al_4C_3 and SiC . Graphite samples containing 10 weight percent Al have been fired for 1 hr at 4000 F. After these samples were removed from the furnace, they expanded overnight to approximately twice their original length. The broken samples gave off an odor similar to tank acetylene, which would support the conclusion that the Al_4C_3 reacted with moisture in the air. X-ray examination did not show the presence of any aluminum carbide.

A recent firing that used argon has proved successful in that a series of 5 samples containing 10 weight percent silicon fired for 1/2 hr at 4000 F gave a good X-ray pattern for SiC . These samples were quite sound and had good general appearance.

To test the thermal expansion compatibility of graphite-oxide samples properly, it will be necessary to impregnate some graphite by soaking up a metal salt solution followed by a decomposition to form the oxide. The volume expansion that is found in dry pressed graphite samples will be done away with by placing the oxide within the pores of the bonded graphite.

Based on the results of these preliminary tests, it is concluded that the most fruitful area of investigation is that of carbide formation. In addition to the Al_4C_3 and SiC , an attempt will be made to form ZrC . This has not been started because of the lack of dry box facilities necessary to handle zirconium metal of less than 325 mesh.

Whenever any of these processes produce suitable specimens, a few bismuth absorption and/or tilting capsule tests are planned to evaluate the effect of bismuth penetration.

FIG. 53: CARBON TUBE FURNACE



F. COATED GRAPHITE

The possibility of obtaining graphite samples coated with a metallic carbide by a process involving the decomposition of a metal halide gas was discussed with a vendor. These samples would be used to determine the types of coated graphite to be tested as in-pile samples within LMFRE. The carbides of niobium, titanium and zirconium appear to have the most desirable properties for LMFR use.

G. BERYLLIUM THIMBLE DEVELOPMENT

The beryllium thimble, to be used for housing the high temperature instrumentation and neutron source, requires special fabrication techniques. The development involves procuring and testing welded and/or mechanically joined beryllium tubing to determine the fabrication techniques necessary to obtain thimbles for LMFRE. Alternate materials being considered for the thimble are molybdenum and Croloy 2-1/4.

H. APPLICATION OF MOLYBDENUM COATING

The research and development program for depositing a molybdenum coating on 2 1/4 percent Cr - 1 percent Mo steel (Croloy 2-1/4) was awarded to Battelle Memorial Institute and covers both the electroless and vapor deposition methods of application.

IV. PROTOTYPE TESTING

A. REACTOR PORT THIMBLE JOINTS

A vacuum or inert gas drybox has been ordered for the beryllium welding studies. Delivery is scheduled for the week of July 21. Equipment related to the health physics of handling beryllium has been received and is being installed. Samples of extruded beryllium tubing are on hand and specimens have been corrosion tested for 1000 hr in the tilting capsule apparatus.

B. 2 1/2-IN. LOOP

All of the major components and material except the dump valve and an expansion joint, have been delivered. The upper and lower tanks are ready to be installed. The control panel has been set in place, but has not been wired.

Small flowmeters will be tested on this loop (Fig. 35). Changes had to be made to accommodate these tests, including the addition of a valve to control the flow rate to the upper tank and an increase in the pump motor size. The upper tank will be used as a calibration tank for the flowmeters.

The dump valve is expected to arrive by late July. It is planned to put the 2 1/2-in. loop into service by late August or early September.

C. VALVE TESTING

Two prototype valves have been received. These are the 1-in. check and the 1-in. glove valves from the Wm. Powell Company. "Out of loop" leakage tests will be performed on these valves to determine the bismuth leak rate of the valves in the as-received condition. After this test, the valves will be installed in the utility loop for a 2400-hr operating period. Then, another leakage test will be conducted to determine the effect of loop operation on the valve leak rate.

D. DEGASSING SPARGER PLATE

Modifications were made to the approach section to obtain uniform distribution of liquid flow over the sparger plate. Modifications were made to the discharge section to obtain constant depth of liquid over the sparger plate regardless of liquid level in the pump sump. Unsuccessful attempts were made to get vendors to supply porous plate of materials compatible with U-Bi mixtures. Three drilled hole sizes were tried in sparger plates to obtain uniform bubbling action across the width of the plate. Recommended arrangement drawings for a plastic test model were made. High speed movies of bursting bubble action were taken to confirm thinking in this regard. Report No. 4247-BAW-1063 was written to complete project work under this E number. A test installation will be made in the ETR in-pile loop.

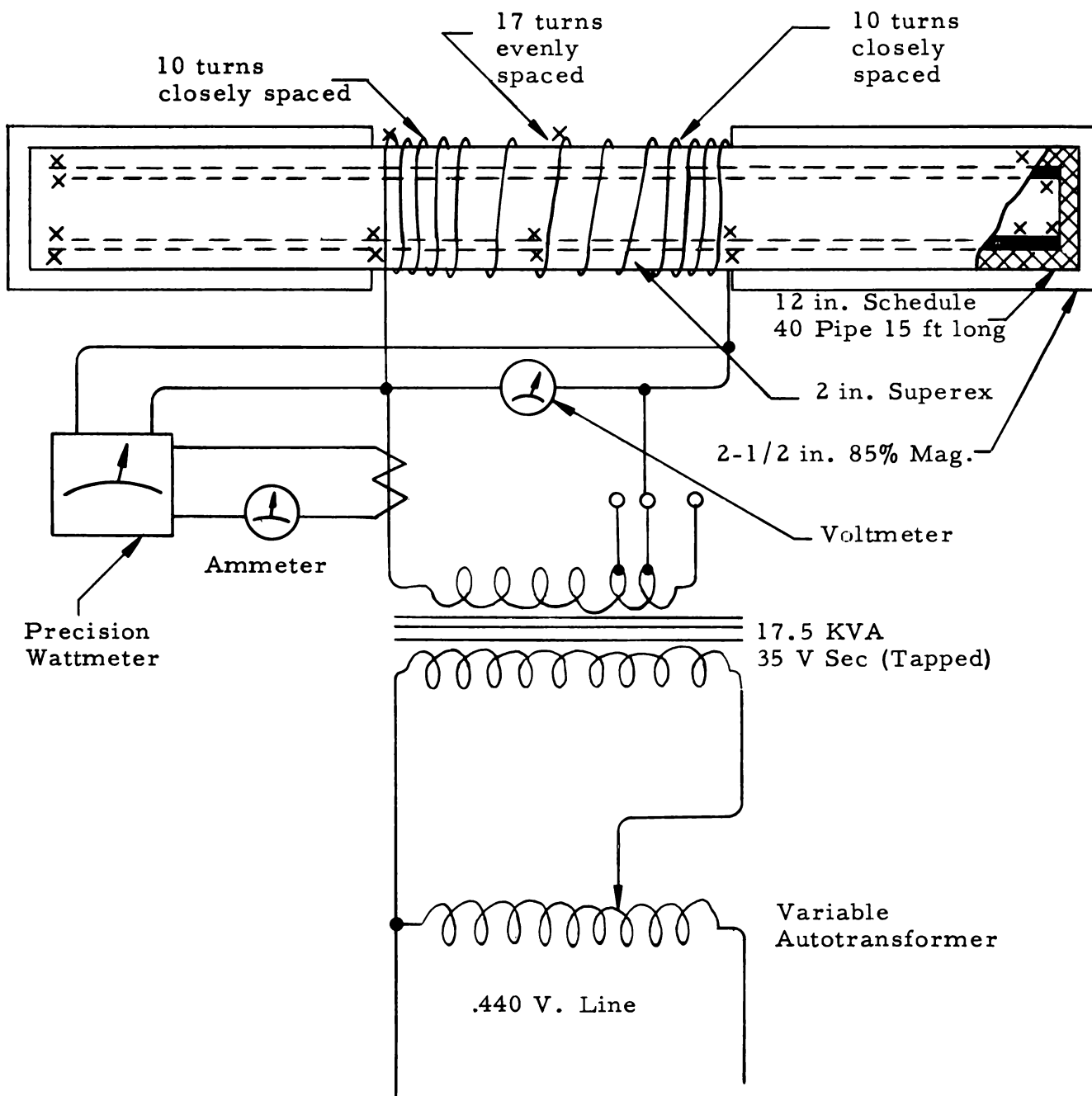
E. 60-CYCLE INDUCTION HEATING

The apparatus to obtain data for low frequency induction heating of a 12-in. schedule 40 pipe is shown in Figure 54. The 15-ft length of pipe was suspended from a frame and insulated over the entire length and on the ends with 2 in. of Johns-Manville "Superex". A coil of 37 turns of 2/0 wire was wound over the center 5-ft section of the pipe and insulated. Power was applied to the coil by means of a 25 KVA variable auto-transformer and a 17.5 KVA stepdown transformer with a 35 volt secondary. The secondary volts and amperes and the secondary power were measured. Thermocouples were attached to the pipe and to the electrical conductors of the coil at the points shown on Figure 54. The temperatures at these points were recorded on an L&N Speedomax recorder.

The pipe was heated with an input power of 4.1 KVA. After 8 hr the center of the pipe reached a temperature of 802 F and the ends of the pipe averaged 400 F. After an additional 12 hr of soaking at this temperature, a difference of 400 F between the center and ends of the pipe still remained.

In an attempt to bring the temperature of the ends nearer to that of the center section, a 2 1/2-in. layer of 85 percent magnesia was added to a 5-ft section at each end. This reduced the differential between the ends and the center to 300 F.

FIG. 54: TEST TO DETERMINE 60-CYCLE
INDUCTION HEATING
REQUIREMENT



X = Thermocouple Locations

The heat losses from the pipe ends would not occur from a continuous pipe and may be amplifying the temperature difference. Therefore, the 5-ft coil will be removed from the pipe and a 2 1/2-ft heated length will be provided at each end of the pipe. If the undesirable temperature differentials persist, the heated length will be increased.

When the proper coil spacing has been determined, tests will be made to determine the power requirements and the optimum coil spacing and diameter.

F. BELLOWS TESTING

When the electrical wiring in progress on both the bellows apparatus and the portable charge rig has been completed, this test facility will be ready for initial operation. The first test bellows are expected early in August. At that time the equipment will be "dry run" with one pair of bellows subject to gas pressure loading only. Subsequent tests will use the U-Bi solution.

G. CAVITATION TESTING - ROTATING DISC

Authorization for this work has been received. Design details are virtually complete except for the rotating shaft vacuum seal. Materials, including the drill press stand, have been ordered and enough are on hand to begin fabrication. The floor model drill press will be used to support the test vessels and to supply the variable speed drive for the rotating discs (Fig. 55).

Initial tests will involve Croloy 2-1/4 discs, subject to various conditions including temperature and velocity static pressure. Other variables to be studied are heat treatment and surface finish. Depending upon the results of this study discs of other materials, notably tantalum and molybdenum (0.5 percent titanium), will be tested.

H. BISMUTH FILTERS

The apparatus to be used for testing bismuth filters has been completed except for electrical wiring (Fig. 56).

FIG. 55: APPARATUS - ROTATING DISC
CAVITATION TEST

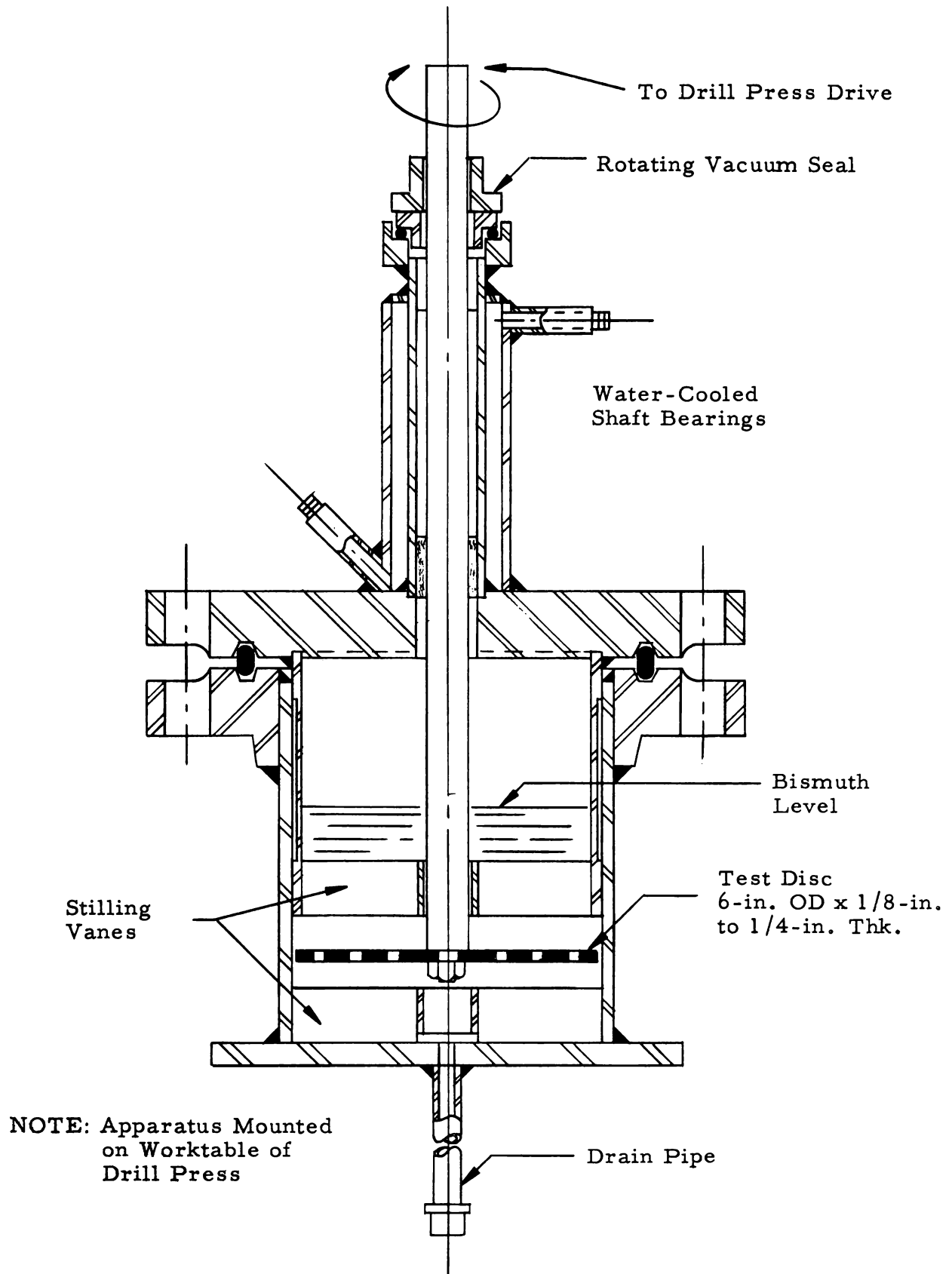
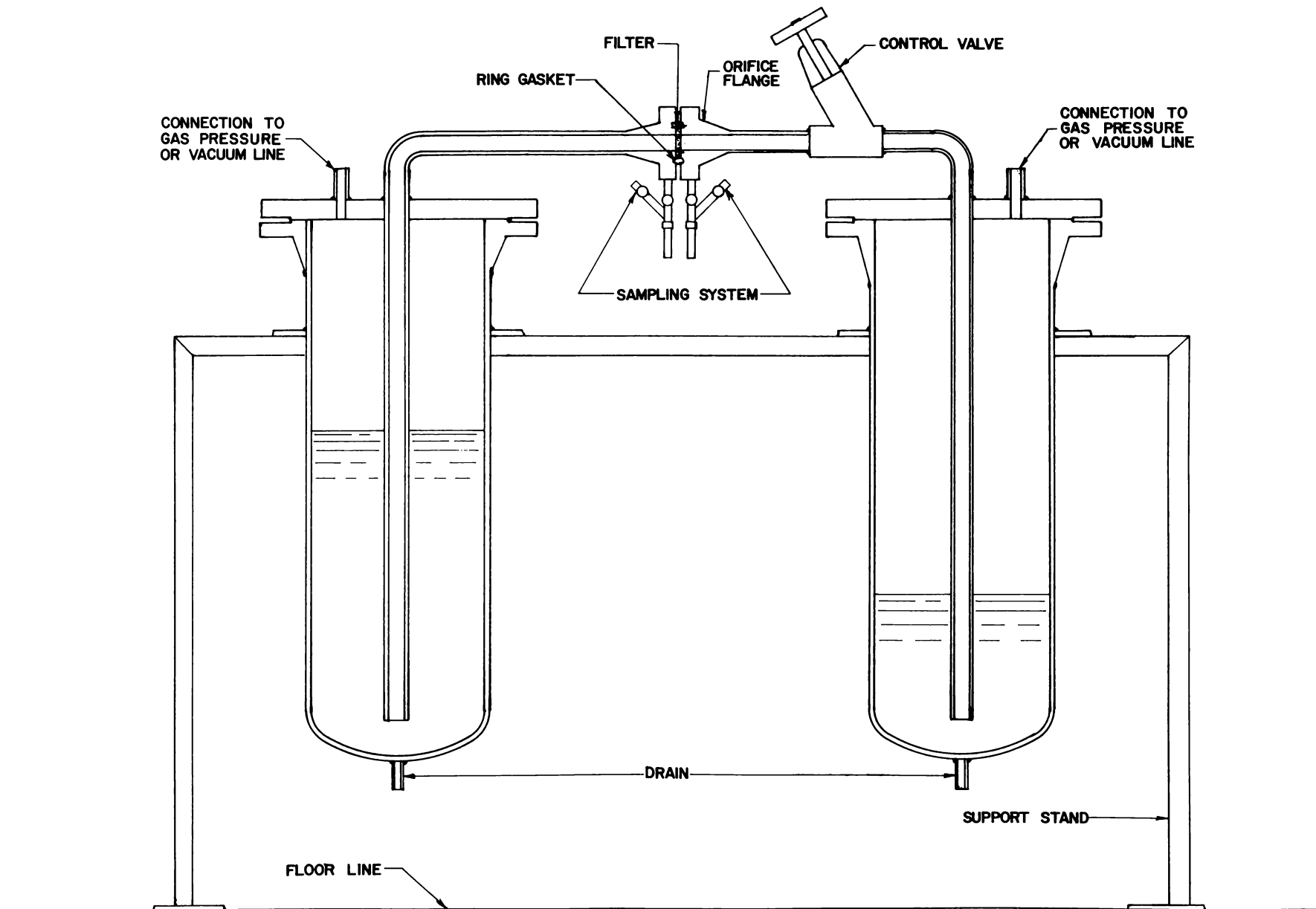


FIG. 56: APPARATUS - BISMUTH FILTER DEVELOPMENT



Only filters of Type 316 stainless steel have been received; filters of Type 431 stainless steel, pure electrolytic iron, and molybdenum are on order. A proposal has been received from Armour Research Foundation for research work necessary to produce satisfactory fiber metal filters for this program. Action will not be taken unless the porous metal filters now on order are tested and found unsatisfactory.

The first tests on the Type 316 stainless steel filters will take place as soon as the apparatus is electrically wired.

I. FLANGE TESTING

Although the reference design specifies an all-welded primary system, efforts to find a satisfactory flange for U-Bi service continue. The Marman Conoseal joint, which appears to have possibilities, is being procured for test. An Oak Ridge design for a freeze flange has been modified for bismuth service and also will be tested.

V. REMOTE MAINTENANCE

REMOTE WELDING

Investigation of remote welding of pipe in the horizontal fixed position continues. Three welding processes have been considered as possibilities for this application: high-frequency induction forge, inert-gas tungsten arc, and gas-shielded metallic arc. Further development of the gas-shielded metallic arc process has been discontinued by mutual agreement of Lynchburg AED and Research Center Personnel. The latest work on this process concerned its application to a sleeve-type joint requiring fillet welds at each end of the sleeve. The fillet welds with the pipe in the horizontal fixed position proved slightly less difficult than groove welds. Figure 57 shows examples of this type of joint. The status of the other two processes follows.

1. High-Frequency Induction Forge Welding

The first progress report issued covered only work done on 3-in. sch 80 pipe size in carbon steel and Croloy 2-1/4. Since then several other sizes have been used, all of Croloy 2-1/4 material

- 2-in. sch 40 pipe
- 2.5 in. OD x .250 in. wall tubing
- 6.625 in. x .313 in. wall tubing
- 4 in. sch 80 pipe (taken from Bi loop)
- 12 in. sch 40 pipe

Two sizes, 2.5-in. OD by .250-in. wall and 6.625-in. OD by .313-in. wall, proved very well suited to our induction welding equipment. With only a few trials on each of these sizes, consistently satisfactory results were possible. On 2-in. sch 40 numerous trials were made, but the thin wall (.154 in.) was very sensitive to slight variations in the

welding parameters. No satisfactory joints were obtained in this size and results were unpredictable. Figure 58 shows some of the results obtained on 2-in. sch 40 pipe and 2.5-in. OD by .250-in. wall tubing.

Some good results have been obtained on 12-in. sch 40 pipe. A technique that gives consistent results, however, is yet to be developed. The results obtained on this size indicate that the inductor size might be increased to improve the heating and thereby improve penetration through the heavier wall (.406-in.) thickness. Figure 59 shows a section of the weld with bends taken from the joint.

The 4-in. pipe salvaged from a bismuth loop was originally tried with an inductor not specifically designed for this size. For this reason there was approximately 1/2-in. radial clearance between the pipe OD and the inductor ID. This proved excessive, and only about 80 percent of the bends taken from this size were satisfactory. Based on the residue of Bi left in the pipe upon welding, it appears that the deficiency of the welding inductor was more detrimental. This inductor has been reduced in diameter and is being installed on the machine for further trial in the presence of bismuth. In this process the temperature of the joint during forging is of utmost importance

For better insight into the heat distribution through the wall thickness, a system of Esterline-Angus recorders has been added to the induction welding equipment (Fig. 60). Through thermocouples preplaced in the joint area and these recorders, accurate data are being obtained on variation of the inside and outside temperatures throughout the welding cycle. This means of measuring temperature has also been a valuable aid in postweld heat treating with the welding inductor.

Future work on this project includes 4-in. sch 80 (taken from Bi-loop), 12-in. sch 40, and 8.625-in. OD with .375-in. wall. A welding inductor is being fabricated for the 8.625-in. size. More efficient means of heat treating by induction are being sought. Figure 60 shows a three-turn heat treating coil in position over a 12-in. sch 40 pipe joint.

2. Inert-Gas Tungsten Arc Welding

Progress of this position-welding machine is being followed.

FIG. 57: GAS-SHIELDED METALLIC ARC WELD IN CROLOY 2-1/4 PIPE
6-1/2 in. OD x 3/8 in. WALL



Photograph shows the overhead position designated by the 6 o'clock marker. The beads were deposited from top to bottom and illustrate the bead pattern and overlapping at the stopping point.

Photograph shows a representative root bead pass illustrating the fusion obtained in each side wall.

FIG. 58: HIGH FREQUENCY INDUCTION FORGE WELDING

(specimen no. 183 in 2-in. sch 40 Croloy 2-1/4 pipe, all others in 2 1/2-in. OD tubing with .250-in. wall thickness)

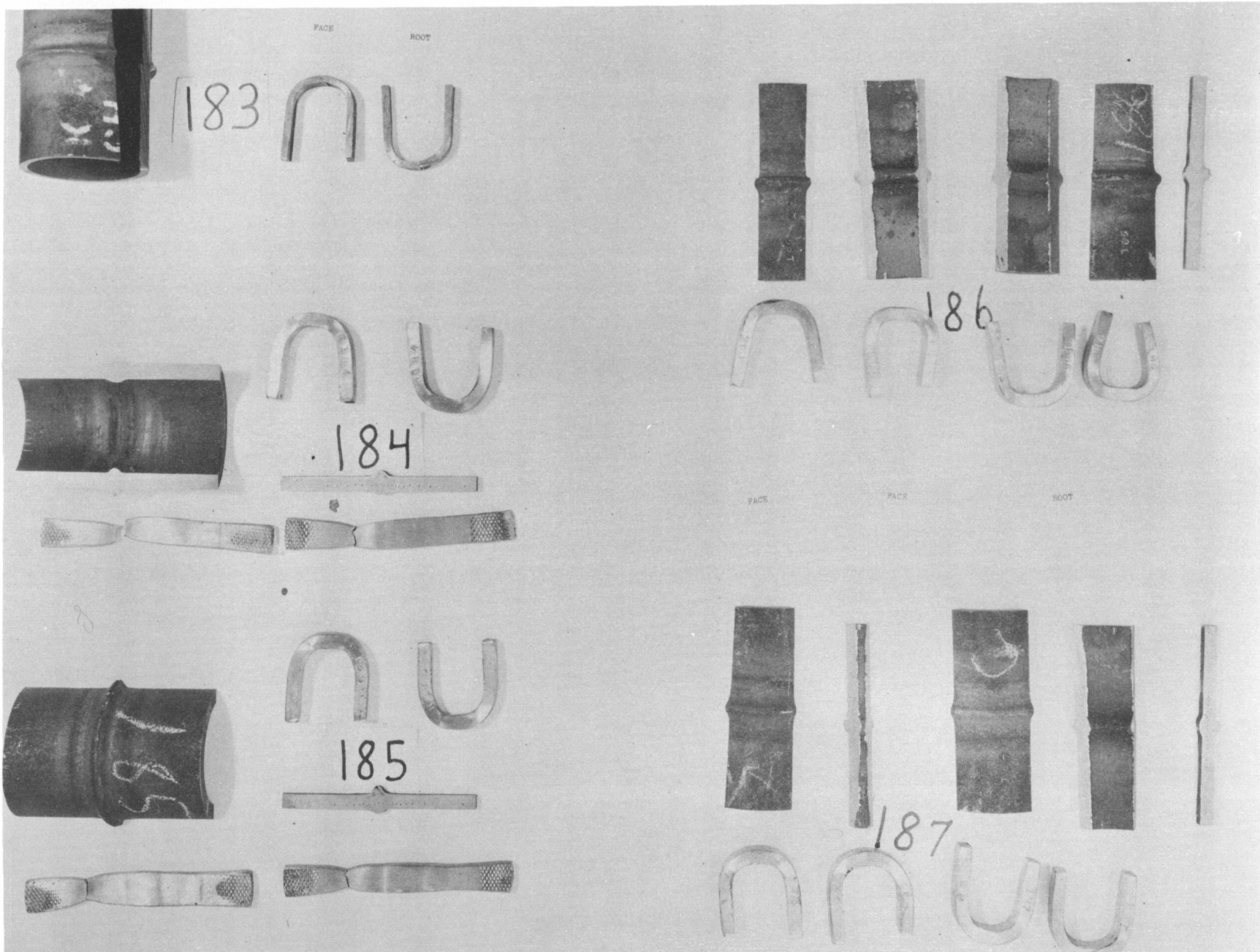
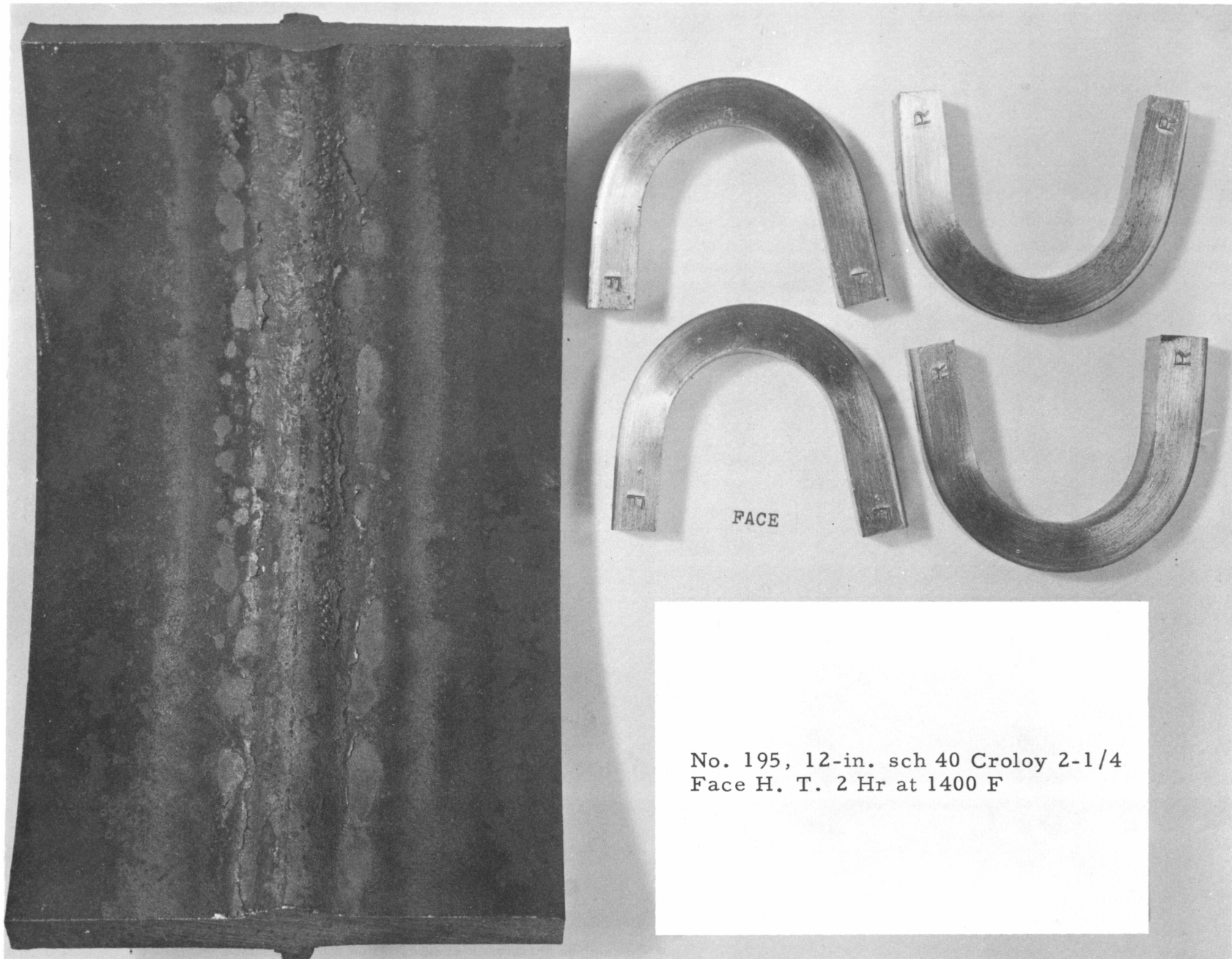
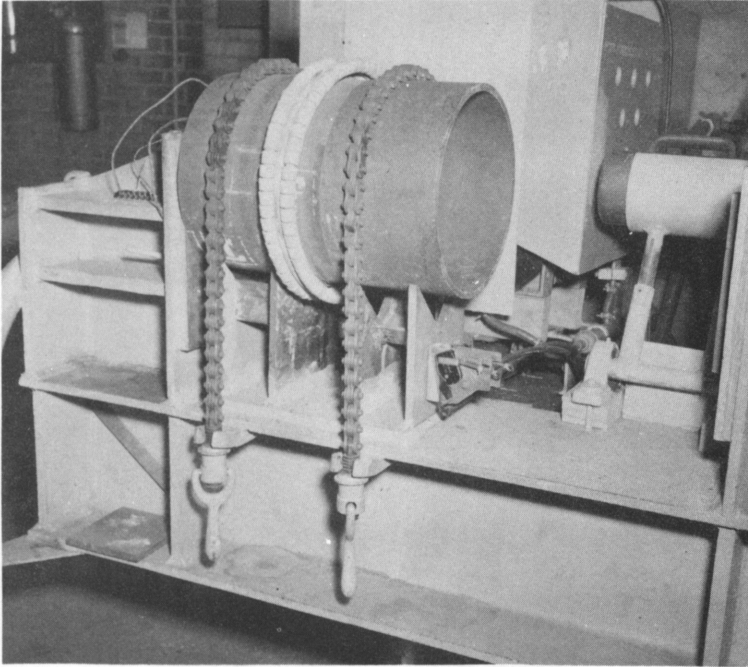


FIG. 59: INDUCTION FORGE WELDED JOINT

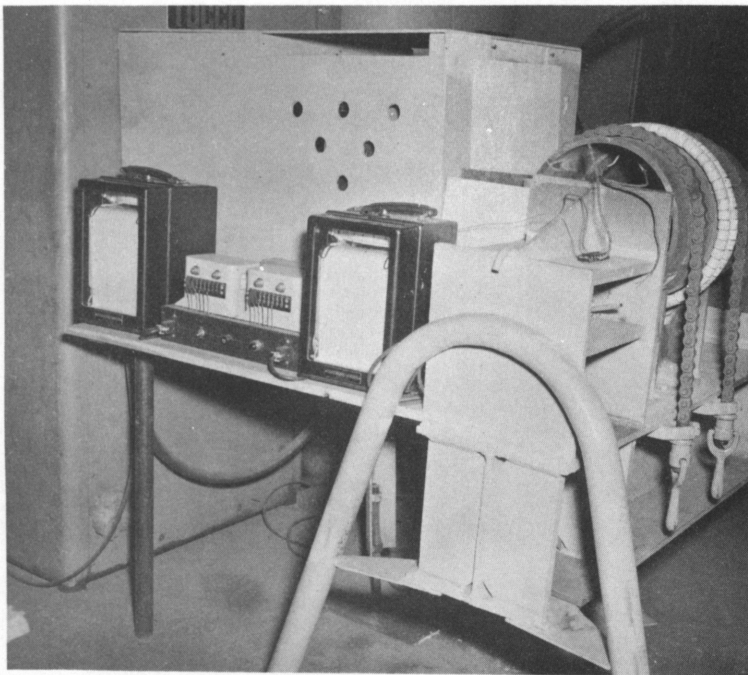


No. 195, 12-in. sch 40 Croloy 2-1/4
Face H. T. 2 Hr at 1400 F

FIG. 60: INDUCTION FORGE WELDING EQUIPMENT



This shows a 3-turn heat treating inductor in position on 12 in. sch 40 Croloy 2-1/4 pipe joint.



Thermocouples preplaced in the joint measure temperature throughout the welding cycle. After the joint is completed, variation of the temperature of both inner and outer regions of the joint relative to time are available for study.

VI. IN-PILE WORK

A. IN-PILE TEST LOOP AT ETR

Fabrication and assembly of the major components in the test area (Fig. 61) is approximately 80 percent complete. There has been some delay on the construction of the pump containment because of a delay in receiving the valves from the vendor. Two valves were received the last week of June. The completion of the order has been promised on a production basis following the delivery of the initial two valves.

The main panel board (Fig. 62) has been received from the vendor and installed in the test area. Construction of two other panel boards that would fit near the test loop at ETR have been completed and installed in the test area. One panel board contains the main switches and power inlets for the loop; the other contains the industrial television and the sampling controls.

The Croloy 2-1/4 pumps for this loop have been received from the vendor. Plastic models of the sump and gas sparger were obtained to study the flow distribution when using these pumps. Plastic model pumps, run with water, were installed, and a performance curve was established. It has been possible to obtain a satisfactory flow distribution within the sump after minor modifications to the pumps.

The mechanism to seal the containment ends during disassembly of the test has been assembled and tested. The results were satisfactory, and work is progressing to fabricate the necessary quantity for the test loop. The remote sampling apparatus has been modified to accommodate a larger air cylinder to move the sampling probe farther from the hot sump. Testing of the sampler continues. The remote cut-off mechanism has been tested using a high-speed solid steel wheel. A satisfactory cut was obtained. However, modifications are being made in the feed rate and wheel speed to get a longer life from the wheel.

FIG. 61: TEST AREA - ETR LOOP

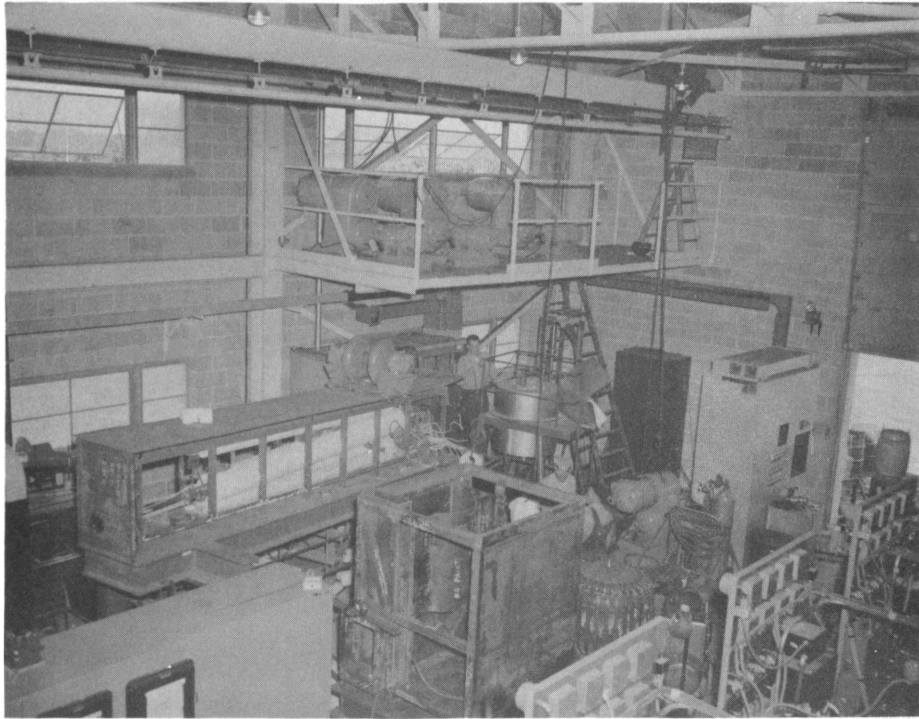
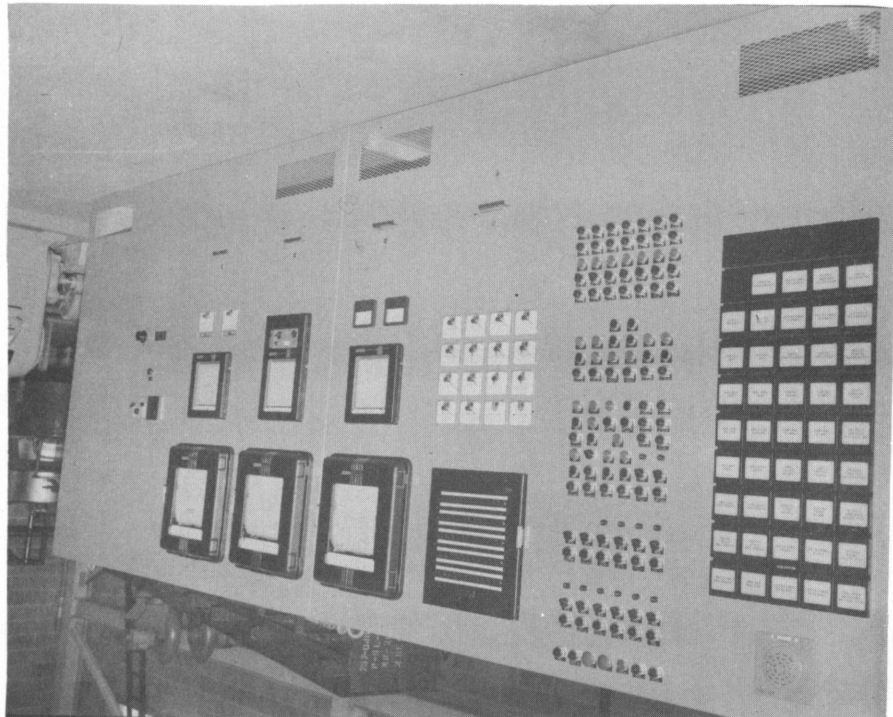


FIG. 62: MAIN PANEL BOARD - ETR LOOP



The detailed design of the in-pile section was completed and fabrication is proceeding in the machine shop. The mockup of the in-pile section was completed and shipped to ETR for critical facility testing. A thermal design study of the in-pile section was completed. A report summarizing the work was submitted as a supplement to "Outline of Information for 320 Approval, Radiation Test Loop No. 2."

Impact and tensile specimens have been coated with aluminum and sent to ETR for irradiation testing.

The journal bearing test using the utility loop pump was concluded at the end of 2238 hr to make the pump available for use on the utility loop. The bearing has performed satisfactorily throughout this test program. This type of bearing is planned for the pumps to be used in the test program. The information obtained on the EM flowmeters from the same test is being compiled.

B. IN-PILE TEST LOOP AT MTR

Detailed design of this loop continues and is approximately 80 percent complete. The functional design of the MTR loop is basically the same as the ETR loop, although the detail design and in-pile section differ considerably because of differences in reactor geometry. The design of many auxiliaries is the same for the two loops.

Components for this loop are now being fabricated, including the dump tank and the fill tank.

C. IN-PILE TEST LOOP AT BNL

1. Loop Assembly

The in-pile section assembly has been completed and installed in its containment. The section containing the deposition gauge, flowmeter, and sampler base has been welded into the loop. The welds have been radiographed, and the entire section has been leak checked and insulated.

The pump cell assembly, complete except for the two valves, was leak-checked to test the welds and suitability of the lead coated gaskets. For this purpose the assembly was put into a plastic bag surrounded by an atmosphere of helium.

All field welds made on the loop proper at BNL were leak-checked.

Two fluid samplers have been fabricated and a test apparatus is being set up for pre-operational checkout.

A check run on the pump cooling system was completed, and the cooling tubes have been led to the pump containment panel.

Final assembly and testing of six pneumatically operated, gas-ballasted valves designed by BNL is almost complete. Using argon, with 80 to 100 psig on the piston and 45 psig across the seat (valve in the closed position), the gas leakage was 10 to 12 ml/min.

The melt-dump tank and containment have been installed, and two disposal tanks have been fabricated and leak checked. Extension of the containment exhaust duct outside of the building has been completed; duct work for the cooler is complete and necessary valves and instrument taps have been installed.

2. Instrumentation

An early warning system, designed to alert the operator of an approaching automatic dump condition, has been installed and tested. Tubing for all draft gauges, and piping for valve operators have been run and checked.

The valve control system modification is complete and the valve operating system has been installed.

A Flexopulse timer has been installed and wired for timing heat pulses to flowmeter.

Control circuits for temperature control of the cold test section and the deposition gauge have been added.

Pressure transmitters have been installed and connected with the control panel.

Twenty-four additional thermocouple switches have been added for general loop surveillance.

3. Gas-Vacuum System

The primary and auxiliary vacuum system manifolds and gas-vacuum panel were completed and partially leak-checked.

The vacuum exhaust line has been extended to the pile face, and a plug for the hole is being fabricated.

The emergency cooling air-carbon dioxide manifold has been assembled.

The helium purification train has been completed and leak checked.

The air supply system for the instruments is almost complete.

4. Deposition Gauge

The new gauge was completed and placed in the loop. The core is made of Croloy 2-1/4 at the junction, which was welded to the pipes to avoid dissimilar metal welds near bismuth. A mu metal shield in the form of two boxes is placed around the unit to reduce the interference from stray fields.

Other details have been changed in the electronic system, the most important being a turned amplifier designed to reject 60 cycles. It was found that a better initial balance may be made by connecting the drive coils in parallel with a potentiometer instead of in series.

5. Flow Gauge

The thermal balance flow gauge has been constructed and placed in the loop.

It was previously reported that the thermal flow gauge read higher than the electromagnetic flowmeter in Loop H. At that time there was no absolute calibration of either gauge. Upon dismantling Loop H, the field in the electromagnetic gauge was calibrated and found to be 26 percent lower than the value reported at the time of manufacturer. Some iron deposit was found in the EM flowmeter. These circumstances place a more favorable light on the thermal flowmeter.

6. Flux Monitors

It is desired to place in the loop neutron flux monitors that would indicate the total irradiation of the in-pile test section. The monitors are required to have a half life of about six months and must be capable of withstanding temperatures of about 500 C. Commercial nickel and thorium metal were chosen. Flux will be measured with the latter by analysis of Co-137 and Co-144 produced

by thorium fission (threshold energy about 1.4 Mev). To prevent oxidation, the thorium was placed in an evacuated quartz capsule which in turn was placed in an evacuated nickel capsule.

The nickel flux monitors were chosen to measure fast flux level by the $Mi-58$ (n,p) $Co-58$ reaction. The threshold for this reaction is approximately the same as that for thorium fission and will serve as an independent check. Commercial nickel contains about 0.1 percent cobalt, which is enough to find the thermal and epithermal flux. Instead of using a cadmium cover, which would melt at the loop temperature, the nickel is covered by a stainless steel envelope that contains cadmium oxide.

A test of cadmium oxide in a stainless sheet showed no corrosion of the stainless steel at 700 C for 48 hr.

7. Loop G

The rebuilding of BNL's loop G nears completion. This loop will be operated to duplicate the in-pile flow and temperature conditions of Radiation Loop No. 1. The maximum and minimum inner film temperatures of the loop will be 500 C (932 F) and 425 C (797 F). Additive concentrations will be: uranium 1400-1500 ppm, magnesium 350 ppm, and zirconium 175-200 ppm. Test duration will be 5000 hr.

A preliminary draft of the Instructions and Procedures for Radiation Loop No. 1 has been completed and reviewed by the Reactor Safety Committee. The first draft of the Testing Program is also complete.

